K4.15 GEOHAZARDS AND SEISMIC CONDITIONS

This appendix contains technical information related to impacts from potential seismic and other geohazards at the mine and port sites, including the following topics:

- Mine site
  - Embankments and impoundments
    - Construction materials
    - Design and construction
    - Seepage analysis
    - Static stability analysis
    - Seismic hazard and deformation analysis
  - Open pit
    - Pit wall stability analysis
- Port sites
  - Seismic hazard analysis
  - Foundation conditions
  - Sheet pile dock stability

K4.15.1 Mine Site

The following discussion addresses mine site facilities that would have the potential to be affected by geohazards, which could include internal erosion and slope failure of embankments and impoundments, and rock wall instability in the open pit.

K4.15.1.1 Overview of Mine Embankments and Impoundments

The mine embankments and impoundments would be designed and constructed to store tailings and contact water during mine operation. The tailings and contact water could pose a risk to the environment if released due to geohazards. The mine site-related embankments and impoundments, shown in Chapter 2, Alternatives, Figure 2-4 and summarized in Table K4.15-1, include the bulk tailings storage facility (TSF), the pyritic TSF, water management ponds (WMPs), and seepage collection ponds (SCPs). Table K4.15-1 presents the buildout dimensions of the embankments and impoundments that would contain tailings, waste rock, and/or contact water at the mine site. These facilities are discussed below.

K4.15.1.2 Embankment Construction Materials

Rockfill, Earthfill, and Engineered Filter Zones

Rockfill and earthfill materials, including the engineered filter zones, used to construct embankments for the tailings and water management facilities would be derived from drilled and blasted bedrock removed from quarries A through C (Chapter 2, Alternatives, Figure 2-4 and Figure K4.15-1). The engineered filter zone materials would be comprised of sand and sandy gravel sourced from the quarries. Both the filter materials and rockfill (also referred to as Zone C materials) would be processed by crushing and screening to meet the required material gradations (PLP 2019-RFI 129). The three rock quarries would be developed in the western portion of the mine site in bedrock consisting of granodiorite associated with the Kaskanak batholith. See Section 3.13, Geology, for further discussion of mine site geology.

Table K4.15-1: Mine Embankment and Impoundment Dimensions

Impoundment/ Embankment Name		Embankment: Max. Height (feet)	Crest Elev. (feet)	Footprint Area (acres)	Max. Crest Length (feet)	Crest Width (feet)	Max. Width at Base (feet)	Downstream Slope (H:V)	Upstream Slope[1] (H:V)	Foundation Strata[2]	Construction Material Volume (M yd³)	Seepage Control Method	Raise Method	Stored Material	Impoundment: Max. Footprint Area[3] (acres)	Pond Surface Area[4] (acres)	Max. Impoundment Volume[5] (acre-feet)
Alternative 1a and Alternative 1																	
Bulk TSF	Main	545	1,730	310	13,700	200	2,340	2.6:1 Overall (including Buttress)	Vertical Serrated	Bedrock	76	Flow-Through Embankment, with Engineered Filter Zones	Modified Centerline	Bulk Tailings	2,875	520 to 940	568,300
	South	300	1,730	90	4,900	200	1,530	2.6:1	3:1	Bedrock	11	U/S Liner (or C/F) & Grout Curtain[6,7]	Downstream	Bulk Tailings			
Bulk TSF Main Seepage Collection Pond		120	1,185	25	3,400	50	500	2.6:1	2:1	Bedrock	2	U/S Liner (or C/F) & Grout Curtain	N/A	Bulk Tailings Seepage	95	35 to 85	3,000
Bulk TSF South Seepage Collection Pond		75	1,395	4	1,300	50	200	2:1	2:1 to 3:1	Overburden	0.1	U/S Liner (or C/F) & Grout Curtain	N/A	Bulk Tailings Seepage	TBD, SCP to be operated with minimum pond volume and freeboard allowance for the required IDF.		
Open Pit Water Management Pond		100	1,123	35	3,700	50	580	2:1	3:1	Overburden	2	Fully Lined	N/A	Open Pit Water	65	40	845
Main Water Management Pond[8]		190	1,295	225	14,600 to 14,700[10]	100	870	2:1	3:1	Bedrock[11]	51[11]	Fully Lined with F/T[14] Zone	N/A	Contact Water	955	750 to 825	56,000
Pyritic TSF[9]	North	335	1,620	350	12,900	200	1,950	2.6:1	3:1	Bedrock	85	Fully Lined	Downstream	Pyritic Tailings	1,000	726	107,800
	East	225	1,620														
	South	215	1,620	100	4,500	200	1,500				30						
Pyritic TSF North Seepage Collection Pond		45	1,325	3	900	50	190	2:1	2:1 to 3:1	Overburden	0.1	U/S Liner (or C/F) & Grout Curtain	N/A	Pyritic Tailings Seepage	TBD, SCP to be operated with minimum pond volume and freeboard allowance for the required IDF.[12]		
Pyritic TSF South Seepage Collection Pond		30	1,425	2	625	50	190	2:1	2:1 to 3:1	Overburden	0.1	U/S Liner (or C/F) & Grout Curtain	N/A	Pyritic Tailings Seepage	TBD, SCP to be operated with minimum pond volume and freeboard allowance for the required IDF.		
Pyritic TSF East Seepage Collection Pond		55	1,400	2	570	50	200	2:1	2:1 to 3:1	Overburden	0.1	U/S Liner (or C/F) & Grout Curtain	N/A	Pyritic Tailings Seepage	TBD, SCP to be operated with minimum pond volume and freeboard allowance for the required IDF.		
Emergency Dump Pond		40	1,335	6	1,800	50	200	2:1	2:1	Overburden	TBD	Fully Lined	N/A	Tailings Slurry	TBD, Emergency Dump pond to remain empty outside of upset conditions in the tailings pipelines. Design storage TBD.		
Alternative 2—Downstream Construction[13]																	
Bulk TSF	Bulk TSF Main	570	1,745	460	14,050	200	2,630	2.6:1 Overall (including buttress)	2:1	Bedrock	124	Flow-Through Embankment, with Engineered Filter Zones	Downstream	Bulk Tailings	2,985	520 to 940	561,800
	Bulk TSF South	320	1,745	5	5,100	200	1,700	2.6:1	3:1	Bedrock	14	U/S Slope Lined & Grout Curtain	Downstream	Bulk Tailings			

Notes:
[1] Upstream slope assumed to be 3 Horizontal (H):1 Vertical (V) for lined embankments, or 2H:1V for C/F seepage control.
[2] Removal of overburden may be required (where not otherwise indicated) based on the geotechnical and hydrogeological information collected during site investigations.
[3] The maximum impoundment footprint area is the entire facility, including embankments and storage/pond surface areas. The embankment footprint and pond surface areas may overlap in some cases.
[4] Range of pond areas indicates normal and maximum operation pond levels.
[5] Max impoundment volume below freeboard and storm storage; TSF storage volume is solids only.
[6] C/F = Core and Filter, a low-permeability and engineered filter zone. The current design concept includes an upstream face liner keyed to grout curtain; however, other options that may be explored during detailed design include incorporating a low permeability core zone keyed into a grout curtain instead of a liner (PLP 2019-RFI 129).
[7] U/S = Upstream. The U/S liner would likely also include low permeability bedding and filter zones (PLP 2019-RFI 129).
[8] The presented embankment height and base width are from the top of the embankment toe backfill (as per discussion between PLP and ADSP), and not the excavated surface.
[9] The ultimate pyritic TSF embankment is a continuous structure between the north, east, and south embankments. The final footprint area, crest length, and fill volume are provided.
[10] Includes 100 to 150 feet at each abutment to reach bedrock (PLP 2019-RFI 108b).
[11] Pebble Limited Partnership (PLP) changes during Environmental Impact Statement (EIS)-Phase failure modes effects analysis, Oct. 24-25, 2018 (PLP 2019-RFI 108, 108a, 108b).
[12] IDF = Inflow Design Flood
[13] Alternative 1 from PLP 2018-RFI 075
[14] F/T = Filter/Transition zone
N/A = not applicable
TSF = tailings storage facility
Source: PLP 2019-RFIs 108, 108a, 108b; PLP 2020d

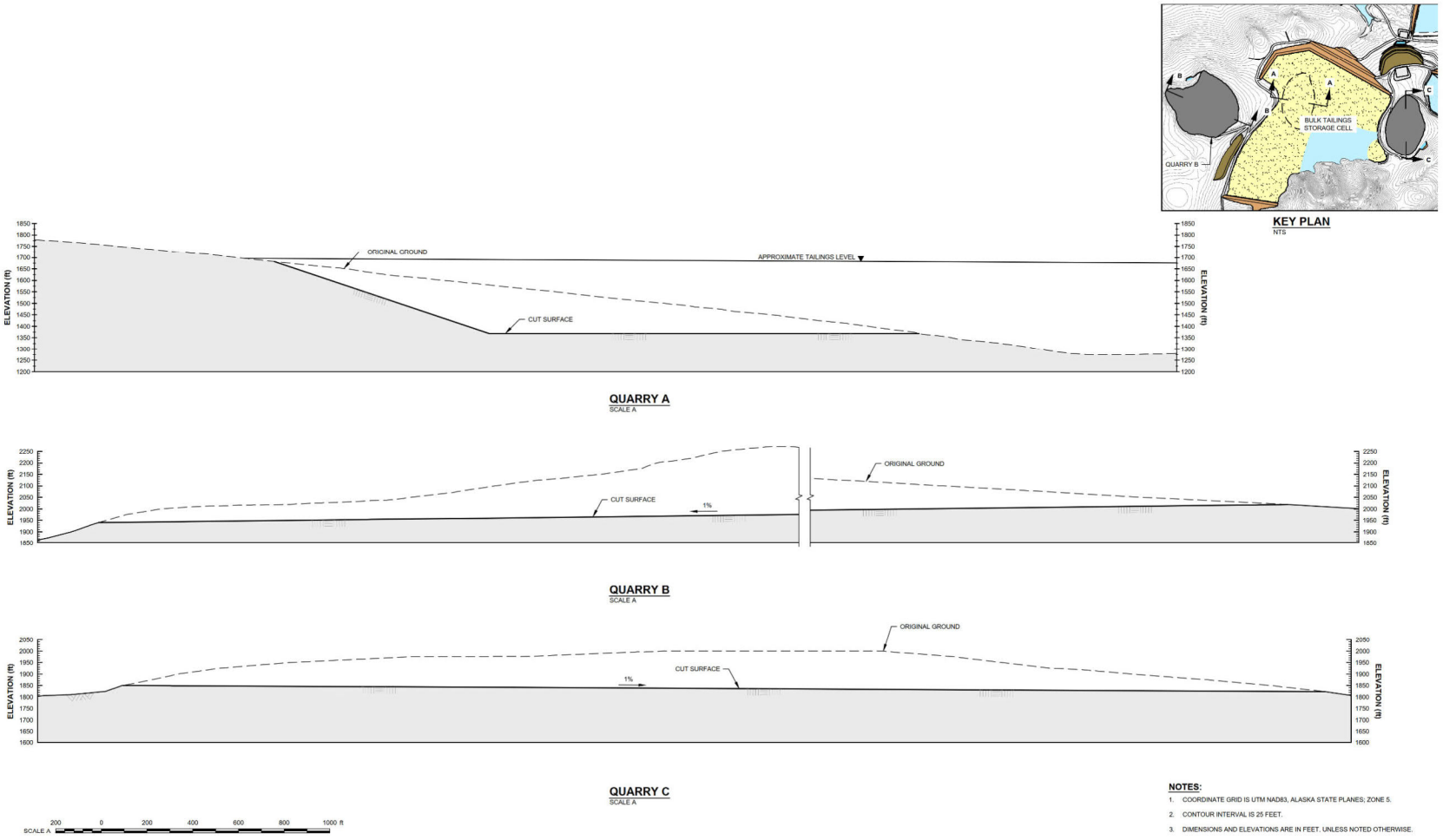

Source: PLP 2019h, Figure MX-009

US Army Corps of Engineers®

PEBBLE PROJECT EIS

QUARRIES A THROUGH C CROSS-SECTIONS - TYPICAL

FIGURE K4.15-1

The characterization of rock types in the three rock quarries and the open pit area was based on both surface geological mapping and geotechnical drillholes (PLP 2018-RFI 015). Additional geotechnical information regarding rock quality and materials balance would be completed for all required embankment rockfill and earthfill materials during detailed design (PLP 2019-RFI 008g and PLP 2019- RFI 129).

Table K4.15-2 presents the estimated rock volumes of the three rock quarries plus the open pit overburden, based on the maximum footprints as presented in Figure 2-4. The table considers the differences between in-place versus post-removal and post-placement volumes and unit densities of the rockfill and earthfill materials, as described in the table footnotes below.

Table K4.15-2: Summary of Available Embankment Rockfill and Earthfill Material

Material Source	Banked Volume		Reduction Factor[1]	Bulking Factor	Loose Volume		Compaction Factor	Compacted Materials		
	(Mft^3)	(Mcy)			(Mft^3)	(Mcy)		(Mft^3)	(Mcy)	(Mton)
Quarry A	1,440	53	0.9	1.6	2,074	77	1.3	1,685	62	101
Quarry B	2,693	100	0.9	1.6	3,878	144	1.3	3,151	117	189
Quarry C	1,208	45	0.9	1.6	1,739	64	1.3	1,413	52	86
Open Pit Overburden	1,573	58	0.5	1.2	944	35	0.95	747	28	41
TOTAL	**6,914**	**256**	**--**		**8,635**	**320**	**--**	**6,996**	**259**	**417**

Notes:
[1]Loose and banked densities based on estimated compacted density and bulking/compaction factors.
Material Definitions:
Banked Volume – Volume before excavation.
Loose Volume – Volume after excavation.
Bulking Factor – Loose volume/banked volume.
Compaction Factor – Compacted volume / banked volume.
Usable Material Reduction Factor (reduction to account for out-of-specification/unusable materials) = 0.9 (quarries), 0.5 (open pit overburden; reduced because of variability of rock quality).
Neatline material volumes were rounded to the nearest million. Quarry volumes based on project description layout.
Material densities assumed as follows:

Material Densities (lb/ft^3)			
Material	Banked	Loose	Compacted
Rockfill	156	98	120
Overburden	105	87	110

Mcy = million cubic yards
Mft^3 = million cubic feet
Mton = million tons
lb/ft^3 = pounds per cubic foot

Source: PLP 2018-RFI 015b

The material banked densities and bulking factors were estimated based on Look (2007) and are considered reasonable or conservative (e.g., bulking factors can range higher than those assumed, yielding potentially larger quantities available). Compaction factors were based on soil properties published by Durham University (1997). The values for compacted density were applied to the material estimates.

Table K4.15-3 presents the estimated amount of rockfill and earthfill material that would be needed to construct the major embankments and perform road maintenance. The data indicate that quarries A through C plus the open pit overburden would generate about 4 to 5 percent less compacted material than needed to construct the embankments. However, if higher bulking

factors were used (e.g., 2.0 for rock and 1.6 for overburden, still reasonable values in the literature [Look 2007]), the calculated available compacted material in Table K4.15-2 would be well above that needed in Table K4.15-3. The material balance (surplus/deficit) would be further refined as the design and site investigation programs are advanced. If necessary, the base elevation of the quarries would be lowered to increase material availability (PLP 2018-RFI 015a).

Table K4.15-3: Embankment Rockfill and Earthfill Material Needs

Rockfill and Earthfill	Total		
	Volume[1]		Weight[2] (Mton[3])
	Mft[3]	Myd[3]	
Pyritic TSF (All Embankments)	3,105	115	186
Bulk TSF Main Embankment	2,295	85	138
Bulk TSF South Embankment	540	20	138
Main Water Management Pond	1,200	44	72
Open Pit Water Management Pond	54	2	3
Main Embankment Seepage Collection Pond	50	2	3
Road Coarse Replacement[3]	22	1	1
Road Sanding[4]	50	2	3
TOTAL	**7,316**	**271**	**439**

Notes:
Mft[3] = million cubic feet
Myd[3] = million cubic yards
Mton: million cubic tons
TSF = tailings storage facility
[1] Neatline material volume (theoretical volume based on geometry of structure) rounded to the nearest million ft[3].
[2] Based on rockfill compacted density assumed to be 120 lb/ft[3].
[3] Road coarse replacement assumes 6 inches of material replaced every 3 years.
[4] Road sanding assumes 150,000 tons per year.
Source: PLP 2019-RFI 108a, RFI 2019-RFI 008e update

Table K4.15-1 shows several smaller impoundments (e.g., sediment ponds) that are not included in Table K4.15-2 and Table K4.15-3. These are generally smaller in height and were of less concern during scoping with regard to geotechnical stability and contents that could be released in the event of failure (sediment versus contact water or tailings in the larger facilities). As with the larger embankments, detailed design, and analysis of the smaller impoundments would be completed as part of the preliminary and detailed designs.

Liner Bedding and Core Zones

Low permeability materials (referred to as Zone S material) would be used as liner bedding in embankments that are either fully lined or have an upstream liner. As noted in Table K4.15-1, the current embankment concepts do not include low permeability core zones; however, other options that may be explored during detailed design include incorporating a low permeability core zone keyed into a grout curtain instead of having an upstream liner (PLP 2019-RFI 129). Low permeability materials may also be used to complete the cover of the bulk TSF at closure, depending on the closure cover design (PLP 2019-RFI 130).

The low permeability materials would be sourced from overburden in the open pit, or if required, from other foundation excavations at the mine site. Surface mapping and drillhole data in the open pit area indicate that the overburden consists primarily of glacial drift and glacial lake deposits

with lesser amounts of colluvium, delta, and beach deposits (Figure 3.13-2). These units consist mainly of low permeability clayey sands and gravels, with areas of silty sands and gravels (PLP 2019-RFI 129).

A preliminary estimate of the total overburden available from open pit stripping is approximately 35 to 40 million cubic yards (Myd^3), and the total available from all mine site sources (including foundation excavations and other surface preparations as well as the pit) is estimated to range from 75 to more than 150 Myd^3 (PLP 2019-RFI 129; SRK 2019d). If for example, liner bedding is specified below the main WMP and pyritic TSF liner systems during future detailed design, approximately 3.5 Myd^3 of Zone S material would be required. An additional 12 Myd^3 of low permeability material would be required for the bulk TSF closure cover, depending on the type of design. Together these volumes represent approximately 38 to 44 percent of the overburden sourced from the open pit or 10 to 20 percent of the total overburden that would be available. If additional material is required at closure, it may also be sourced from deconstruction of certain mine facilities (e.g., main WMP, pyritic TSF), if suitable. Thus, it is expected that the pit and other mine site areas would provide a sufficient amount of low permeability materials to meet the Zone S requirements specified in detailed design (PLP 2019-RFI 129).

The overburden at the pit would be selectively stockpiled in designated areas for use as construction material in the appropriate zone, as determined by material gradation. As described in Chapter 5, Mitigation, detailed characterization of the pit overburden materials and a materials balance would be completed during detailed design to assist with the development of a pit pre-stripping plan to segregate the different materials to be stockpiled for construction use (PLP 2019-RFI 129).

Growth Media

Growth media, consisting of topsoil and overburden, would be stockpiled during construction for future use in reclamation activities at closure. Based on the Reclamation and Closure Plan (SRK 2019d), as well as footprint and elevation data (PLP 2020b), approximately 20 to 24 Myd^3 of growth media would be placed in the growth medium stockpiles north of the main WMP and west of the bulk TSF.

SRK (2019d) estimates that a total of about 35 Myd^3 of growth media would be needed for reclamation. A separate estimate based on GIS footprint data for specific reclaimed facilities (see Figure 4.16-6) yielded lower volumes of growth media needs ranging from 9 to 14 Myd^3. This estimate does not include some miscellaneous infrastructure and roads (e.g. power plant, camp) that may continue to be used in post-closure, and assumes that quarries A and C would require about 3 feet of growth media on cut surfaces and sloped areas, and that remaining reclaimed areas would receive a minimum of 6 to 12 inches of growth media (SRK 2019d). Growth media depth may vary depending on existing overburden type; for example, rocky areas would require more growth media than those with some remaining soil (SRK 2019d). The GIS-based estimates are considered a minimum, as they do not include areas (other than quarries) that may require more than 1 foot of growth media, or small contiguous areas in between specific facility outlines.

It is possible that volume of growth media needed for reclamation (9 to 35 Myd^3) may exceed the estimated volumes in the growth media stockpiles (20 to 24 Mcy^3). Additional growth media would also be sourced from the overburden stockpiles (PLP 2020b, Figure MX-005). The available volume of overburden with fines (see above under “Liner bedding and Core Zones”), that would also be appropriate for use in growth media, is expected to be sufficient to meet the needs of reclamation. Material balance (surplus/deficit) would be further refined as the design and site investigation programs are advanced (PLP 2018-RFI 015a; PLP 2019-RFI 129).

K4.15.1.3 Design and Construction of Embankments and Impoundments

The various embankments and impoundments at the mine site would be constructed of rockfill. Inherent in the construction of rockfill embankments and impoundments is the potential for groundwater to seep through the structures. The seepage would have the potential to reduce the stability of the structures by causing internal erosion or adding pore water pressure, which could affect resistance to sliding failure. Therefore, the embankments and impoundments would be designed and constructed to minimize internal erosion and control the phreatic surface (groundwater table) during operation. The facilities would also be designed for stability during static (non-seismic) and seismic (earthquake) conditions.

As described in Section 4.15, all embankments would be subject to State of Alaska regulations per Chapter 17 in Title 46 of the Alaska Statutes (AS 46.17) and Article 3—Dam Safety of Chapter 93 in Title 11 of the Alaska Administrative Code (11 AAC 93). The Dam Safety and Construction Unit (Dam Safety) of the Alaska Department of Natural Resources (ADNR) would be responsible for "supervision" of the safety of the embankments and for administration of the ADSP. A draft revision of "Guidelines for Cooperation with the Alaska Dam Safety Program (dam safety guidelines) (ADNR 2017a) is in the public domain, but has not yet been formally adopted by ADNR. A portion of the dam safety guidelines regarding periodic safety inspections were formally adopted by ADNR in 2003 by reference in 18 AAC 93. Subsequent revisions to the guidelines (ADNR 2005b, 2017a) have not been adopted in regulations, and may not be enforceable under AS 46.17 or 11 AAC 93 (ADNR 2020).

The regulatory requirements are obligatory, and typically considered as the "minimum" standard of care. The intent of the ADSP is to provide for the protection of human lives, property, and the environment, including anadromous fish streams, through consistency in design approach, construction, and operation of water and tailings storage facilities. The draft ADSP dam safety guidelines do not dictate how a facility is to be designed and constructed, but do describe a minimum standard of care, indicating that designs should follow a higher standard based on accepted industry standards and procedures (i.e., what a reasonable person or expert in the industry would consider foreseeable risk and the standard of care).

Prior to construction, all embankment starter dams and all embankments that are to be built to their full height at the outset would undergo initial application package preparations, preliminary and detailed designs, final construction package applications, safety reviews, and submittals to ADNR for Certificates of Approval to Construct a Dam. Also prior to construction, each embankment raise would undergo a separate set of preliminary and detailed design and safety reviews that would be adjusted as necessary based on knowledge from previous raise constructions, TSF operations, and tailings characterizations, followed by submittals to ADNR for a Certificate of Approval to Modify a Dam.

Prior to operations following the completion of each starter dam, full embankment, or embankment raise construction, a construction completion report would be submitted to ADNR for a Certificate of Approval to Operate a Dam. Therefore, no operations can start until the construction completion report is approved and the certificate is issued. Also, all dam repairs, removals, and abandonments require separate designs, safety reviews, and submittals to ADNR for Certificates of Approval to Repair, Remove, and Abandon a Dam, respectively.

The following discussion explains the general design and construction features relevant to geohazards, including elements for preventing internal erosion and instability, relevant closure-related aspects, and management and monitoring.

Bulk TSF

General—The proposed bulk TSF would consist of a main embankment (downgradient in terms of groundwater flow) and a south (upgradient) embankment (Figure 2-8). Important considerations for siting a stable and resilient tailings facility include site-specific topography and geology (van Zyl 2015). The bulk TSF would be in watersheds that flow north into the North Fork Koktuli (NFK) River and the South Fork Koktuli (SFK) River, and would be mostly surrounded by bedrock knobs and slopes. Bedrock foundation conditions beneath the embankment footprint and abutments are described below under "Stability-Related Elements."

The two bulk TSF embankments would be constructed of rockfill and earthfill sourced primarily from quarry A. These materials would be placed and compacted in planned and specified sequences and raise heights (PLP 2020d).

Under the Alternative 1a, Alternative 1, and Alternative 3—North Road Only, the upper 280 feet of the 545-foot-high bulk TSF main embankment would be centerline-constructed with downstream buttresses. That is, during the raising of the dam, rockfill and earthfill would be placed concurrently on top of both the centerline and the downstream slope of the previous raise. This would result in a near-vertical upstream face at the dam crest for the upper portion of the embankment, with some rockfill placed on upstream coarse tailings beach material during construction of the dam raises, resulting in a vertical zigzag of alternating tailings and rockfill in a cross-section view (Figure 2-8). Under Alternative 2—North Road and Ferry with Downstream Dams, the bulk TSF main embankment would be downstream-constructed (Figure 2-47).

In contrast, the south embankment would be downstream constructed under all alternatives. That is, during the raising of the embankment, rockfill and earthfill would be placed on top of the downstream slope of the previous raise, which would result in a nearly symmetrical embankment (Figure 2-8).

The size of the bulk TSF assumes that the split in tailings from the process plant would be an average of 88 percent bulk tailings and 12 percent pyritic tailings, based on batch flotation tests of drillhole samples from the pit area. If this split were to deviate substantially from that planned, the embankment raise schedules for the bulk and pyritic TSFs would be adjusted to accommodate the changed tailings volumes. The bulk tailings volume and related sizes of the bulk TSF embankments also assume that the tailings would be thickened to 55-percent-solids slurry by weight. The thickened tailings content was determined based on a tradeoff study conducted to optimize the minimum water content that would be moveable as a slurry. If this amount of thickening could not be achieved and greater water volumes were generated, additional pumping capacity would be provided to transfer the tailings slurry from the process plant to the TSFs and pump additional supernatant water from the TSFs and their seepage ponds (PLP 2018-RFI 010).

Embankment lifts and freeboard requirements would be reviewed as part of each embankment raise and safety review, and would be adjusted as necessary to reflect actual tailings throughput, settled densities, mine water management conditions, and different site conditions encountered.

Seepage-Related Elements—The bulk TSF main embankment (both the centerline- and downstream-constructed options) would use a flow-through design to prevent internal erosion by minimizing water buildup in the TSF and seepage pressure on the embankment, and to provide controlled flow away from the other embankments (PLP 2018-RFI 006a; PLP 2019-RFI 006c). In contrast, the south embankment would use a liner on the upstream slope face and would not include a flow-through design (Figure 2-8).

The bulk TSF main embankment would include engineered filter zones and a crushed or processed aggregate drain at a topographic low point, which would provide a preferential seepage path from the tailings mass to downstream of the embankment toe. Additional underdrains running

parallel to the embankment would allow for the drainage of seepage collected along the embankment (PLP 2020d).

The main embankment engineered filter zones would consist of a gradation of sand- to gravel-sized particles in two to three zones, which would be designed based on industry-accepted no-internal-erosion filter criteria developed by Sherard and Dunnigan (1985) (Fell et al. 2015; USACE 2004; USDA 2017; PLP 2018-RFI 006). A coarse-grained tailings unit would be located immediately upstream of the embankment (PLP 2018-RFI 006), which would be expected to minimize the amount of finer-grained tailings entering the upstream rockfill and earthfill part of the embankment. Rockfill and earthfill are typically composed of pervious material. The engineered materials zones are expected to control the migration of materials between adjacent fill zones while providing the necessary drainage capacity in the embankment structure (PLP 2019-RFI 008h). The embankment would be constructed in a manner to ensure the design performance of the engineered filter zones (AECOM 2018k). Material zones would be placed sequentially and not concurrently, and it is expected that the height differential would be limited to the thickness of one material lift. The engineered materials would be processed on site from the quarry sources and would be subject to ongoing quality control and assurance testing consistent with industry best practices and as defined in the design documentation. Materials that do not meet gradation specifications would be repurposed as non-critical materials such as road crush (PLP 2019-RFI 006a; PLP 2019-RFI 008h).

The main embankment zones and underdrains would be designed with consideration for the potential for cementation or partial plugging of seepage flows due to geochemical breakdown or under-performance of drainage materials. The underdrains would be built using suitable rockfill materials sourced from the quarries, which were analyzed for geochemical characteristics using acid rock drainage-predictive testing and determined to be non-acid generating. Samples of bulk tailings water were analyzed using the same methods and also determined to be non-acid generating. Iron could originate from oxygen-limited conditions in the tailings mass and accumulate in underdrains if flow through the drain is not rapid enough. In certain circumstances, iron hydroxide precipitates can plug drains and hinder flow. This would be mitigated by oversizing the underdrains. With these design considerations, there is low risk that chemical reactions would occur that could cause potential plugging and hindrance of seepage flow out of the TSF. The design criteria for the various drainage zones and design capacity of the drains would be determined and confirmed during preliminary and detailed design phases (PLP 2019-RFI 006c).

The bulk TSF south embankment would be constructed with an upstream liner keyed into a grout curtain. Other options that may be explored for the bulk TSF south embankment during final design and permitting include the use of low permeability (Zone S) material as liner bedding, incorporating a low permeability core zone into the embankment, or incorporating low permeability liner bedding zones and filter zones into the embankment without a specified core zone (PLP 2019-RFI 129). As described above under “Embankment Construction Materials,” the low-permeability and engineered filter zone materials would be developed and sourced from locations in the mine site to meet design gradation specifications. Materials with fines content between 30 and 60 percent passing a #200 sieve are expected to be suitable for use as core zone material. Materials meeting these gradation requirements were identified in the open pit area during geotechnical investigation programs completed between 2004 and 2011 (PLP 2018-RFI 006a; PLP 2019-RFI 129). The quantity of on-site, low-permeability core materials would be confirmed during additional geotechnical investigations as the design progresses. If sufficient quantities of these materials are determined to not be available on site, alternatives such as a low-permeability face liner or asphalt core would be used.

Control of water in the bulk TSF is an important consideration in achieving a stable tailings deposit and embankment. Best available technology (BAT) principles established following the Mount

Polley dam failure (Morgenstern et al. 2015) include eliminating or minimizing surface water in impoundments and promoting unsaturated conditions in tailings through drainage provisions. The size and location of the bulk TSF supernatant pond would be controlled during operations by pumping excess water to the main WMP or bulk TSF main embankment SCP. The embankments would include basin and embankment underdrains to help maintain a reduced phreatic surface in the facility. The stability benefit of maintaining a minimal supernatant pond size is advocated by comments on the 2014 Mount Polley Mine dam failure as follows:

- "Structural failure of the embankment alone did not cause the breach, but coupled with the condition of the tailings pond – with insufficient beaches and too much supernatant water – a progressive erosional failure of the embankment rapidly widened into a complete breach";
- "Adequate beaches could not be continuously maintained primarily as a result of too much supernatant water"; and
  "Beaches can serve as a buffer to maintain separation between water in the tailings pond and the embankment structure" (BCMOE 2015).

Tailings deposition and pond water would be managed to allow the continual development and maintenance of a tailings beach behind the bulk TSF main embankment. This would serve to protect the dam from seepage pressure that could reduce stability (Knight Piésold 2018a, 2019o; PLP 2018-RFI 006; RFI-008f; PLP 2019-RFI 006c). Tailings are expected to segregate following slurry deposition into three grain size zones (coarse, transition, and fine tailings units), with coarse tailings deposited closest to the spigots and fine tailings in the center of the impoundment. A tailings beach would also be developed along the west side of the impoundment, behind the south embankment, and in the eastern corner of the bulk TSF to promote pond development up against bedrock slopes to the southeast and direct subsurface drainage away from topographic saddles. As described in Chapter 5, Mitigation, a tailings deposition plan would be developed to limit the settlement of fine tailings near the embankments by controlling the location and duration of active spigots and alternating discharge locations (PLP 2019-RFI 006c).

During the failure modes effects analysis (FMEA), an identified concern was the potential for uneven deposition of tailings around the perimeter of the bulk TSF, caused by spigot spacing and segregation of thickened tailings, leading to smaller beaches and added seepage pressure on the embankments. As described in Appendix M1.0, Mitigation Assessment, deposition of tailings on ice in the winter (practiced at Red Dog Mine, Alaska) was discussed as a possible method to mitigate this effect (AECOM 2018k).

A grout curtain would be installed near the downstream toe of the south embankment to prevent upgradient groundwater from flowing into and beneath the impoundment (see Figure 2-8) (PLP 2018-RFI 008f). The grout curtain would be keyed into bedrock underlying the embankment before the placement of the embankment materials (bedrock conditions beneath the footprint are summarized below under "Stability-Related Elements"). Estimates of the depth and lateral extent of the grout curtain and the volume of grout required would be based on further analysis of bedrock hydraulic conductivity beneath the footprint, to be confirmed during detailed design and ongoing site investigation programs (see Chapter 5, Mitigation). A concrete plinth would be pre-constructed on top of the prepared bedrock surface to help create a seal between the grout curtain and liner; the grout curtain zone would be injected through pipe sleeves embedded along the plinth; and the upstream face liner (or low permeability core zone materials) would be tied to the plinth/grout curtain to create a continuous low permeability zone in the embankment. The actual grout curtain extent would be confirmed during construction, and grouting operations would continue until the bedrock would not accept additional grout (PLP 2018-RFI 006a; Knight Piésold 2018t).

The design freeboard of the bulk TSF would contain the entire volume of the inflow design flood (IDF) above the tailings beach. The freeboard would also account for wave run-up and wind set-up protection and post-seismic settlement (Knight Piésold 2018a; PLP 2018-RFI 019a, PLP 2018-RFI 028). Freeboard is further discussed in Section 4.16, Surface Water Hydrology. Water levels and freeboard in the bulk TSF pond would be maintained through proactive raise construction to account for the IDF in the elevation of the tailings beach (AECOM 2018k). Excess water would be controlled by pumping to the main TSF SCP or the main WMP (Knight Piésold 2018a).

Stability-Related Elements—The TSF embankment foundations would be prepared by removing overburden to expose competent bedrock before placement of the rockfill/earthfill material, as advocated by Morgenstern (2018). Should colluvium and/or talus surficial deposits be encountered beneath the structure footprints, which could result in downslope movement (described in Section 3.15, Geohazards and Seismic Concerns), they would be removed to avoid posing a stability issue for the embankments and/or liners.

Six geotechnical drillholes have been drilled to date beneath (or within about 100 feet of) the bulk TSF main embankment footprint and abutments, and five beneath the bulk TSF south footprint. Those beneath the main embankment encountered granodiorite, monzonite, and basalt rock types with depths to moderately weathered bedrock ranging from about 15 to 80 feet (see Figure 3.15-4). Drillholes beneath the south embankment footprint encountered rhyolite, porphyry, brecciated monzonite and basalt, sandstone, and mudstone with depths to moderately weathered bedrock ranging from 5 to 92 feet. Additional zones of weak rock were commonly encountered below these depths beneath both embankments, such as small faults or shear zones with gouge, zones of very poor rock quality designation[1] (RQD < 25%), occasional lost circulation while drilling, and rubble or highly fractured zones in the more competent rock mass (e.g., drillholes GH06-065, GH06-068, GH07-81, GH07-82, and GH08-148 in PLP 2019-RFI 014b).

Rock mass rating (RMR) values from the drillholes (see Section 3.15, Geohazards and Seismic Conditions) were used to develop rock strength parameters used in the stability analyses described later in this appendix (Table K4.15-5). Future geotechnical investigation programs would include additional investigation along the embankment alignments to further evaluate their location relative to faults and other weak zones (PLP 2019-RFI 014b) (Chapter 5, Mitigation).

As noted above, the bulk TSF main embankment under Alternative 1a, Alternative 1, and Alternative 3 would use centerline construction to reduce the footprint. The upstream portion of successive dam raises would partially rest on tailings, and additional buttresses would be provided downstream to enhance overall stability. Alternative 2 would use a downstream construction design, which is typically considered more stable than centerline construction. The results of the preliminary stability analyses for both the centerline and downstream alternatives are described below under “Static Stability Analysis.”

The bulk TSF embankments would be regulated as Class I (high) hazard potential dams as described in ADSP draft guidelines (ADNR 2017a), with an operating basis earthquake (OBE) and maximum design earthquake (MDE) established in accordance with criteria described in Section 4.15, Geohazards and Seismic Concerns and below under “Seismic Hazard Analysis.”

The main embankment’s internal filter zone would be thick enough to fulfill standard filter zone design criteria to prevent internal erosion and also remain intact after the MDE. The thickness of the filter zone must be wider than the maximum horizontal deformation that the embankment

[1] RQD is a rough indication of the degree of jointing and fracturing, measured as the total length of core pieces >4 inches long, divided by total length of the core run, and expressed as a percentage. RMR is based on a combination of RQD and data on compressive strength, groundwater conditions, and discontinuities.

would undergo as a result of the MDE. For example, assume the filter zone thickness is determined to be *X*, and the maximum horizontal deformation is calculated to be *Y.* In this case, the filter zone must be at least *X*+*Y* thick so that it would remain continuous and functional, with a thickness of at least *X* throughout the full height of the embankment after it has been sheared by the *Y* movement. The *X* and *Y* details would be conceptually developed after geotechnical programs are completed, the results analyzed, and dimensions finalized as design progresses.

Closure—The bulk TSF would be closed in place after Year 20 and would undergo dry closure and become a permanent landform (PLP 2018-RFI 024). Free water would be pumped out, and the tailings would be allowed to consolidate until they became suitable for equipment traffic. The permeable design of the main embankment would allow the tailings to continue to drain, thereby lowering the phreatic level and improving embankment stability. The tailings surface would be regraded to facilitate surface drainage away from the TSF. The stability benefits to a dry surface cover are summarized by Cobb (2019) as follows: "At the end of the operating life the risk is immediately reduced if the operational pond can be removed, resulting in a "dry" closure. After that, the risk is dependent on the nature of the design and the post-closure maintenance requirements." The bulk TSF post-closure maintenance requirements would be developed as part of the closure design and post-closure objectives.

The closure cover would consist of a low-permeability layer covering the tailings surface, constructed of either compacted overburden (glacial till) or a synthetic liner; an overlying capillary break layer composed of rockfill to promote horizontal drainage and minimize infiltration; topsoil and growth media placed over the capillary break; and revegetation (PLP 2020d; PLP 2018-RFI 091). Surface drainage controls, such as a sloping surface, and preferential pathways, such as small armored swales, would be used to convey runoff and reduce infiltration (PLP 2019-RFI 130).

PLP 2019-RFI 130 provides additional details on how the tailings surface would be prepared and trafficked during the transition from operations to closure, as well as a discussion of the trade-offs between the two options for the low permeability layer. Glacial till is available on site, does not require specialized equipment or crew to install, but has higher permeability (approximately 3 x 10^{-7} to 3x10^{-8} ft/s) than a synthetic liner. The liner option would provide a lower permeability barrier to infiltration (approximately 3x10^{-9} to 3x10^{-13} ft/s), though seepage could result from liner defects during installation and operation. The long-term lifespan of a geosynthetic liner is unclear due to these materials being relatively new, but it is expected to maintain performance for more than 100 years. With the addition of a soil cover that would protect against ultraviolet light, human, and animal damage, the lifespan is expected to be similar to that expected from lined tailings and other waste disposal facilities throughout North America. As described in Chapter 5, Mitigation, the selection of closure cover option, liner type, and thickness would be based on a trade-off study in final design (PLP 2019-RFI 130).

Infiltration rates through the closure cover could range from as low as 0 in/yr for a liner system to 15 in/yr for a compacted overburden cover, with the higher estimate representing about one-third of total precipitation. Preliminary seepage estimates through the main embankment are estimated to reduce from about 8 cfs on average at the end of operations to 0.5 to 1.2 cfs in post-closure, depending on cover design. Most of the reduction is expected in first phase of closure (once tailings slurry deposition stops, which contributes 48 cfs of flow into the TSF) and would continue to decrease as the pond is removed, surface regraded, cover installed, and terminal consolidation reached (PLP 2019-RFIs 006c; PLP 2019-RFI 130; Knight Piésold 2019o). Additional details regarding seepage estimates in post-closure are presented below under "Seepage Analysis."

BAT principles that promote long-term stability include achieving dilatant conditions throughout the tailings deposit by compaction (Morgenstern et al. 2015). The flow-through design would

promote long-term consolidation and safe post-closure management of the tailings. It is estimated that the freely draining tailings in the proposed flow-through design would reach a terminal consolidation of about 80 to 85 percent in post-closure.

As in operations, the saturation of the tailings mass is expected to vary spatially in post-closure due to grain size variability, ranging from coarse near the embankments to fine in the center. Tailings consolidation, limited infiltration, and long-term draining of the tailings are expected to reduce the level of saturation in the tailings mass in closure. Analysis of tailings properties would be completed in detailed design, and the properties monitored throughout operations. If required to achieve drainage and stability goals (maintaining a reduced phreatic surface and pore pressures at the embankments), alternative drainage-enhancing features would be considered, such as vertical or horizontal drains (PLP 2019-RFI 130).

Management and Monitoring—Monitoring would be included in all phases of the TSF, and would include the following elements (PLP 2017, 2019d; ADNR 2017a):

- Construction quality assurance (CQA) and construction quality control (CQC) plans to assure that the TSF embankments are built in accordance with the approved design, drawings, and specifications, as well as design modifications that might arise during construction as a result of differing site conditions.
- An emergency action plan (EAP) that includes a dam break analysis with inundation maps and describes actions to be taken in the event of dam failure, along with information and in-place preparations needed to take those actions immediately and without unnecessary delays.
- An operations and maintenance (O&M) manual describing procedures to be implemented under normal and extreme water levels; an operator training program; monitoring to confirm that embankments are performing in accordance with the design; periodic safety inspections; extraordinary inspections after extreme events (e.g., major earthquakes, large floods, vandalism); and mitigation to conduct repairs or structural modifications if the dam is not performing as designed.
- Monitoring after closure, including inspections for mass stability, seepage flows, and inspections after extreme events. Inspections and maintenance of the closure cover would be completed throughout post-closure (regardless of the design) to ensure that it continues to meet design criteria, or that maintenance issues such as cracking, erosion, or differential settlement are remediated. Monitoring would be conducted on a regular basis by onsite personnel, annually during formal dam safety inspections, and in response to specific events such as major earthquakes or storm events (PLP 2019-RFI 130).
- Post-closure monitoring and inspections would be funded through financial assurance mechanisms approved by ADNR and ADEC, which would be updated on a 5-year cycle (PLP 2019-RFI 115; SRK 2019d).

Comparison with Other Centerline-Constructed Dams—PLP (2019-RFI 008h) provides a summary of centerline dams that are currently operating globally and have some similarities to the bulk TSF main embankment. The response to Item #11 of RFI 008h (Table 1—Summary of Comparable Centerline Dams) provides a list of 10 mine sites with centerline tailings dams that are considered comparable to the planned bulk TSF main embankment. Eleven tailings dams in total are listed because two tailings dams are listed under Highland Valley Copper. However, as described below, only three of these dams are directly comparable to the planned bulk TSF main embankment from a structural perspective; three more are somewhat comparable; and the remaining five are not comparable.

- Three dams are directly comparable to the planned bulk TSF main embankment with regard to centerline construction (Constancia, Highland Valley H-H, and Continental). The Constancia dam is zoned rockfill with a vertical clay core and is higher than 328 feet. The 318-foot-high Highland Valley H-H Dam is an earthfill dam with a vertical core, random fill, and tailings placed upstream; and variable waste fill placed downstream. The 750-foot-high Continental dam is rockfill with a centerline-constructed segment. All three dams have configurations and materials similar to those planned for the bulk TSF main embankment, except that Constancia and Highland Valley H-H have vertical cores, so they are not "flow-through" dams. The engineered filter zones in the bulk TSF, consisting of graded sands and gravels, are expected to be more effective than the low-permeability core examples in lowering the phreatic surface in the embankment and promoting stability. The Continental dam has alluvium on its upstream face to prevent tailings migration into the dam, so it can be considered a partial flow-through dam. The Constancia and Highland Valley H-H dams are lower—and the Montana Resources dam is higher—than the planned bulk TSF main embankment. The dams are still being raised.
- Three of the 11 dams are described as "modified centerline" dams, or hybrids of centerline and upstream or downstream construction with rockfill raises (Alumbrera, Fort Knox, and Montana Tunnels dams). They are somewhat comparable to the planned bulk TSF main embankment configuration. The Alumbrera dam is described as a rockfill/earthfill dam; is projected to be 540 feet high; and has a free-draining starter dam. The Fort Knox dam is rockfill; is 350 feet high; and had planned centerline raises, but was raised as a downstream-to-centerline hybrid. The Montana Tunnels dam is rockfill; was permitted to 410 feet in 2008; and started downstream with raises closer to upstream than centerline.
- The remaining five of the 11 dams are being raised by using cyclone sand instead of rockfill, so they are not comparable to the planned bulk TSF main embankment (Brenda, Cerro Verde, Gibraltar, Highland Valley L-L, and Thompson Creek dams). These dams have rockfill or earthfill starter dams followed by cyclone sand raises, and actual or permitted heights ranging from 385 to 985 feet. In addition, the Gibraltar TSF was raised by the upstream method, not centerline. Several of these dams have reported sand boils or sinkholes, such as the Brenda TSF seepage and sand boils, Gibraltar dam sinkholes and internal erosion, and seepage and exit erosion from the sand fill toe at the Highmont part of Highland Valley dam. Regardless, these are not relevant to the planned bulk TSF main embankment that is not planned to be raised using cyclone sands.

Pyritic TSF

General—The pyritic TSF is planned to impound pyritic tailings, potentially acid-generating (PAG) waste rock, and metal-leaching (ML) materials in a co-disposal manner during operations. These impounded materials would be moved to the open pit at closure. This TSF would include a continuous embankment around the northern, eastern, and southern sides that have been named the north-, east-, and south embankments, respectively.

The general term "co-disposal" refers to the mixing of the fine and coarse waste streams. Other terminology is used in the mining industry to define the point at which the mixing occurs, or how the independent waste streams are placed. These are summarized as follows:

- **Co-placement—**Tailings and coarse waste rock material are transported independently, but not mixed to form a single discharge stream. Examples are waste rock end-dumped into a tailings facility, or waste rock used to create internal berms or

retaining walls of a tailings facility. The planned pyritic TSF is an example of co-placement, with waste rock placed as a ring around the inner perimeter of the TSF and tailings placed in the waste rock ring. Other examples worldwide include facilities at the Nunavik Nickel Mine in Quebec, Navachub Gold Mine in Namibia, and Neves Corvo Mine in Portugal, in which waste rock was used to construct perimeter embankments or interior dikes for tailings cells (Habte and Bocking 2017).

- **Co-deposition—**Very similar to co-placement, but the waste streams are generally placed in independent layers, allowing the deposited tailings to naturally enter the voids in the underlying rock. A further layer of rock is then added, and the process continues. An example is end-dumping of waste rock with subsequent tailings deposition down the rill face prior to further end-dumping (e.g., Pogo and Greens Creek mine dry stack TSFs in Alaska).
- **Co-mingling—**Tailings and coarse waste rock material are transported independently and mixed together (usually by mechanical means) in a waste storage facility or as a single discharge stream when pumped. The mixing promotes filling of the voids (mingling) to maximize the density of the material.

All of these forms of tailings and waste rock co-disposal are in common use globally. A summary of additional existing and planned co-disposal TSF operations is provided by Habte and Bocking (2017).

The pyritic TSF would consist of a continuous embankment around the north (downgradient) and east sides, and a separate embankment on the south (upgradient) side (Figure 2-4 and Figure 2-9). This facility would be designed to isolate the most contaminated tailings and waste rock in a fully lined, subaqueous storage cell during operations to minimize acid generation (PLP 2020d). The majority of the pyritic TSF would be located in a single tributary valley that drains north toward the NFK, referred to as the “NFK east site.” The southern portion of the pyritic TSF south embankment would be situated in a drainage divide between the NFK east watershed and a tributary that drains south toward the SFK River.

As with the bulk TSF, the embankments would be regulated as Class I (high) hazard potential dams under ADSP draft guidelines (ADNR 2017a). An OBE and MDE would be established similar to those described above for the bulk TSF.

Seepage-Related Elements—The pyritic TSF would be a fully lined facility using a high-density polyethylene (HDPE) geosynthetic membrane to retain water. Therefore, the facility would not include engineered filter zones as described for the bulk TSF main embankment (PLP 2018-RFI 055). SCPs with pumpback and groundwater monitoring wells would be situated downgradient of the north, east, and south embankments.

A bedding layer would be placed under the liner. The surface of the liner would be protected with processed materials (sand and gravel) after installation to prevent damage from equipment punctures or damage during placement of potentially acid-generating (PAG) waste rock material. Waste rock would be end-dumped in 20-foot lifts. Concern was expressed in the Environmental Impact Statement (EIS)-phase FMEA that this could result in liner damage even with a protective layer. Placing waste rock in smaller lifts was discussed as a possible method to minimize the risk of liner damage (AECOM 2018k).

Liner installation would be completed in accordance with manufacturer specifications, quality control and assurance guidelines, and standard industry practices for similar facilities, such as heap leach pads. Minimum material specifications would be provided, such as tensile strength and elongation at break; tear, puncture, and stress-crack resistance; and density requirements. Installation procedures would include directions for liner placement, seam welding, and inspection

and testing requirements. Installation would be closely monitored to confirm proper welding of the seams. Industry standards typically require visual inspections and continuity testing for all field seams or repairs. Inter-seam pressure (air testing) and testing using a vacuum box are considered acceptable methods of continuity testing. Strength and destructive testing are also typically undertaken during liner installations. The frequency and allowances of testing results are commonly outlined in a quality manual, which would be developed prior to installation (PLP 2018-RFI 019c; Knight Piésold 2018n).

The likelihood of liner leakage leading to internal erosion and potential failure of the embankment was the subject of failure modes in the EIS-phase FMEA (AECOM 2018l) as discussed in Section 4.27, Spills. Liner failure from chemical causes is considered unlikely because the pyritic tailings and PAG waste rock would be inundated throughout the mine life with a 5-foot water cover, which would limit the potential for the materials to be oxidized, turn acidic, and potentially react with the liner material. HDPE geomembranes are well understood to be extremely durable products with design service lives of up to several hundred years. The service life of an HDPE membrane is typically defined as its half-life, which is the point at which a 50 percent reduction in a specific design property is expected to occur (PLP 2018-RFI 055).

Referring to Figure 2-9, potentially acid generating (PAG) waste rock would be placed in a ring over the processed sand and gravel around the inside perimeter of the TSF. Pyritic tailings would be discharged into the TSF from sub-aqueous discharge points into the interior of the facility to minimize oxidation and potential acid generation, with deposition occurring concurrently with waste rock placement (PLP 2018-RFI 055). The tailings surface level would be maintained at all times below the waste rock surface level. Water cover on top of the both the tailings and waste rock would be maintained for the life of the facility. Water quality would be monitored during the operation to confirm that acidic conditions are not developing (PLP 2018-RFI 055). As with the bulk TSF, water levels and freeboard in the facility would be maintained to account for the IDF, wave run-up, and wind set-up. Excess water would be controlled by pumping to the main WMP (Knight Piésold 2018a; PLP 2018-RFI 019a; PLP 2018-RFI 028; PLP 2018-RFI 028a; PLP 2018-RFI 028b).

Stability-Related Elements—The embankment foundations would be prepared by removing overburden to competent bedrock, including colluvium and solifluction surficial deposits if encountered beneath the embankment footprint. These types of deposits have been mapped on the west and east sides of the watershed and could be subject to gradual downslope frost creep (described in Section 3.15, Geohazards and Seismic Conditions).

Twelve geotechnical drillholes have been drilled beneath or within several 100 feet of the pyritic TSF embankment footprint. These encountered primarily granodiorite and monzonite rock types, with heavily fractured siltstone and graywacke in the northeast area of the embankment, and breccia in the southeast corner of the embankment. Depths to moderately weathered bedrock were highly variable, ranging from less than 5 to 255 feet (Figure 3.15-4). Faults were mapped intersecting the east side of the embankment and were encountered in a drillhole along the northern edge of the embankment (GH08-189 in PLP 2019-RFI 014b). Other areas of potentially weak rock with very poor RQDs were documented in the drillhole logs.

Data from the drillholes were used to develop rock strength parameters used in the stability analyses (Table K4.15-5). As indicated in Chapter 5, Mitigation, future geotechnical programs would include additional investigation along the embankment alignments to further evaluate their location relative to faults and other weak zones, which would be incorporated into detailed stability analyses as design progresses (PLP 2019-RFI 014b).

In areas of the impoundment that do not lie directly on the embankment, some native soil would be excavated prior to the placement of liner bedding and installation of the liner; however, not all

overburden would be removed. The liner would be installed on the prepared slope and anchored at the top of the facility (PLP 2018-RFI 055). If placed all at one time, the upper part of the liner could be exposed to the elements for years as the impoundment is filled gradually during mine operations. While the lifetime of the exposed HDPE liner is expected to be greater than the life of the facility (Koerner et al. 2011), it could be subject to stretching from underlying frost creep and the weight of the liner over the long side slopes. Liner deformation is expected to be minimized by the placement of liner bedding and the placement of PAG waste rock fill on top of the liner, which would eventually buttress such movement.

Closure—At closure, the pyritic tailings and PAG waste would be placed into the open pit, the liner would be removed, and the facility would be reclaimed (PLP 2018-RFI 024). The pyritic tailings would be removed from the pyritic TSF as a slurry using floating dredge pumps during closure. Water in the TSF (supernatant pond, pore water, run-on, direct precipitation) would be used to re-slurry the tailings; additional water would be reclaimed from the pit for use in re-slurry activities as needed (PLP 2018-RFI 092). The tailings slurry would be pumped via pipeline to the open pit for long-term storage. The PAG waste rock material would be removed using conventional hauling methods (excavators and haul trucks) and trucked into the open pit via the pit haul ramps. It is expected that the start of waste rock removal would lag behind tailings removal by approximately 1 year to allow the tailings and supernatant pond level to be lowered to dewater the waste rock. The tailings would be deposited subaqueously into the open pit, and the PAG waste rock would be inundated to limit exposure to a maximum of approximately 1 year. A minimum water cover would be maintained above the PAG waste rock and pyritic tailings throughout long-term closure.

After closure, the embankments would be breached, flattened, and contoured/graded to conform to the surrounding landscape, and promote natural runoff and drainage. Therefore, potential impacts associated with static and seismic stability of this facility would last no longer than the 20-year mine life.

Management and Monitoring—Monitoring would be included in all phases of the TSF (PLP 2017, 2018d). In accordance with ADNR (2017a) guidelines, monitoring would include the same elements as described for the bulk TSF.

Water Management Ponds

General—Two WMPs would be at the mine site (see Figure 2-4 and Table K4.15-1): the main WMP north of the pyritic TSF, and the open pit WMP. Each of these facilities would require an embankment or berm with design considerations and potential geohazards effects similar to those described for the bulk TSF.

The size of the main WMP, comprising a 750- to 825-acre reservoir with 190-foot-high embankment, would be in line with the world's largest geomembrane-lined water storage facilities. The technology for designing, constructing, and operating similarly sized and lined facilities is well developed (Scuero et al. 2017a, b, c; Vaschetti et al. 2019; Carpi 2020). A comparable reservoir example is the Columbus Upground Reservoir in Ohio (EPI 2020), which is a pump-storage water facility 843 acres in size, approximately the same size as the planned main WMP area. The Columbus Upground Reservoir operates in a similar way as the main WMP; that is, water is pumped from a source (in this case, a nearby river), stored for future use, and released when needed (for city water supply). Other large geomembrane-lined reservoir examples include the 147-acre Panama Canal Expansion Water Savings Basin and the 97-acre Tampa Bay Reservoir in Florida. A comparable mine embankment example is the water retention and tailings storage facility at Las Bambas Mine in Peru that has a 443-foot-high geomembrane-lined embankment, and is planned to ultimately be 754 feet high. The first 134 feet of this embankment were used to

store water for mine start-up, and then the reservoir became a TSF. Other comparably high geomembrane-lined water reservoir embankments include the 182-foot concrete-type Filitranos Dam in Greece and 298-foot rockfill Runcu Dam in Romania.

A benefit of operating the main WMP as a flexible-sized water reservoir is advocated by the comments on the 2014 Mount Polley dam failure as follows:

- "An adequate water management plan did not exist… failed in its management of the water balance with respect to long term planning, including site integration, effective treatment, discharge plans and permits"; and,
- "There was no qualified individual responsible for the water balance, and [Mount Polley Mining Corporation] MPMC did not adequately characterize the risk of surplus supernatant water, which had been compounding since the mine reopened in 2005" (BCMOE 2015).

Seepage-Related Elements—WMP berms or embankments would be constructed using rock and earthen fill (PLP 2017, 2018d) and the same general approach as described for the bulk TSF. The embankments would be fully lined.

One issue identified during the FMEA was that the number of seepage pumpback wells currently proposed around the perimeter of the main WMP may be insufficient to identify and capture liner seepage along this 9,000-foot-long embankment. As indicated by PLP, the number of wells would be determined during final design based on additional field investigations and may exceed those proposed to date (PLP 2019-RFI 135). Deep continuous drains around the perimeter were also discussed as possible mitigation for intercepting potential seepage flow from the main WMP (AECOM 2018k). Additional discussion of WMP seepage flow and pumpback wells is provided in Section 4.17, Groundwater Hydrology.

Stability-Related Elements—The foundation materials at the WMPs would be prepared and the embankments designed and constructed to be stable under static and seismic conditions. The embankment foundation of the main WMP would be prepared by removing overburden to competent bedrock (design change by PLP based on the results of the October 2018 EIS-phase FMEA) (AECOM 2018k, 2018l; PLP 2018-RFI 101), and as advocated by Morgenstern (2018).

Eight geotechnical drillholes have been drilled beneath (or within a few hundred feet of) the main WMP embankment footprint. These encountered mostly gabbro (a type of basalt) and granodiorite, with depths to moderately weathered bedrock ranging from about 25 to 70 feet (see Figure 3.15-4). Additional zones of weak rock were encountered below these depths, such as sections of increased fracturing in the more competent rock mass and occasional lost circulation while drilling (e.g., drillhole GH07-101 in PLP 2019-RFI 014b).

The open pit WMP, which would be founded on overburden, was formerly located in an area with glacial lake deposits mapped at the surface. Since the DEIS was published, the location of the open pit WMP was moved to the west near the contact between glacial lake and glacial drift deposits and would rest mostly on the latter (Figure 3.13-2). Drillholes and test pits in the vicinity of the new location encountered mostly compact to very dense sand and gravel with some silt (PLP 2019-RFI 014b). Overburden extends to depths of about 70 to 90 feet in this area and overlies relatively competent granodiorite bedrock. The design concept for the open pit WMP embankment requires addressing any potential weak foundation conditions encountered in the overburden materials (e.g., clayey glacial lake deposits found in this area) by excavating that material.

Any potential mitigation requirements (including removal of overburden if required) would be addressed based on current and future geotechnical and hydrogeological information collected in the area. As indicated in Chapter 5, Mitigation, these would include additional investigation along

the embankment alignments to further evaluate their location relative to clays or weak bedrock zones, which would be incorporated into detailed stability analyses as design progresses (PLP 2019-RFI 014b).

Closure—The WMPs would be removed and reclaimed in post-closure when they are no longer required for water management and treatment (PLP 2018-RFI 024). Embankments and berms would be breached, flattened, and contoured/graded to conform to the surrounding landscape and promote natural runoff and drainage.

Therefore, the potential impacts of seepage and internal erosion on the static and seismic stability of these facilities would be long term, lasting until some point in post-closure after reclamation activities are complete and monitoring is no longer required; however, the potential impacts would not be permanent.

Management and Monitoring—Monitoring would be included in all phases of the WMPs (PLP 2017, 2018d), and would include the same elements as described for the bulk TSF.

Seepage Collection Ponds

General—SCPs would be located downstream of the TSF embankments and WMPs (see Figure 2-4 and Table K4.15-1). These include SCPs associated with the bulk TSF main and south embankments, and the pyritic TSF north, east, and south embankments. These facilities would require an embankment or berm with design considerations and potential seismic and geohazards effects similar to those described for the bulk TSF south embankment. The SCP embankments are proposed to be downstream-constructed as water retention reservoirs.

Seepage-Related Elements—The SCP embankments would use similar design features as the bulk TSF south embankment, including an upstream face liner (or low-permeability core zone) with filter and transition zones; grout curtains to control seepage and enhance embankment stability; and downstream groundwater pumpback and monitoring wells to pump groundwater back into the TSF and monitor the quality of the downstream groundwater (PLP 2018-RFI 006). The depth and lateral extent of the grout curtain and volume of grout required would be determined as described above for the bulk TSF south embankment.

Stability-Related Elements—As with the TSFs and WMPs, the foundation materials beneath the SCP embankments would be prepared and the embankments designed and constructed to be stable under static and seismic conditions. The bulk TSF main SCP would be founded on bedrock, and the other SCPs on overburden (Table K4.15-1). The bulk TSF main SCP would be located near the north end of tributary NK 1.190 between two north-facing hillslopes to take advantage of the geomorphic constriction and relatively shallow bedrock in the area upstream of where the tributary enters the wide part of NFK valley.

Six drillholes were advanced beneath (or within about 100 feet of) the footprint of the main SCP embankment. Depths to moderately weathered bedrock at these locations range from 4 to 86 feet, and the bedrock consists of basalt (gabbro) and volcaniclastic breccia.

Closure—The SCPs associated with the pyritic TSF would be removed and reclaimed in post-closure, similar to the description of the WMPs (PLP 2018-RFI 024). Therefore, potential impacts of seepage and internal erosion on the static and seismic stability of these facilities would be long term, lasting until some point in post-closure after reclamation activities are complete and monitoring is no longer required; however, the potential impacts would not be permanent.

The SCPs associated with the bulk TSF would remain in post-closure indefinitely, or until no longer required for water management and treatment. It is expected that seepage flow through the bulk TSF embankment would slow with increasing consolidation and reduced infiltration in

closure. A preliminary estimate of the maximum consolidation of the bulk tailings is on the order of 50 years (AECOM 2018k). However, there are no current plans to remove the bulk TSF SCPs. Therefore, potential impacts associated with the seepage and stability of these facilities would range from long term to permanent.

An analysis of the time it would take for the bulk TSF main SCP to fill to the point of overflow in the event that the reclaim pipeline ruptured in an earthquake (or other reason such as pump failure or corrosion) is provided in PLP 2019-RFI 130. Based on a combination of SCP inflow from both TSF seepage and precipitation ranging from dry to wet conditions (4 to 13 cfs), and a range of starting water levels (pond capacities) from an empty pond to the maximum operating level, the amount of storage time remaining before overflow occurs ranges from about 3 weeks to 15 months. The low end of this estimate represents an earthquake-caused rupture occurring during a relatively wet season when the pond is already at its maximum operating level. While this combination of conditions may be unlikely, it could plausibly occur sometime during the post-closure period. As described in Chapter 5, Mitigation, personnel and redundant equipment would be maintained onsite throughout post-closure, so that repairs could be conducted as needed (PLP 2019-RFI 130).

Management and Monitoring—Monitoring would be included in all phases of the WMPs (PLP 2017), and would include the same elements as described for the bulk TSF.

K4.15.1.4 Seepage Analysis

Preliminary seepage analyses were completed to support the design of the bulk TSF, which as noted above (see Section K4.15.1.3) would include a flow-through design with engineered filter zones to control seepage and internal erosion. The results of the preliminary analyses are presented below.

The pyritic TSF and main WMP would be fully lined facilities, and the requirements for engineered filter zones for these lined structures would be evaluated during the design process.

Bulk TSF

Methods and Input Parameters—The rate of seepage through the bulk TSF main embankment was estimated by Knight Piésold (2018t, 2019o) and PLP (PLP 2018-RFI 006; PLP 2018-RFI 006a; PLP 2019-RFI 006b; PLP 2019-RFI 006c) using a two-dimensional seepage model that incorporated conceptual project design assumptions and referenced available seepage rates at existing mine facilities with similar flow-through designs. The purpose of the seepage analysis was to conduct a preliminary analysis of seepage flow to provide a range of flow estimates for input into the site-wide water balance model (discussed in Section 4.16, Surface Water Hydrology). It was not intended to be used to predict phreatic surfaces for use in stability models, or for predicting the migration of contact groundwater. Phreatic surfaces evaluated in stability modeling are discussed below under “Stability Analysis”; a more comprehensive three-dimensional model was developed to predict groundwater flow and the migration of contact water away from the bulk TSF as described in Section 4.17, Groundwater Hydrology.

The preliminary seepage analysis was completed using the publicly available numerical modeling software SEEP/W (Geoslope 2019). The steady state analysis was conducted using sections representing the maximum configuration of the bulk TSF at the end of operations and post-closure. The model output provided a unit rate of seepage per foot of distance along the embankments, which was then multiplied by the characteristic length of dam through which the same seepage rate would apply, assumed to be two-thirds of the total length of each dam.

Input parameters to the model included hydraulic conductivity (K) of tailings and bedrock, recharge to the exposed tailings surface, anisotropy of the tailings (ratio of vertical to lateral K), length of segregated tailings units, length of the bulk TSF embankments, location of the supernatant pond with respect to the main embankment, cover type in post-closure, and presence or absence of a seasonal pond in post-closure. Recharge values that were increased by nearly 300 percent over the base case in the sensitivity analysis, as well as a pond size increase by 1,500 feet closer to the dam, effectively demonstrate the potential influence of increased precipitation due to climate change on seepage flow through the embankment. K values and anisotropies were assumed for three tailings units (coarse, transition, and fines/slimes) based on values in the literature (Vick 1990) and preliminary grain size analyses of grind establishment test work conducted on ore samples from the pit (Figure K4.15-2), which show that tailings are predicted to range from medium sand- to clay-sized particles depending on grind size. The assumed distribution of tailings units in the seepage model is shown in Figure K4.15-3. Uncertainties regarding the ability of the thickened tailings to segregate into these units are discussed below under “Stability Analysis.”

The rockfill and earthfill zones in the embankments, including the engineered filter zones, were not assigned any material properties that would restrict flow. It was assumed in the model that the main embankment would be free-draining and not impede seepage flow, and that seepage flow would be controlled by the lower K tailings mass. The effect of this assumption was evaluated by comparing models that did and did not include the embankment as a material zone, which resulted in less than a 5 percent difference between seepage flow estimates.

Input parameters to seepage models can affect seepage rates by orders of magnitude. The model was run as an initial case, considered the best estimate of input parameters, as well as several sensitivity scenarios to evaluate the effect of uncertainties in input parameters and heterogeneities expected in the tailings mass. The range of input parameters is listed in Table K4.15-4. The selection of certain parameter values (such as K) were on the higher side of observed field data in order to conservatively estimate the amount of seepage flow that would require management. It is unclear if ranges in parameters or boundary conditions due to seasonal effects were considered in the model (other than the seasonal pond in post-closure). Recommendations are provided in Appendix M1.0, Mitigation Assessment, to consider such effects in future detailed design analysis.

Boundary conditions in the model included a constant head boundary on top of tailings in the area of the supernatant pond; recharge rates assigned to the exposed tailings beach; seepage face boundaries along the lower perimeter of the embankments; a no-flow boundary at the upstream face of the south embankment (representing a geosynthetic liner and grout curtain); and seepage face and constant head boundaries at the ground surface downstream of each embankment. In post-closure, a constant head boundary was assigned to a seasonal pond and the top of the tailings, with a recharge rate that varied depending on closure cover type (compacted overburden or synthetic liner).

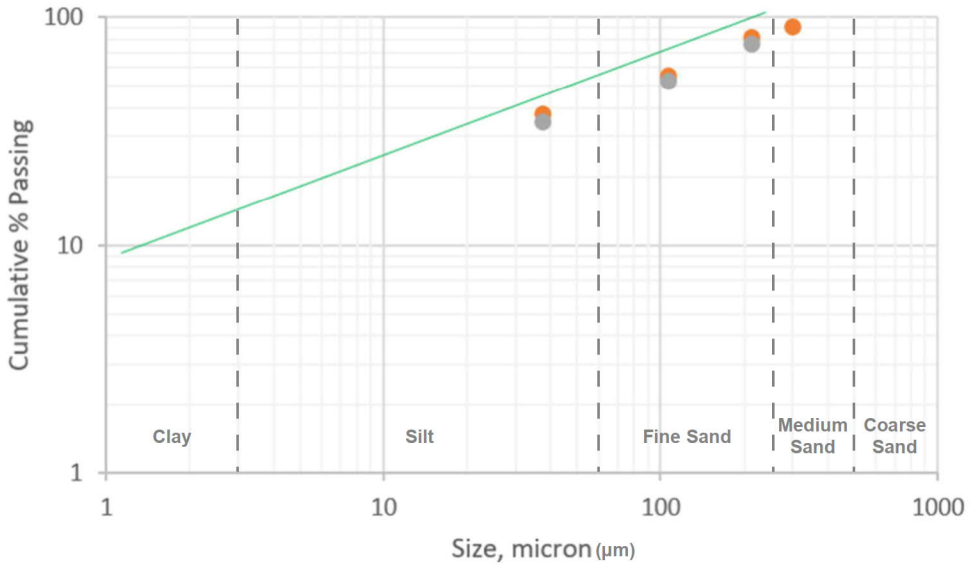

Source: PLP 2019-RFI006c

Tailings Particle Size Distribution from Grind Establishment Testwork

Sample Results for Ore Grind of D80 = 180 µm

Expected Distribution for Finer Grind where D80 = 135 µm

Notes:
1. D80 = diameter at which 80% of sample mass is less than this value
2. 1 micron or µm = 0.001 mm

US Army Corps of Engineers®

TAILINGS GRAIN SIZE DISTRIBUTION

PEBBLE PROJECT EIS

FIGURE K4.15-2

Table K4.15-4: Bulk TSF Preliminary Seepage Analysis Input Parameters and Results

Mine Phase	Parameter Changed in Sensitivity Analysis		Parameter Range for Sensitivity Analyses			Seepage Results (cfs)		
			Reduced Value	Initial Case Value	Increased Value	Minimum	Initial Case	Maximum
Main Embankment[1]								
End of Operations	Normal Operating Conditions—Pond 2,000 ft from Dam	K^2 of Coarse Tailings	x 0.1	$6.6x10^{-6}$ ft/s	x 10	4.0	5.2	5.3
		K of Transition Tailings	x 0.1	$6.6x10^{-7}$ ft/s	x 10	5.2		7.8
		K of Fine Tailings/Slimes	x 0.1	$6.6x10^{-8}$ ft/s	x 10	5.2		5.3
		Anisotropy of Coarse Tailings (K_v/K_h)	0.1	1	-	4.6		-
		K of Shallow Bedrock and Bedrock[3]	x 0.1	$3.3x10^{-6}$ ft/s	-	5.0		-
		Recharge on Tailings Beach[4]	75 in/yr	110 in/yr	300 in/yr	3.6		13.2
		Length of Coarse Tailings Unit	1,000 ft	1,800 ft	3,600 ft	3.7		7.8
	Pond 500 ft from Dam	Anisotropy of Coarse Tailings (K_v/K_h)	0.1	-	1	4.6	-	18.2
Post-Closure	Seasonal Pond[5]	Recharge[6]	0 in/yr	-	15 in/yr	0.5	-	1.2
	No Seasonal Pond		3 ft/yr	-	15 in/yr	0.3	-	1.1
South Embankment[1]								
Post-Closure	Seasonal Pond[5]	Recharge[6]	0 ft/yr	-	15 in/yr	0.2	-	0.6
	No Seasonal Pond		3 ft/yr	-	15 in/yr	0.1	-	0.5

Notes:
[1]The characteristic length of the embankments (assumed to be two-thirds of total length) is 8,770 feet for the main embankment and 3,067 feet for the south embankment. These were used to derive seepage volume estimates by multiplying the two-dimension model result (per 1 foot unit along the embankment) by the characteristic length.
[2]K = hydraulic conductivity.
[3]Shallow bedrock is assumed to be 50 feet thick. K for shallow bedrock is $6.6x10^{-6}$ ft/s and for deep bedrock is $6.6x10^{-7}$ ft/s. Initial case value represents the average of K for shallow bedrock and deep bedrock, or a case where shallow bedrock is removed from beneath the embankments and deep bedrock K is one-half an order of magnitude higher.
[4]The range of recharge of the tailings beach in operations is equivalent to 7% to 30% of total water spigotted in with the tailings slurry (48 cfs) and reflects the relatively wide uncertainty associated with this value.
[5]Seasonal pond assumed to be 3,000 feet from the dams in post-closure.
[6]Range of recharge in post-closure encompasses both a synthetic cover type (0 ft/yr) and compacted overburden cover (15 ft/yr).
cfs = cubic feet per second ft = foot/feet ft/s = foot per second
ft/yr = foot per year in/yr = inches per year
Source: Knight Piésold 2019o, PLP 2019-RFI 006b, PLP 2019-RFI 006c

Preliminary Seepage Analysis Results—The results of the sensitivity analyses for the main embankment at the end of operations showed that seepage flow is most sensitive to recharge on the tailings beach, the distance of the pond from the dams, and isotropy of the coarse tailings unit. It is less sensitive to changes in tailings and bedrock K values. Overall sensitivity results ranged from 3.6 to 18 cfs at the end of operations through the main embankment. Based on the likelihood that the tailings would be anisotropic, Knight Piésold (2019o) selected a range of 3.5 to 5.5 cfs as a best estimate for use in the site-wide water balance model.

In post-closure, the preliminary seepage rates were estimated to range from 0.3 to 1.2 cfs through the main embankment, and 0.1 to 0.6 cfs through the south embankments, depending on closure cover type. The post-closure results were less sensitive to the presence or absence of a seasonal pond.

While the model was not intended to be used to predict phreatic surfaces for use in embankment stability modeling, it can provide useful information about these, subject to conceptual-level boundary conditions and input assumptions. As indicated on Figure K4.15-3, the phreatic surface next to the main embankment is expected to vary in operations with the history of spigotting in the area, as well as the success of tailings segregation. A well-graded, non-segregated, low-permeability, thickened tailings deposit could result in significantly different predictions about seepage performance. For example, a reduction in the K value of the coarse tailings by an order of magnitude, and reduction in the length of this unit by 800 feet, resulted in 30 to 40 percent lower seepage rates compared to the initial case (Table K4.15-4), with potentially related increases in phreatic surface elevations.

As described in PLP 2019-RFI 008h and below under “Stability Analysis,” operational practices that would be employed to maintain the desired width of the tailings beach and keep the pond away from the dams would include varying the tailings discharge locations, resulting in a phreatic surface elevation that could vary along the length of the embankment at any given time. The seepage model also shows how the phreatic surface is expected to decline in early closure after the end of spigotting (PLP 2019-RFI 006b).

Detailed seepage analyses would be completed for each embankment during the preliminary and detailed design stages (PLP 2018-RFI 006). Refined seepage analyses in the preliminary and detailed designs would consider tailings grain size distribution based on additional test work and the plan for discharging tailings into the impoundment (e.g., spacing of spigots, time to discharge from each point) when estimating representative values for the modeled tailings deposit. Future analyses for the preliminary and detailed designs would consider a range of values for permeability, anisotropy, and unit length to assess a plausible range of flow conditions that could exist (PLP 2019-RFI 006c).

K4.15.1.5 Stability Analysis

Structural integrity is the most important priority in the design and management of tailings facilities (van Zyl 2015). As described above, all embankments and impoundments in the mine site area would store water or potentially liquid-behaving contents that could pose a risk to the environment if released. The mine site facilities were designed to be stable during both static (non-seismic) and seismic conditions, which are addressed in the following subsections.

Preliminary Static Stability Analysis

Input Parameters—The preliminary analyses of static slope stability considered conceptual-level embankment configurations and homogeneous material parameters. Table K4.15-5 presents the geotechnical values assumed for these analyses.

MAIN EMBANKMENT SECTION - MATERIAL LAYOUT:

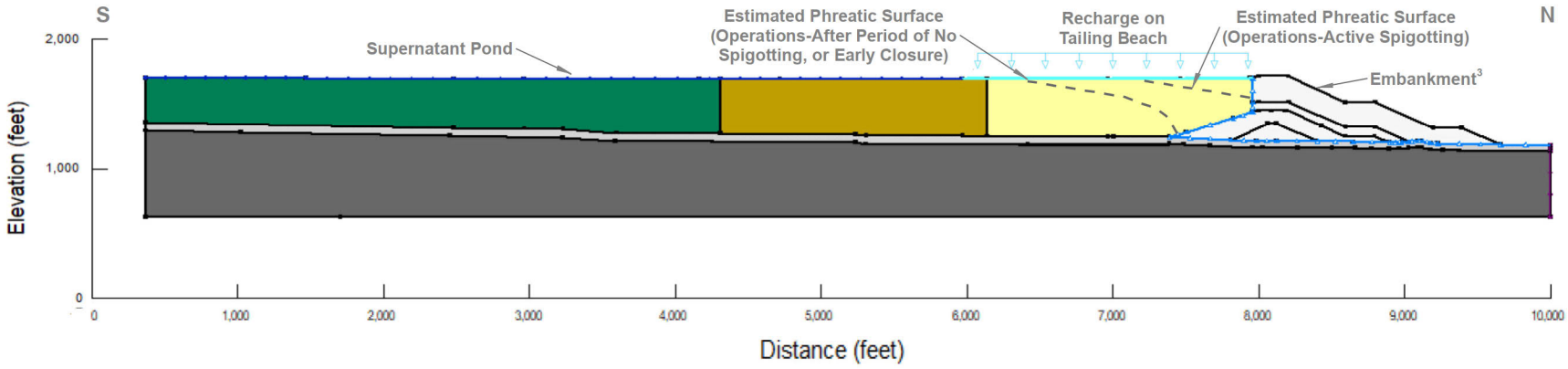

SOUTH EMBANKMENT SECTION - MATERIAL LAYOUT:

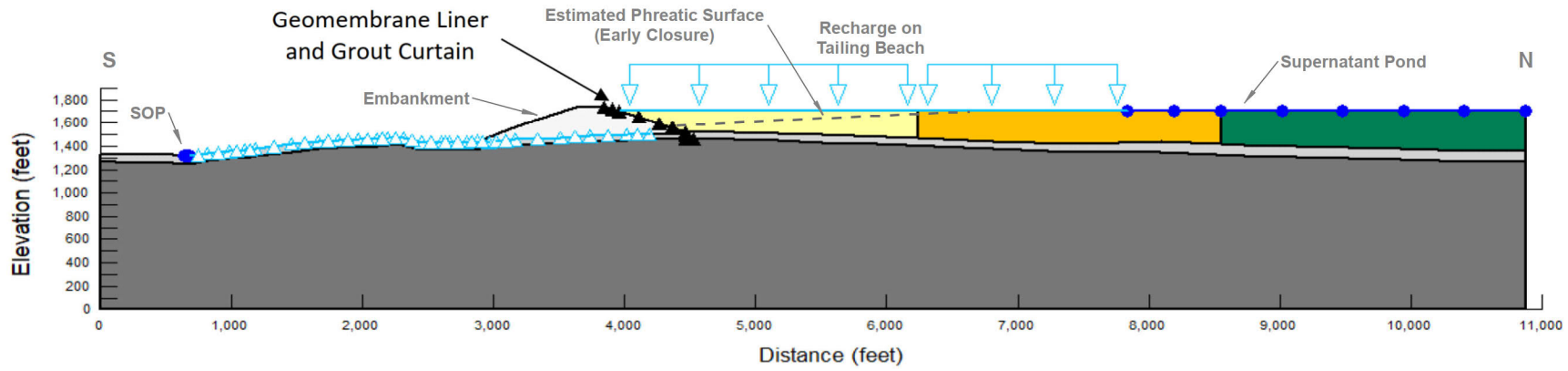

Source: KP 2019o; PLP 2019-RFI006b, c

Boundary Conditions Assigned to Model:

- Recharge on Exposed Tailings
- Constant Head to Top of Tailings in Area of Pond
- Seepage Face and Constant Head Representing Drainage Downstream of Embankments

Notes:
1. Sections represent end of operations and early closure.
2. The embankments were not specified as material zones in the model.
3. Phreatic surfaces are results of model simulations and vary with model parameters in sensitivity analyses.
4. Ability of tailings to segregate into units shown and reduce phreatic surface is uncertain, and would be further analyzed in detailed design.

Legend
- Coarse Tailings
- Transition Tailings
- Fine Tailings
- Shallow Bedrock
- Bedrock

US Army Corps of Engineers®

BULK TSF SEEPAGE MODEL

PEBBLE PROJECT EIS

FIGURE K4.15-3

Table K4.15-5: Geotechnical Material Parameters Used in Preliminary Stability Analyses

Embankment	Material	Unit Weight[1] (pcf)	Strength Function[2]	Tau/Sigma Ratio[3]	Cohesion (psf)	Phi[4] (°)
Bulk TSF Main Embankment	Bedrock	160	N/A	N/A	0	40
	Tailings	90	N/A	0.25	N/A	N/A
	Rockfill	145	Low-density, poorly graded, weak particles	N/A	N/A	N/A
Bulk TSF South Embankment	Bedrock	160	N/A	N/A	0	40
	Tailings	90	N/A	0.25	N/A	N/A
	Rockfill	145	Low-density, poorly graded, weak particles	N/A	N/A	N/A
Pyritic TSF Main Embankment	Bedrock	160	N/A	N/A	0	40
	Tailings	100	N/A	0.25	N/A	N/A
	Rockfill	145	Low-density, poorly graded, weak particles	N/A	N/A	N/A
Main Water Management Pond	Overburden[5]	120	N/A	N/A	0	35
	Bedrock	160	N/A	N/A	0	40
	Rockfill	145	Low-density, poorly graded, weak particles	N/A	N/A	N/A
Open Pit Water Management Pond	Overburden[5]	120	N/A	N/A	0	35
	Rockfill	145	Low-density, poorly graded, weak particles	N/A	N/A	N/A
Bulk TSF Main SCP	Bedrock	160	N/A	N/A	0	40
	Rockfill	145	Low-density, poorly graded, weak particles	N/A	N/A	N/A

Notes:
° = degrees
N/A = Not Applicable
pcf = pounds per cubic foot
psf = pounds per square foot
SCP = seepage collection pond
TSF = tailings pond facility

[1] The basis for the selection of the densities for bulk tailings, pyritic tailings, rockfill, and bedrock was the results of geotechnical laboratory testing performed in conjunction with previous field studies.

[2] Shear strength for rockfill was defined based on Leps (1970), using a function that defines the variation of shear strength with normal stress, rather than using a single friction angle or cohesion value.

a. Rockfill shear strength typically reduces at higher stresses because of the crushing of particle contact points in the material and a reduction in material dilatancy. Rockfill shear strength is also related to the density and durability of the material and the particle size distribution.

b. A lower-bound strength function (representative of low-density, poorly graded, weak particle rockfill) was considered. The lower-bound strength function was based on published information on the shear strength properties of rockfill materials.

[3] The basis for selection of the tau/sigma ratio of 0.25 for tailings was the peak undrained strength ratio (Su/p') for hard rock fine-grained tailings materials, which is typically in the range of 0.2 to 0.3. A value of 0.25 was assumed for the preliminary stability analyses.

[4] The basis for the selection of the phi angles for bedrock was the results of past geotechnical drillhole investigations, which indicate that the bedrock underlying the bulk TSF area comprises Cretaceous sedimentary and volcanic rocks, including mudstone, siltstone conglomerate, sandstone, and basalt; and Cretaceous intrusive rocks comprised of monzonite, diorite, and gabbro.

a. Bedrock was defined as a homogeneous geological unit for the stability analyses.

b. A friction angle of 40 degrees was used in the stability analyses based on the findings of past geotechnical drillhole investigations.

[5] The basis for the selection of overburden values included typical unit weight values for silty sands and gravels, and mine site geotechnical drillhole data for the phi angle.

Source: PLP 2018-RFI 008a; PLP 2018-RFI 008b; PLP 2019-RFI 008i; PLP 2019-RFI 008j, PLP 2019-RFI 014b

For the purposes of the preliminary stability analyses, bedrock was defined as a homogeneous unit, with RMR values used to develop shear/normal strength functions for use in the analyses of embankments founded on bedrock. For embankments founded on overburden, parameter values were derived from both drillhole data and typical values for silty sands and gravels, which appear reasonable based on values in the literature (Geotechdata 2013). Future geotechnical investigation programs would include additional investigation along the embankment alignments to confirm or update these values, and further evaluate deep-seated slide risks to the alignments relative to faults and other weak zones. The results would be included in future stability analyses to be conducted for the preliminary and detailed design phases and through the State of Alaska permitting process (PLP 2019-RFI 008g, PLP 2019-RFI 014b) (Chapter 5, Mitigation).

The preliminary stability analyses were completed for embankment configurations under static loading conditions using the assumptions presented in Table K4.15-5 and the limit equilibrium computer program SLOPE/W to model potential slip surfaces and resulting factor of safety (FoS) values. Cross-sections were generated showing critical circles and calculated FoS for the major mine site embankments as described below.

Bulk TSF Main Embankment—The bulk TSF main embankment is proposed to operate as a drained facility to promote long-term drainage and stability of the bulk tailings mass. The main embankment would be approximately 530 feet high, with an overall downstream slope of approximately 2.6:1 horizontal:vertical (H:V). Under Alternative 1a and Alternative 1 and Alternative 3, centerline construction methods with buttressing would be used to limit the footprint and enhance stability, which would result in a serrated near-vertical upstream face at the dam crest for the upper 280 feet of the embankment (see Figure 2-8). The preliminary stability analysis for this design calculated an FoS value on the order of 1.9 to 2.0 under static loading conditions. Figure K4.15-4 shows a schematic section of the main embankment at its ultimate height with the predicted potential slip surface.

The stability of the conceptual buttressed centerline design was reviewed by geotechnical and tailings subject matter experts (SMEs) from the US Army Corps of Engineers (USACE) EIS team (AECOM), the State of Alaska, and Pebble Limited Partnership (PLP) (including its geotechnical contractor, Knight Piésold) during the EIS-phase FMEA in October 2018. Failure mode reviews were based on the recognized potential that embankment design concepts would be refined over time and that industry standard-of-care would be followed in design and construction. Participants discussed that although the upstream portion of successive dam raises in the upper half of the embankment would partially rest on tailings, the results of initial stability analysis do not rely on the strength of these materials; rather, they rely on the strength of the rockfill materials directly beneath and downstream of successive raises, materials in the engineered filter zones, and rockfill buttressing the downstream side of the filter zones. In other words, regardless of the strength of the tailings, the overall embankment did not fail in a downstream direction in the stability analysis. The potential for instability on the upstream side of the raises would be buttressed by the tailings mass, in such a manner that an unstable condition would likely occur only in an upstream direction (toward the tailings deposit) along an isolated slip surface restricted to the last raise/lift, which would not overwhelm freeboard (designed to be contained in the elevation of the tailings beach). Therefore, the SMEs concluded that the likelihood of global instability of the buttressed centerline embankment design would be very low (probability less than 1 in 10,000) (AECOM 2018k, 2018l). Additional stability analysis of the embankment in the event of liquefaction of the tailings in an earthquake is discussed below under “Post-Liquefaction Analysis.”

There are three areas of uncertainty with respect to embankment static stability at the present level of design: 1) the extent that the thickened tailings would segregate to promote a deeper phreatic surface near the embankment; 2) the extent that pore pressures in the newly placed,

potentially soft and loose tailings would reduce sufficiently to provide a stable upstream slope of the first raise; and 3) how to schedule and construct the first raise with its upstream part over tailings placed in less than 2 years (estimated time for starter dam to fill to capacity). These uncertainties need to be resolved during the final design process and early during the first year of operations to avoid the potential of a possible deeper failure surface up to the depth of the lowest centerline raise, resulting in the possibility that more of the centerline part of the embankment below just the most recent raise could slide into potentially undrained tailings, setting the mass in motion with adverse consequential effects on the TSF in a downstream direction.

The uncertainty of building part of the first centerline raise with its upstream part near a significant height of tailings placed in less than 2 years is related to the need to have the first centerline raise in place before the tailings beach reaches the starter dam's design freeboard elevation. The starter dam is planned to have a maximum height of 265 feet, so its upstream face would have a maximum height on the order of 200 feet, and the starter dam is planned to store the first two years' of tailings. This means that tailings geotechnical investigations consisting of field explorations and laboratory testing to address the first two uncertainties described above, plus the raise design using the geotechnical results, embankment seepage and stability analyses, tailings liquefaction potential analyses, certificate of approval to construct the raise, raise construction and completion report, and certificate of approval to operate with the first raise in place, all need to be completed within 2 years of the start of tailings deposition.

The technical key to addressing these three uncertainties is to obtain geotechnical characteristics of the tailings, which can only be accomplished after tailings deposition has begun and actual deposited tailings become available for geotechnical investigations and raise design, including seepage, stability, consolidation, and liquefaction analyses. Initial geotechnical investigation results obtained in the first year of operations are needed to provide data on the extent of segregation that is being achieved, pore pressures within the tailings, consolidation rates of the tailings, and depth of the phreatic surface in the tailings and embankment. These geotechnical data can then be used in analyses to provide stable and safe centerline raises, starting with the first raise above the starter dam and initial deposited tailings. Chapter 5, Mitigation, describes some of the additional geotechnical investigation and engineering design work that would be completed during the preliminary and detailed design work, including additional seepage, stability, and liquefaction analyses. Additional recommendations for tailings geotechnical investigation and stability analyses are provided in Appendix M1.0, Mitigation Assessment. The scope of additional work would be specified in an initial design package after the EIS is complete (PLP 2019-RFI 008g).

Under Alternative 2, the main embankment would be downstream-constructed, and would also include downstream buttresses to increase the stability. The preliminary stability analysis for the downstream-constructed main embankment calculated an FoS value on the order of 1.9 to 2.0 under static loading conditions, similar to the buttressed centerline design, thereby offering minimal additional stability over the proposed design. Figure 2-66 shows a schematic section of the main embankment under Alternative 2 at its ultimate height with the predicted potential slip surface. Some of the uncertainties discussed above for the modified centerline construction would also apply to the downstream alternative. In particular, the uncertainty regarding whether tailings would sufficiently segregate near the embankment crest, potentially leading to a high phreatic surface near the dam, could also reduce the stability of the downstream-constructed embankment.

It is noted that although the embankment FoS values are adequate for the current conceptual levels of design, acceptably reliable FoS values for preliminary and detailed design and final construction package purposes would be more accurately evaluated during the advanced preliminary and detailed stages of the designs based on additional geotechnical investigation of

tailings and the embankment fill characteristics. The current conceptual-level design FoS values are considered adequate for determining low probabilities of instability; for comparing different types of embankments such as downstream and centerline; and for PLP project planning.

The reduction in seepage flow that would occur during closure is expected to enhance the long-term stability of the main embankment. This would be achieved through removing the pond, promoting runoff, limiting infiltration, tailings consolidation, and ensuring long-term internal drainage. As described above, most of the seepage reduction is expected in the first phase of closure once tailings slurry deposition stops; it would continue to decrease as the pond is removed, the surface is regraded, the cover is installed, and terminal consolidation achieved (PLP 2019-RFI 006c, PLP 2019-RFI 130; Knight Piésold 2019o). The saturation of the tailings mass in the post-closure phase is expected to vary spatially depending on tailings grain size, distribution, and anisotropy. Analysis of the tailings properties throughout closure would be completed during the closure preliminary and detailed designs, based on monitoring during the TSF operations. As described in Chapter 5, Mitigation, if required to achieve drainage and stability goals (i.e., maintaining reduced phreatic surface and pore pressures at the embankment), alternative drainage-enhancing features would be considered, such as vertical or horizontal drains (PLP 2019-RFI 130).

Bulk TSF South Embankment—The bulk TSF south embankment would be downstream constructed with a fully lined downstream dam face. The conceptual south embankment would be approximately 305 feet high, with an overall downstream slope of approximately 2.6H:1V (PLP 2018-RFI 008b). Figure K4.15-5 shows a schematic section of the current concept for the south embankment at its ultimate height with the predicted potential slip surface. The preliminary stability analyses for the south embankment calculated an FoS value on the order of 1.9 to 2.0 under static loading conditions.

Pyritic TSF North Embankment—The pyritic TSF is proposed to be a fully lined facility. The north, south, and east embankments would be approximately 335, 225, and 215 feet high, respectively; with overall downstream slopes of approximately 2.6H:1V, and upstream slopes of 3H:1V (Figure 2-9). The stability of the upstream slopes would be enhanced by placement of PAG waste rock. Figure K4.15-6 shows a schematic section of the north embankment of the pyritic TSF at its ultimate height with the predicted potential slip surface. The preliminary stability analyses calculated an FoS value on the order of 1.9 to 2.0 under static loading conditions. Based on this conceptual design, the EIS-phase FMEA panel concluded that the likelihood of global instability of the north and south embankments of the pyritic TSF would be very low (probability less than 1 in 10,000) (AECOM 2018l).

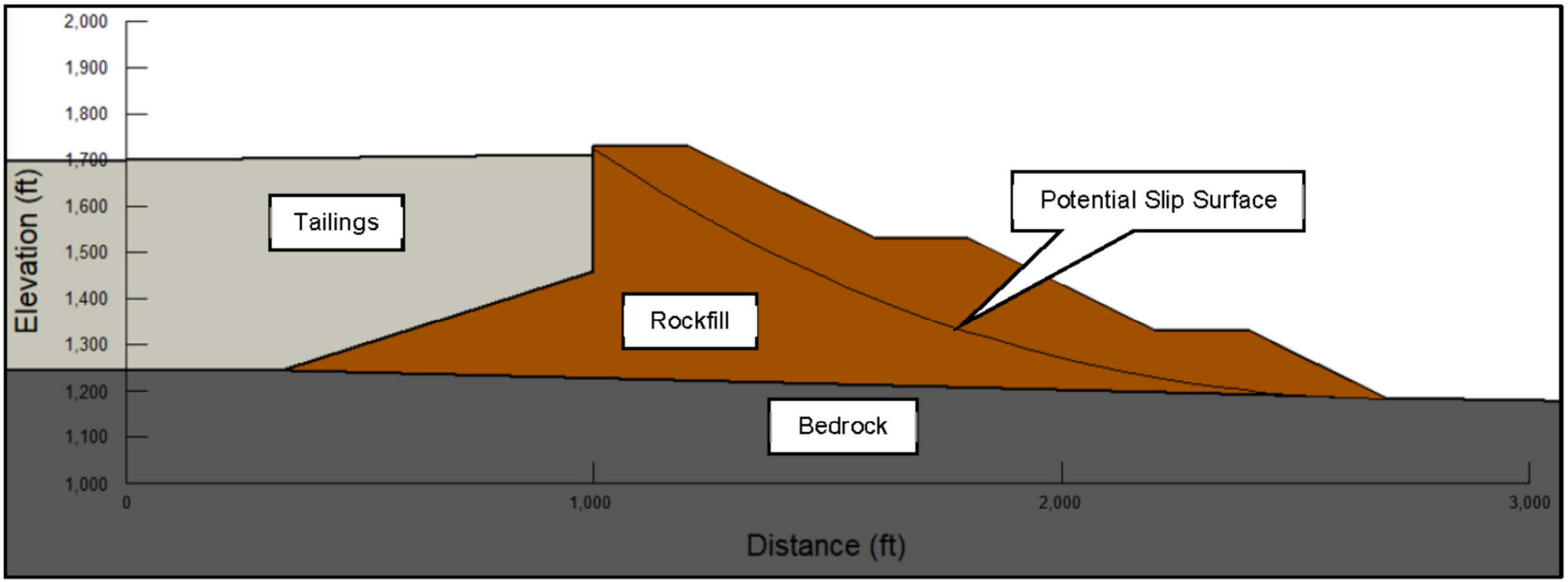

Source: PLP (2018-RFI 008); SRK (2018c), Figure 3

US Army Corps of Engineers®

BULK TSF MAIN EMBANKMENT STATIC STABILITY ANALYSIS - BUTTRESSED CENTERLINE CONSTRUCTION

PEBBLE PROJECT EIS

FIGURE K4.15-4

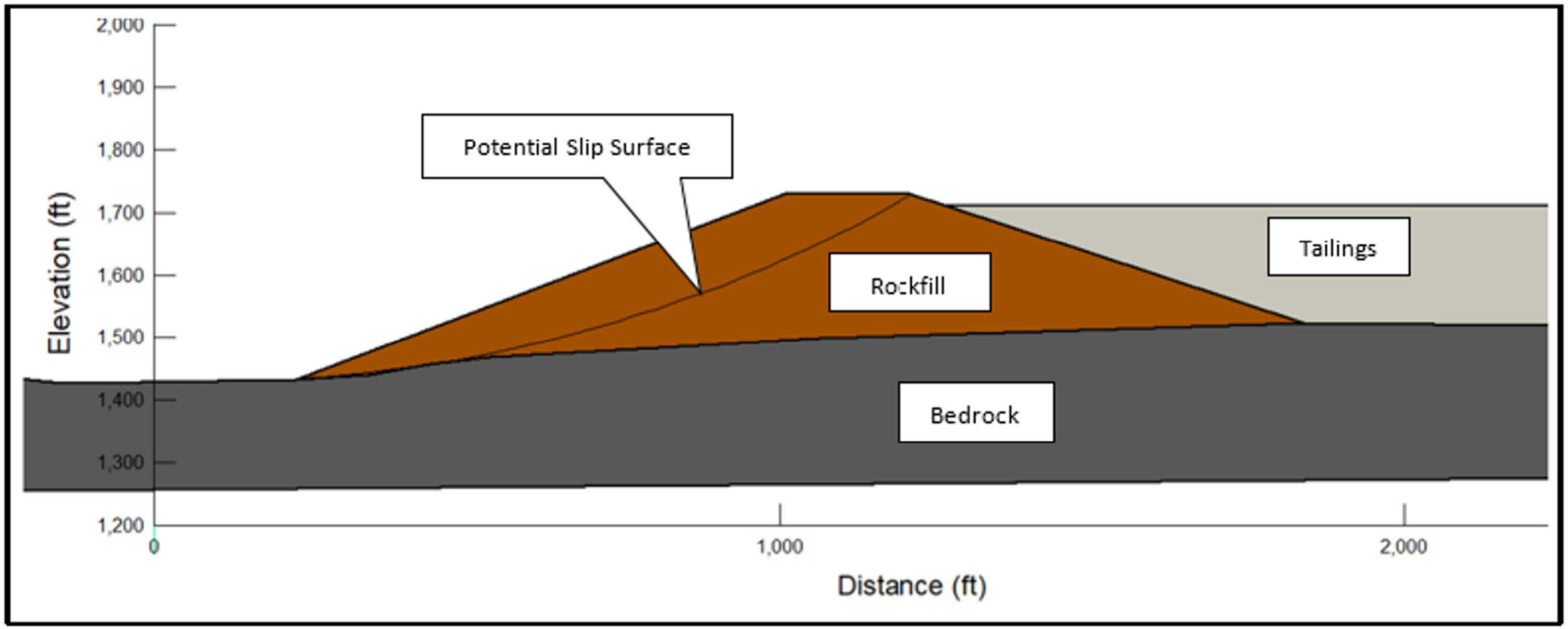

Source: PLP 2018-RFI 069

US Army Corps of Engineers®

BULK TSF SOUTH EMBANKMENT STATIC STABILITY ANALYSIS

PEBBLE PROJECT EIS

FIGURE K4.15-5

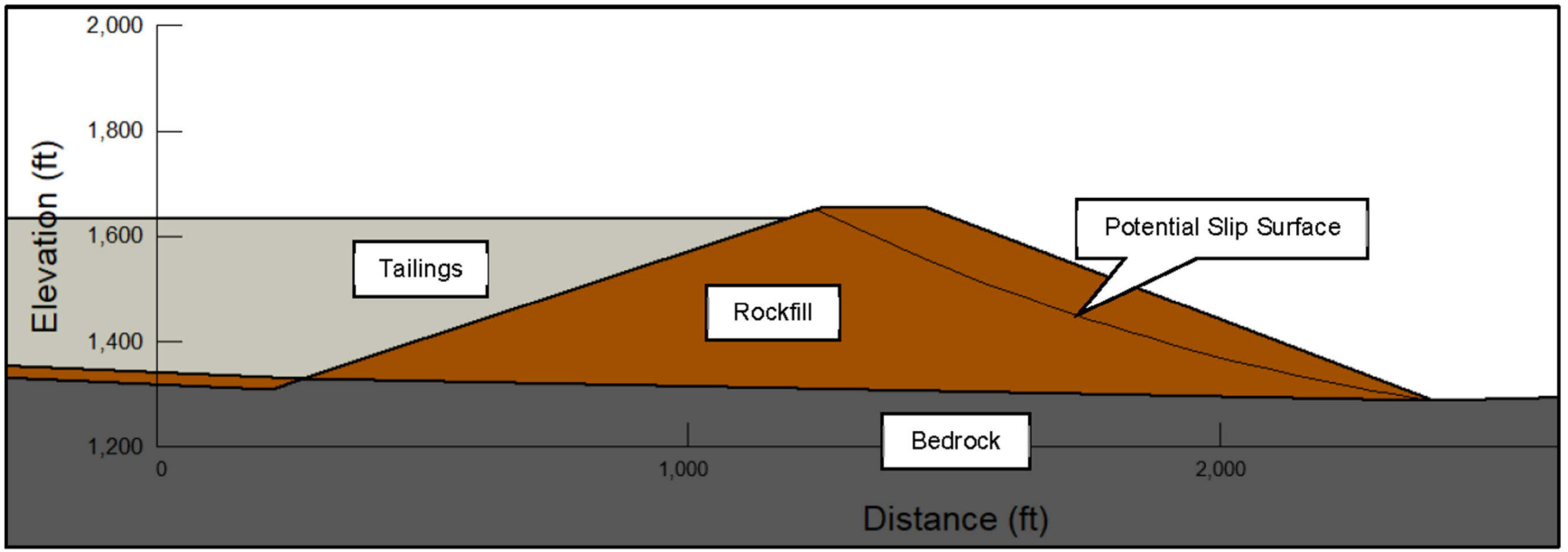

Source: PLP (2018-RFI 008); SRK (2018c), Figure 4

US Army Corps of Engineers

PYRITIC TSF NORTH EMBANKMENT STATIC STABILITY ANALYSIS

PEBBLE PROJECT EIS

FIGURE K4.15-6

Main WMP—The main WMP would be the primary water management structure at the mine site and would be a fully lined water retention facility. The embankment would have a maximum height of approximately 190 feet, with an overall downstream slope of approximately 2H:1V.

The initial design of the main WMP included the embankment being founded on overburden. During the EIS-phase FMEA, geotechnical experts expressed concern regarding the possibility that weak foundation conditions (such as a buried glacial clay layer) could be undetected by geotechnical investigations and concluded that the probability of global instability could range from very low to low (less than 1 in 10,000 to 1 in 1,000). As a result, PLP proposed a design change to remove overburden to the depth of competent bedrock in the embankment foundation.

Figure K4.15-7 shows a schematic representation of the static stability analysis with the potential slip surface. The preliminary analysis calculated an FoS value on the order of 1.9 to 2.0 under static loading conditions, based on the input parameters in Table K4.15-5 and assuming that overburden below the embankment is removed and the embankment is founded on suitable bedrock material. Based on this revised conceptual design, the EIS-phase FMEA panel concluded that the likelihood of global instability of the main WMP embankments would be very low (probability less than 1 in 10,000) (AECOM 2018l).

Open Pit WMP—The open pit WMP would be founded on overburden, constructed using the downstream method, fully lined, and would have an overall downstream slope of approximately 2H:1V and an upstream slope of 3H:1V (PLP 2018-RFI 008b). At approximately 40 feet high, the embankment of this structure would be much smaller than that of the main WMP. Figure K4.15-8 shows a schematic representation of the stability analysis results for this embankment with the predicted potential slip surface.

The open pit WMP was not evaluated in the EIS-phase FMEA (Section 4.27, Spill Risk, provides the rationale for the selection of structures for analysis in the FMEA). Potentially weak layers such as glacial lake deposits may be present under part of the open pit WMP area (see Figure 3.13-2)and could underlie the embankment foundations. However, the concern that potentially undetected layers could affect global stability is less than at the main WMP, because the embankment height would be lower and glacial lake deposits would be targeted and analyzed as design progresses. Assuming that any potential weak foundation conditions encountered in the overburden materials would be mitigated during design and construction after the collection of additional geotechnical drillhole investigation data, the preliminary stability analyses calculated an FoS value on the order of 1.9 to 2.0 under static loading conditions.

Bulk TSF Main SCP—The bulk TSF main SCP is proposed to be constructed using downstream methods. The embankment would be approximately 120 feet high, with an overall downstream slope of approximately 2.6H:1V and an upstream slope of 2H:1V (PLP 2018-RFI 008b). The preliminary stability analyses for this embankment used the same input parameters as for the bulk TSF and calculated a downstream FoS value on the order of 1.9 to 2.0 under static loading conditions. Figure K4.15-9 shows a schematic representation of the stability analysis results for the bulk TSF SCP with the predicted potential slip surface.

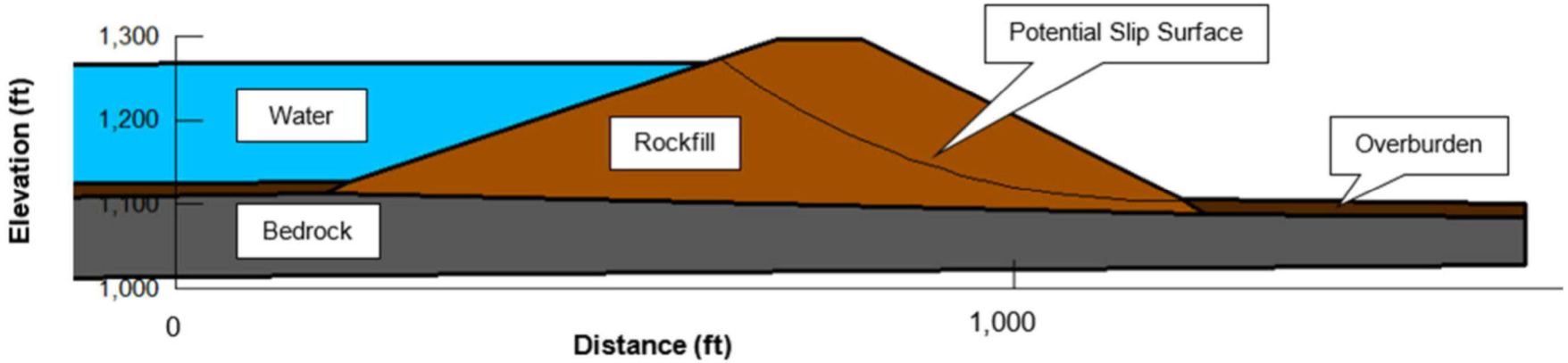

Source: PLP 2019-RFI 008j

US Army Corps of Engineers®

MAIN WMP STATIC STABILITY ANALYSIS

PEBBLE PROJECT EIS

FIGURE K4.15-7

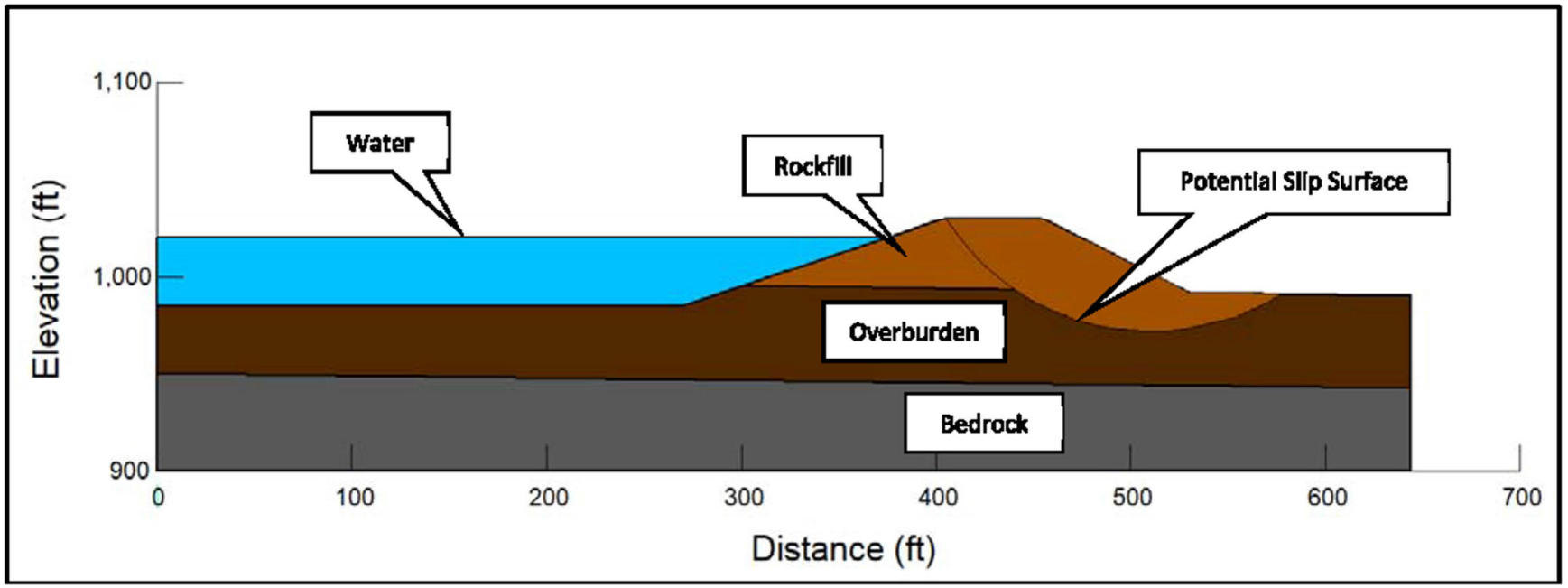

Source: PLP (2018-RFI008b), Figure 2

US Army Corps of Engineers®

OPEN PIT WMP STATIC STABILITY ANALYSIS

PEBBLE PROJECT EIS

FIGURE K4.15-8

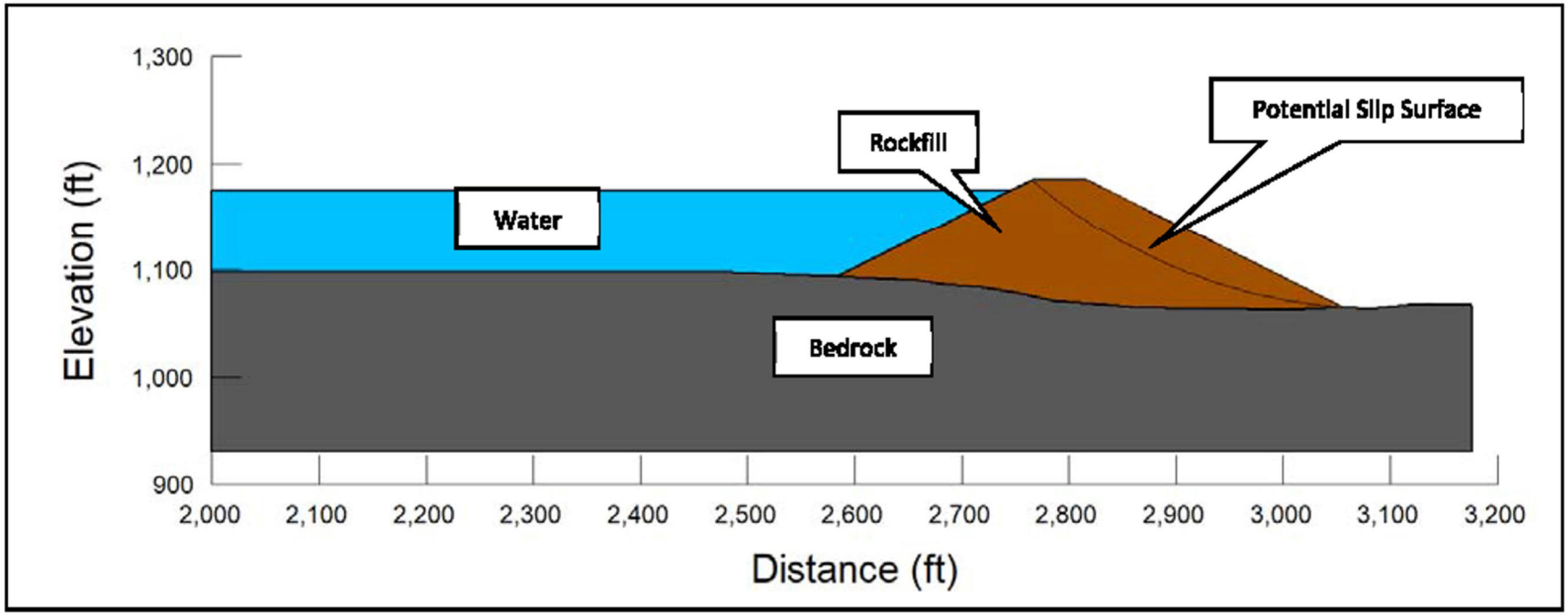

Source: PLP (2018-RFI 008b), Figure 1

US Army Corps of Engineers®

BULK TSF SCP STATIC STABILITY ANALYSIS

PEBBLE PROJECT EIS

FIGURE K4.15-9

Summary of Static Stability Analysis Results—Table K4.15-6 summarizes the results of the static stability analysis.

Table K4.15-6: Summary of Static Stability Analysis Results

Embankment	Construction Method	Max. Height (feet)	Downstream Slope Angle	Factor of Safety
Bulk TSF Main Embankment (Alternative 1 and Alternative 3)	Buttressed Centerline	545	2.6H:1V	1.9 to 2.0
Bulk TSF Main Embankment (Alternative 2)	Downstream	570	2.6H:1V	1.9 to 2.0
Bulk TSF South Embankment	Downstream	300	2.6H:1V	1.9 to 2.0
Pyritic TSF North Embankment	Downstream	335	2.6H:1V	1.9 to 2.0
Main WMP	Fully Lined Rockfill	190	2H:1V	1.9 to 2.0[1]
Open Pit WMP	Fully Lined Rockfill	100	2H:1V	1.9 to 2.0
Bulk TSF Main SCP	Rockfill with Upstream Liner	120	2.6H:1V	1.9 to 2.0

Notes:
[1] Results based on a revised design of constructing the embankment on suitable bedrock foundation (AECOM 2018k, 2018l; PLP 2019-RFI 008j)
H:V = horizontal/vertical
TSF = tailings storage facility
Sources: PLP 2018-RFI 008, -RFI 008b, -RFI 069, -RFI 075; PLP 2019-RFI 008j

Allowances were included in the conceptual embankment cross sections for internal filter and transition zones, which were represented as a homogeneous rockfill material in the model domains. These zones would be defined further and included in future stability modeling. Potential future modifications to the embankments are not expected to affect the embankment footprint.

The static stability analyses would be updated for each embankment structure as the design progresses through state permitting and additional field data are collected to support the understanding of geotechnical and hydrogeological conditions.

Seismic Hazard Analysis

Seismic Sources—The mine site is situated in a seismically active area because of the convergence of the Pacific and North American tectonic plates (Figure K4.15-10 and Figure K4.15-11). The most important seismically active geologic structure near the mine site is the Alaska-Aleutian Megathrust, which lies about 120 miles to the southeast. Figure K4.15-10 shows the relatively high concentration of earthquake events associated with this structure. A description of the megathrust and other active faults in the project area is provided in Section 3.15, Geohazards and Seismic Conditions.

Section 3.15 also provides a summary of evidence and uncertainties in the interpretation of the recency of faulting on the closest potentially active fault to the mine site, the Lake Clark fault. The closest documented surface exposure of this fault is located 14 miles away from the mine site. Several possible extensions of this fault as close as 6 miles away from the mine site have been identified based on regional geophysical data (Figure 3.15-2), though these are not necessarily active in the Holocene. Evidence of repeated paleo-liquefaction events as close as 8 miles

southwest of the mine site (Higman and Riordan 2019) could suggest Holocene earthquake activity on either a buried Lake Clark fault extension or deeper subduction-related seismicity. The implication of these uncertainties for the impact analysis includes the following:

- If the locations of the extensions in Figure 3.15-2 were shown to be active, there could be the potential for surface rupture of the mine access road and pipeline where they cross the faults. The location of these where they cross the different alternatives is discussed in Section 4.15, Geohazards and Seismic Conditions. The amount of potential surface fault displacement on an active surface fault can be estimated based on empirical relationships between displacement and magnitude, rupture length, or slip rate (Wells and Coppersmith 1994; Honegger 2017). For example, the average displacement on a fault experiencing an earthquake of magnitude (M) 7.0 to 7.5 is predicted to be on the order of 3 to 7 feet, based on regression relationships for earthquakes worldwide (Wells and Coppersmith 1994), and may warrant special fault crossing design for the pipeline. On the other hand, if the potential extensions are not confirmed to be faults or have very low slip rates as suggested by Koehler and Carver (2018), displacements could range from zero to de minimis values that would not warrant special crossing design.
- As described below under "Deterministic Seismic Hazard Analysis," Knight Piésold (2019d) selected the closest mapped surface exposure of the Lake Clark fault (14 miles away) to assess the magnitude of potential ground shaking that could occur at mine site embankments from a major earthquake on this fault. If its location and recency of activity were determined to be closer to the mine site, the estimate of ground shaking at mine site embankments would be higher from this particular fault, but lower than other design earthquakes considered. The predicted peak ground acceleration (PGA) from a maximum credible earthquake (MCE) of M7.5 located 14 miles away is 0.32g (Table K4.15-9), and the predicted value if the same MCE occurred on the closest fault extension 5.9 miles away would be 0.57g, which is less than the value of 0.61g determined for the M8.0 intraslab earthquake defined as one of the four maximum design events (MDE) for the mine site embankments.
- The paleo-liquefaction events do not affect the interpretation of ground shaking described above for the Lake Clark fault, or below under "Deterministic Seismic Hazard Analysis" for other seismic sources (PLP 2019-RFI 139). Evidence of liquefaction is expected across much of the region due to the generally high seismicity in the area (Figure K4.15-10) and the occurrence of large crustal, intraslab, and megathrust earthquakes in the region, any of which could cause liquefaction in susceptible soil types.

Chapter 5, Mitigation describes PLP plans to continue to investigate the Lake Clark fault as design progresses (PLP 2019-RFI 139), and Appendix M1.0, Mitigation Assessment, provides additional fault study recommendations to be considered during these investigations that would help identify or rule out the potential locations and recency of faulting closer to the mine site.

Design Earthquakes—Seismic hazard analyses were completed in support of the proposed Pebble project. Draft ADSP guidelines (ADNR 2017a) indicate that seismic analyses of dams should include both OBE and MDE scenarios. Table K4.15-7 shows the OBE and MDE return periods as related to ADSP classification of dam hazards.

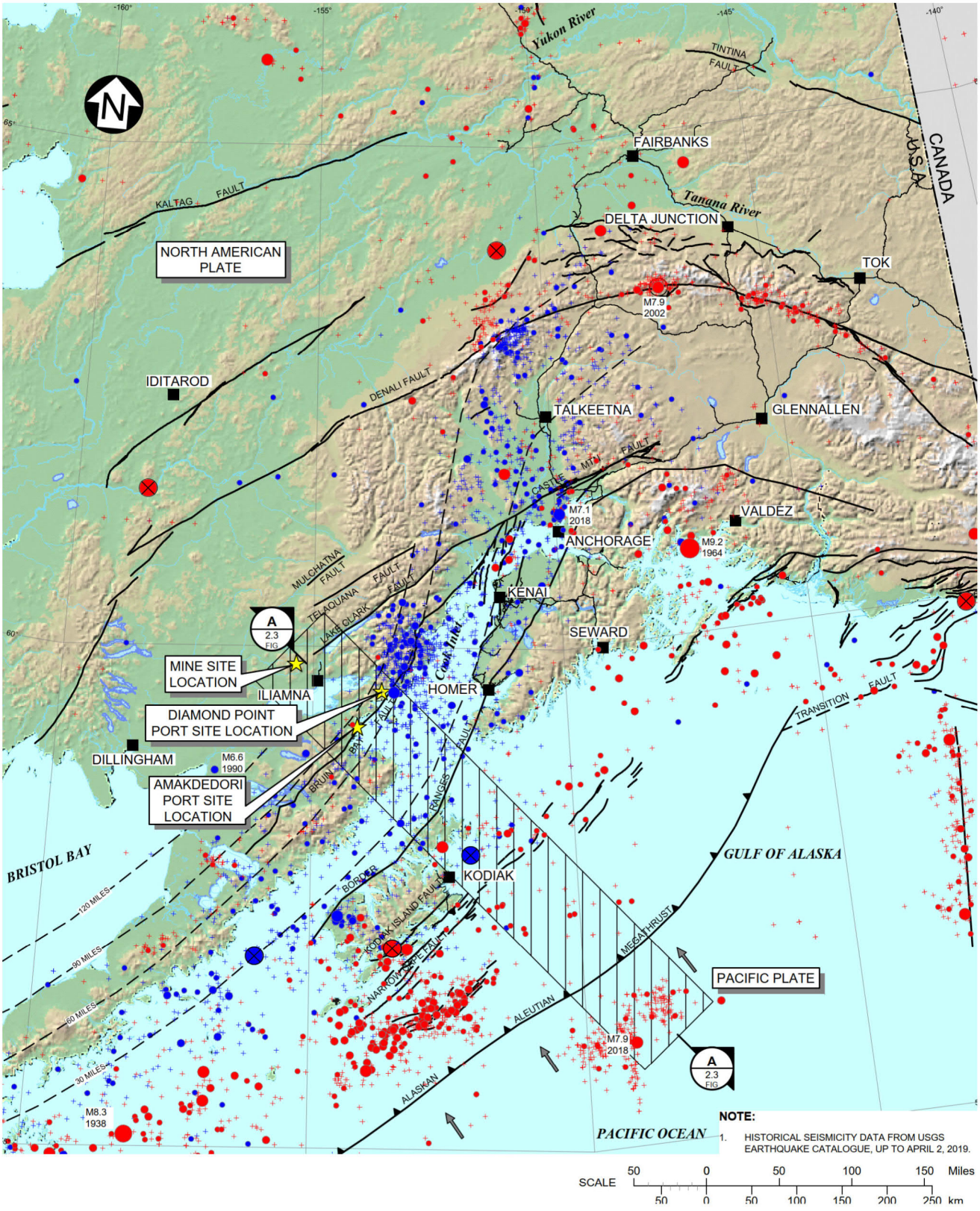

Source: KP 2019d (Figure 2.2)

SYMBOL SIZE PROPORTIONAL TO MAGNITUDE

- 4.0 - 4.9
- 5.0 - 5.9
- 6.0 - 6.9
- 7.0 - 7.9
- 8.0 - 8.9
- 9.0 +
- LARGE MAGNITUDE EARTHQUAKES RECORDED BETWEEN 1899 & 1904

EARTHQUAKE FOCAL DEPTH

- DEPTH ≤ 25 MILES
- DEPTH > 25 MILES

LEGEND:

- ACTIVE AND POTENTIALLY ACTIVE FAULTS
- ALIGNMENT OF ALEUTIAN TRENCH
- DIRECTION OF TECTONIC PLATE MOVEMENT
- CONTOUR OF APPROXIMATE OCEANIC SLAB DEPTH
- ZONE OF RECORDED EARTHQUAKES INCLUDED ON SECTION A-A

US Army Corps of Engineers®

SEISMICITY AND EARTHQUAKE DEPTH

PEBBLE PROJECT EIS

FIGURE K4.15-10

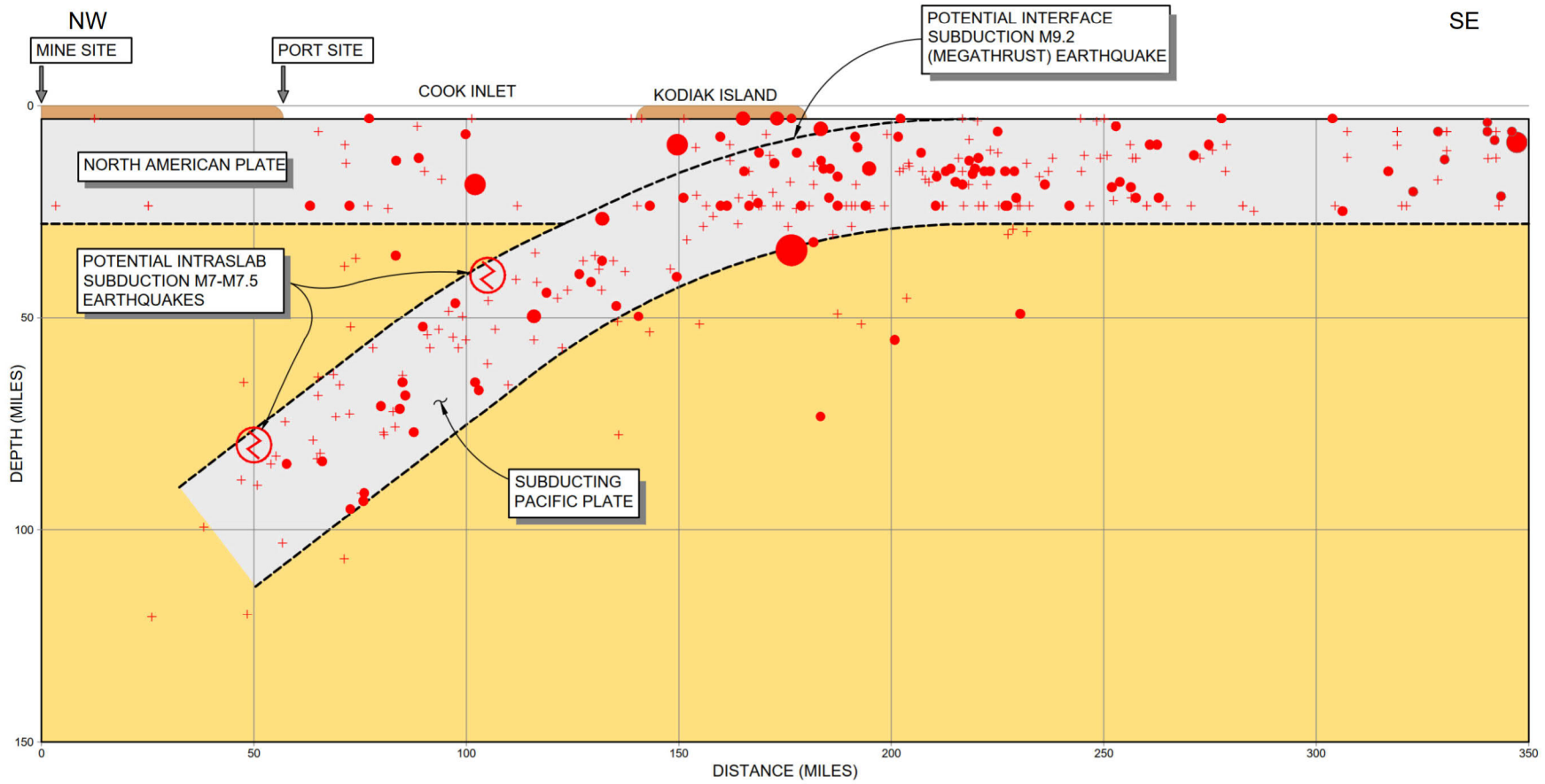

Source: KP 2019d (Figure 2.3)

SYMBOL SIZE PROPORTIONAL TO MAGNITUDE

- 4.0 - 4.9
- 5.0 - 5.9
- 6.0 - 6.9
- 7.0 - 7.9
- 8.0 +

US Army Corps of Engineers®

CROSS-SECTION THROUGH ALASKA SUBDUCTION ZONE

PEBBLE PROJECT EIS

FIGURE K4.15-11

The OBE represents the ground motions or fault movements from an earthquake considered to have a reasonable probability of occurring during the functional life of a project. All critical elements of a structure need to be designed to remain functional during the OBE, and any resulting damage should be easily repairable in a limited time. The OBE can be defined based on probabilistic evaluations, in which the level of risk (the probability that the magnitude of ground motion would be exceeded during a particular length of time) is determined relative to the hazard potential classification and dam location (ADNR 2017a).

The MDE represents the ground motions or fault movements from the most severe earthquake considered at the site, relative to the acceptable consequences of damage in terms of life and property. All critical elements of a dam and appurtenant structures for which the collapse or failure could result in or precipitate an uncontrolled release from the reservoir must be designed to resist the MDE. The MDE may be defined based on either probabilistic or deterministic evaluations, or both (ADNR 2017a).

Table K4.15-7: Earthquake Return Periods for Alaska Dam Hazard Classifications

Dam Hazard Classification	Return Period, Years	
	Operating Basis Earthquake	Maximum Design Earthquake
I	150 to >250	2,500 to MCE
II	70 to 200	1,000 to 2,500
III	50 to 150	500 to 1,000

Notes:
MCE = Maximum Credible Earthquake.
1. The MCE is defined as the largest earthquake magnitude that could occur along a recognized fault or in a particular seismo-tectonic province or source area under the current tectonic framework.
2. TSFs and the main WMP have a Class I dam hazard classification. Other mine site embankments may have a lower dam hazard classification.
Source: ADNR 2017a

As shown in Table K4.15-7, the OBE should be selected from a range of return periods from 150 years to more than 250 years for a dam with a Class I hazard classification. A conservative OBE corresponding to a return period of 475 years was adopted for the Pebble TSF designs. The MDE should be selected from a range of return periods from 2,500 years up to the maximum credible earthquake (MCE) for a dam with a Class I hazard classification range. The MCE was selected as the MDE for the Pebble TSFs. As discussed below, both probabilistic and deterministic evaluations were completed for the Pebble Project to evaluate potential ground shaking associated with these earthquakes. The proposed design earthquakes associated with the OBE and MDE are presented in Section 4.15, Geohazards and Seismic Conditions, and highlighted in bold in Table K4.15-8 and Table K4.15-9.

Probabilistic Seismic Hazard Analysis—A probabilistic seismic hazard analysis is conducted to assess the likelihood that a given level of ground shaking could occur at a site from a combination of potential earthquake sources. The probabilistic analysis was used to select the OBE for the mine site embankments. Shown in Table K4.15-8, the maximum ground shaking (acceleration) values for different return periods and probabilities of occurrence were determined by Knight Piésold (2019d) based on gridded US Geological Survey (USGS) data and ground motion maps for Alaska (Wesson et al. 2007). The Knight Piésold (2019d) report is a revised version of a similar analysis completed prior to the DEIS (Knight Piésold 2013), which was updated based on more recent USGS data, comments received on the DEIS, and RFIs. The estimated maximum acceleration selected for the 1-in-475-year earthquake (OBE) at the mine site is 0.16g.

Table K4.15-8: Probabilistic Seismic Hazard Analysis for Mine Site

Return Period (Years)	Probability of Exceedance [1]	Maximum Acceleration [2] (g)
50	63	0.06
100	39	0.08
200	22	0.11
475	**10**	**0.16**
1,000	5	0.21
2,500	2	0.29
5,000	1	0.36
10,000	0.5	0.43

Notes:
[1] Probability of exceedance calculated for a design life of 50 years; Q = 1 – exp (-L/T), where Q = probability of exceedance, L = design life in years, T = return period in years.
[2] Maximum accelerations are for values on firm rock.
Information based on the USGS Seismic Hazard Program 2017 database.
Bold = proposed OBE
Source: Knight Piésold 2019b, 3; PLP 2019-RFI 008g; PLP 2019-RFI 139

While the probabilistic data were not used to develop MCEs or MDEs for the mine site, for comparison purposes, the PGA predicted for the 2,500-year return period earthquake in the probabilistic analysis (0.29g), is lower than three of the four MCE scenarios developed based on the deterministic seismic hazard analysis (described below). At 0.43g, the probabilistic 10,000-year earthquake also has a predicted ground shaking value less than the highest values for the MDE in the deterministic analysis, such that the mine site structures would be designed to take the results of both analyses into account.

The USGS 2007 probabilistic database and maps do not incorporate some of the more recent ground motion models that have been developed since that time, and they next plan to update these for Alaska in 2023. PLP (2019-RFI 008h) provides a discussion of other ground motion models that are available and could be considered in the interim to improve upon the existing probabilistic analysis. For example, the latest update to Next Generation Attenuation (NGA) ground motion prediction equations for crustal earthquakes (Bozorgnia et al. 2014) supersede the equations used in the 2007 USGS database. The new crustal equations were developed using a larger database of events, including more recent earthquake records. Current probabilistic seismic analysis software, EZ-FRISK, includes the recent NGA crustal models and several more recent subduction zone models. Another NGA study is ongoing to provide further revisions to ground motion equations for subduction zone earthquakes. It is anticipated that the next revision to the USGS model and maps for Alaska would incorporate the latest equations applicable to both crustal and subduction zone earthquakes (Knight Piésold 2019d).

Because the mine site embankments would be designed for the deterministic MCE scenarios defined for the mine site (described below), these events and not the OBE control the design of the dams. De-aggregation information provided by USGS indicates that subduction zone earthquakes contribute approximately 90 percent of the probabilistic seismic hazard for the 475- and 2,500-year earthquakes. As such, using the latest software with updated crustal earthquake models is expected to have only a minor effect on the predicted PGA for the OBE. In addition, a review of recently published subduction models of Abrahamson et al. (2016) indicates that the predicted PGA would be similar or lower than those developed using the 2007 USGS database (PLP 2019-RFI 008h).

The seismic hazard analysis for the mine site would be updated as design progresses. A seismic report is one of the engineering reports to be included in the preliminary design package submitted

to ADNR. The analysis would incorporate current best practices for analysis and updated USGS ground motion data as available (PLP 2018-RFI 008c, RFI 008h).

Deterministic Seismic Hazard Analysis—The deterministic method assesses the maximum ground shaking that could occur at a site from major seismic sources based on magnitude, distance, and fault type, using appropriate ground motion prediction models. Unlike the probabilistic method, it does not take into account the relative likelihood that earthquakes would occur on different faults.

Table K4.15-9 shows the results of the deterministic analysis for the mine site based on the regional seismic sources. Similar to the probabilistic analysis, the deterministic analysis was updated by Knight Piésold (2019d) based on more recent ground motion models since the version presented in the DEIS, and Table K4.15-9 reflects the revised analysis. The results of the deterministic analysis were used to select the MDE for the mine site embankment, based on the four MCE scenarios shown in bold in Table K4.15-9. These are described further in Section 4.15, Geohazards and Seismic Conditions.

The maximum acceleration values in Table K4.15-9 were determined based on three ground motion models for subduction zone events (Atkinson and Boore 2003; Abrahamson et al. 2016; Zhao et al. 2006), and a set of five models in Bozorgnia et al. (2014) for shallow crustal earthquakes. Values for the crustal faults were calculated using the appropriate reverse or strike-slip ground motion prediction equations. In the case of the unknown background fault, a reverse faulting mechanism was conservatively assumed because it provided the highest result from the ground motion equations.

Seismic activity since these models were developed included the following large earthquakes in the region, which were within the magnitude and maximum acceleration values shown in Table K4.15-9:

- Magnitude 7.1 earthquake experienced northwest of Anchorage (about 200 miles north of the mine site) on November 30, 2018
- Magnitude 7.9 earthquake experienced in the Gulf of Alaska (about 600 miles southeast of the mine site) on January 23, 2018
- Magnitude 7.1 earthquake experienced about 7 miles east of Iliamna Bay (about 75 miles east/southeast of the mine site) on January 24, 2016

As indicated above, PLP plans to update the seismic hazard analyses as design progresses, incorporating current best practices into the analysis, such as the NGA subduction ground motion equations, once they have been formally released (AECOM 2018f; PLP 2018-RFI 008c, RFI 008h).

Table K4.15-9: Deterministic Seismic Hazard Analysis for Mine Site

Earthquake Source Type	Earthquake Source Name	Source/ Fault Mechanism	Maximum Magnitude	Epicentral Distance[1]	Focal Depth	Peak Ground Acceleration[2]	
			(Mw)	(miles)	(miles)	Median (g)	84th Percentile (g)
Interface Subduction	**Alaska-Aleutian Megathrust**	**Thrust**	**9.2 (8.5)[3]**	**120**	**25**	0.09	**0.16**
Intraslab Subduction	Intraslab Event	In-slab	7.5	110	40	0.05	0.11
			8.0	110	40	0.09	0.18
	Deep Intraslab Event	**In-slab**	7.5	50	80	0.17	0.34
			8.0	**50**	**80**	**0.31**	**0.61**
Shallow Crustal Fault[4]	**Lake Clark Fault (Mapped)**	**Strike-slip**	**7.5**	**14**	**3**	0.17	**0.32**
	Castle Mountain Fault	Strike-slip	7.3	170	3	<0.01	0.01
	Bruin Bay Fault	Reverse (Thrust)	8.0	60	3	0.07	0.12
	Border Ranges Fault	Strike-slip	8.0	130	3	0.02	0.04
	Kodiak Island / Narrow Cape Faults	Strike-slip	7.5	190	3	<0.01	0.01
	Telaquana Fault	Strike-slip	7.0	40	3	0.05	0.09
	Mulchatna Fault	Strike-slip	6.5	55	3	0.02	0.04
	Denali Fault	Strike-slip	8.0	125	3	0.02	0.04
	Maximum Background Earthquake[5]	**Reverse (Thrust)**	**6.5**	**< 1**	**~7**	**0.30**	**0.56**

Notes:
[1] Fault locations are from Knight Piésold (2011c, 2015a).
[2] PGAs are for values on firm rock.
[3] The PGAs for the megathrust event were calculated using a representative magnitude 8.5 for the ground motion prediction equations of Atkinson and Boore (2003) and Zhao et al. (2006), and a magnitude 9.2 for Abrahamson et al. (2016).
[4] The adopted faulting mechanism for each shallow crustal fault was based on a review of available information defining the fault type. The predominant faulting mechanism assumed for all of the shallow crustal faults is strike-slip, with the exception of the Bruin Bay fault for which reverse faulting was used. Reverse faulting was also conservatively assumed for the maximum background earthquake. PGAs for the crustal faults were calculated using the appropriate reverse or strike-slip ground motion prediction equations of Bozorgnia et al. (2014).
[5] Seismic event with no apparent association with known faults, but which could contribute to the seismic hazard.
MW = megawatt
PGA = peak ground acceleration
Bold = MCE scenarios considered in TSF design
Source: Knight Piésold 2019b, d; PLP 2019-RFI 008g, RFI PLP 2019-RFI 139

Knight Piésold (2019d) and PLP (PLP 2019-RFI 008h) provide a discussion of various considerations used in the selection of ground motion models for the deterministic analysis, and the effect of recent developments on the results. For example, the five equations in Bozorgnia et al. (2014) used for crustal earthquakes were given equal weight in the deterministic analysis. The effect of dropping one of these, as USGS has done recently (having to do with soft soil parameters), would result in a slight decrease in the PGA for the MCE on the Lake Clark fault (from 0.32g to 0.31g), and slight increase for the background earthquake (from 0.56g to 0.58g), which would still be less than the maximum determined for the intraslab event (0.61g). More recent subduction models of Abrahamson et al. (2018) were compared to the results using Abrahamson et al. (2016) and found to result in very similar or significantly lower PGA values for the megathrust and intraslab events. Thus, PLP plans to maintain the higher, more conservative deterministic results shown in Table K4.15-8 until the NGA subduction models currently under development are available.

Response Spectra—Each of the four MCE scenarios bolded in Table K4.15-9 were recommended to be used for the design of mine site embankments because there could be different ground shaking characteristics (frequency and duration) and damage potential associated with each of them (Knight Piésold 2019d). An earthquake response spectrum is used to represent the influence of a given earthquake on a structure with time during the period of ground shaking. Response spectra showing the predicted ground acceleration with time for each of the four deterministic MCE scenarios are provided in Table K4.15-10 and shown in Figure K4.15-12.

Table K4.15-10: Deterministic Response Spectra for Maximum Design Earthquake Scenarios

Spectral Period (seconds)	Spectral Acceleration (g)			
	Magnitude 9.2 Interface Subduction	Magnitude 8.0 Intraslab Subduction	Magnitude 7.5 Shallow Crustal Fault	Magnitude 6.5 Shallow Crustal Fault
PGA	0.16	0.61	0.32	0.56
0.02	0.161	0.606	0.320	0.576
0.03	-	-	0.354	0.638
0.05	0.192	0.877	0.449	0.823
0.075	0.235	1.093	0.577	1.078
0.10	0.283	1.310	0.652	1.247
0.15	0.342	1.391	0.720	1.405
0.20	0.334	1.251	0.698	1.349
0.25	0.335	1.125	0.645	1.224
0.30	0.344	0.985	0.594	1.093
0.40	0.362	0.744	0.507	0.887
0.50	0.260	0.600	0.438	0.733
0.75	0.226	0.419	0.311	0.485
1.0	0.210	0.332	0.234	0.349
1.5	0.148	0.237	0.154	0.198
2.0	0.104	0.187	0.113	0.130

Table K4.15-10: Deterministic Response Spectra for Maximum Design Earthquake Scenarios

Spectral Period (seconds)	Spectral Acceleration (g)			
	Magnitude 9.2 Interface Subduction	Magnitude 8.0 Intraslab Subduction	Magnitude 7.5 Shallow Crustal Fault	Magnitude 6.5 Shallow Crustal Fault
3.0	0.047	0.082	0.075	0.069
4.0	0.033	0.053	0.056	0.042
5.0	0.023	0.034	0.045	0.030
7.5	0.014	0.013	0.028	0.014
10.0	0.010	0.008	0.018	0.008

Notes:
1. Spectral Accelerations are 84th percentile values for firm rock site conditions
2. The spectral accelerations provided for the interface subduction (megathrust) event have been calculated using a representative magnitude of 8.5 for the ground motion prediction equations of Atkinson and Boore (2003) and Zhao et al. (2006) and a magnitude of 9.2 for Abrahamson et al. (2016).
3. The magnitude 7.5 shallow crustal fault represents an earthquake on the mapped Lake Clark fault.
4. The magnitude 6.5 shallow crustal fault represents the maximum background earthquake (MBE).
5. Spectral accelerations for the interface subduction and intraslab subduction events for periods of 3.0 to 5.0 seconds are average values provided by the ground motion prediction equations of Zhao et al. (2006) and Abrahamson et al. (2016).
6. Spectral accelerations for the interface subduction and intraslab subduction events for periods of 7.5 and 10.0 seconds are values provided by the ground motion prediction equation of Abrahamson et al. (2016).

Source: Knight Piésold 2019d, Table 4.2

As shown in Figure K4.15-12, the period of greatest concern with regard to ground shaking impacts on the mine site embankments is not just the PGA at the very beginning of an earthquake, but the highest accelerations that would be experienced between about 0.1 and 0.3 seconds, as well as the effects of continued shaking beyond that. Although the PGA associated with the interface (megathrust) event is much less that those of the intraslab and shallow crustal earthquakes, the duration of strong ground motion for the interface event would be longer. De-aggregation information provided by the USGS indicates that intraslab subduction earthquakes contribute about 80 percent of the seismic hazard for the short period ground motions, while interface (megathrust) earthquakes contribute about 52 percent of the hazard during long period motions (Knight Piésold 2019d).

The PGA and response spectra provided above are for ground motions on firm rock. Peak ground motions in the tailings deposit, embankments, and foundations may be higher due to local amplification of ground shaking. Because the TSFs are designed to be founded on bedrock, amplification in the foundations is likely to be minimal. The ability of embankment fill materials and the tailings deposit to transmit seismic ground motions is dependant on their dynamic stiffness and damping characteristics.

The deterministic response spectra presented in Table K4.15-10 were used as input to the seismic displacement analysis described below under “Pseudo-Static Stability Analysis” for mine site dams founded on bedrock (PLP 2019-RFI 008h). For the open pit WMP embankment that would be founded on overburden, the average shear wave velocity in the top 100 feet of the foundation was estimated based on local drillhole data and used with appropriate ground motion equations to develop site-specific response spectra for use in the pseudo-static analysis (PLP 2019-RFI 008i).

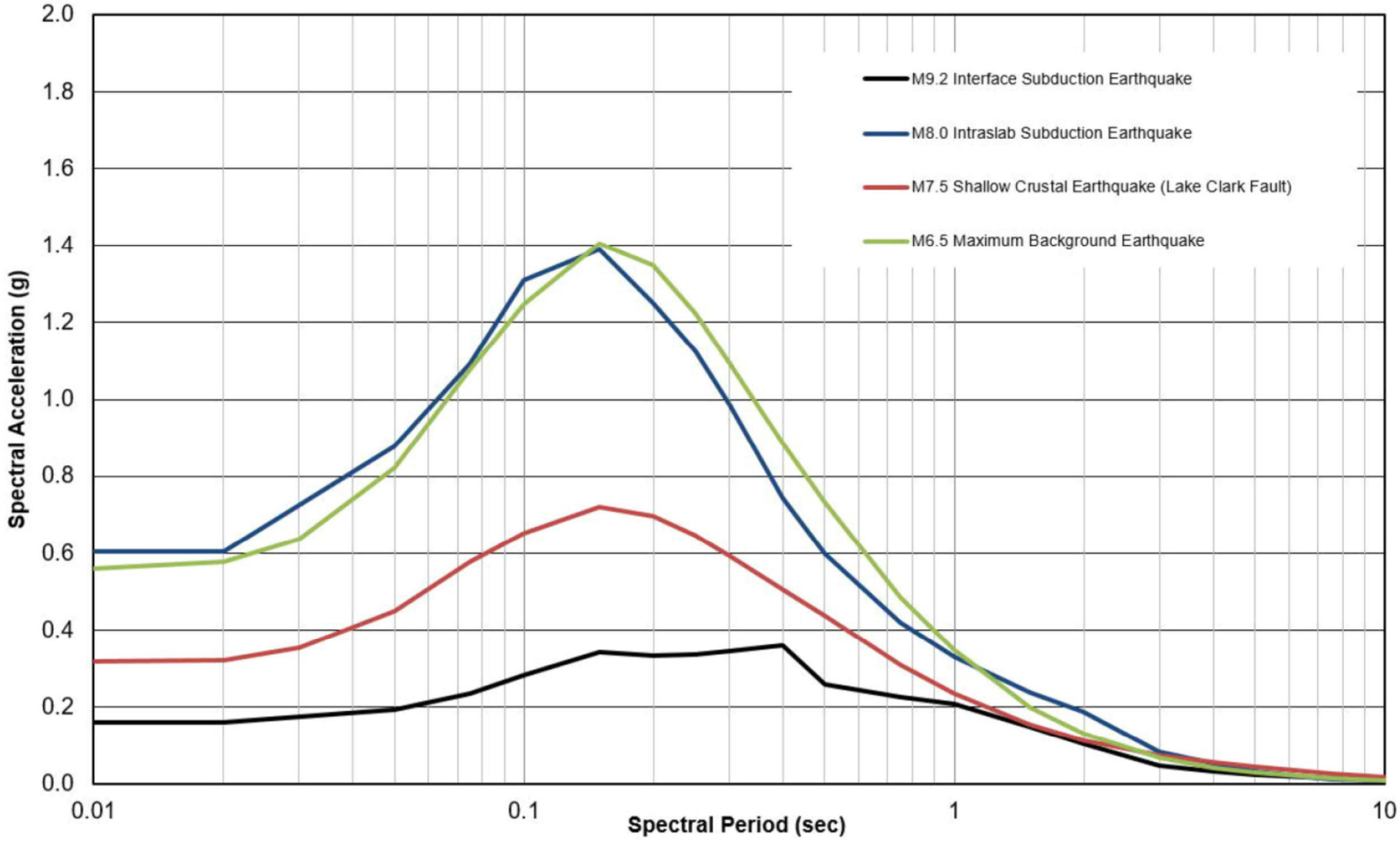

Source: PLP 2019-RFI008h; KP 2019d

US Army Corps of Engineers®

DETERMINISTIC RESPONSE SPECTRA FOR TSF MAXIMUM DESIGN EARTHQUAKE SCENARIOS

As noted in Chapter 5, Mitigation, foundation conditions would be further characterized as design progresses, including assessments of rock stiffness, fracturing, and weathering. Dynamic site response analyses would be carried out to determine potential amplification as seismic waves propagate through the foundation, tailings deposit, and embankment (Knight Piésold 2019d). Acceleration time histories from past earthquakes would be required as input excitation for nonlinear response analyses of mine site embankments. Acceleration time-history records would be selected to represent each of the four MCE scenarios defined for the mine site based on consideration of the magnitude, rupture mechanism, focal mechanism, source directivity, and recording site location, geology, and topography. A minimum of eight earthquake time-history records would be adopted for each design MCE. Each of the records would be modified by scaling and spectrally matching to the corresponding MCE response spectrum (PLP 2019-RFI 008h).

Preliminary Seismic Stability Analyses

Preliminary Pseudo-Static Analysis—The stability of mine site embankments during hypothetical earthquake loading conditions was preliminarily assessed based on the conceptual level of design by performing a pseudo-static analysis using SLOPE/W and the method of Bray and Travasarou (2007) (PLP 2019-RFI 008g, PLP 2019-RFI 008i). The Bray method is a simplified predictive relationship for estimating displacement due to seismic deformation. This method considers earthquake magnitude, the natural period of the dam structure (related to dam height and stiffness), and the spectral acceleration of earthquake motions when estimating horizontal displacement in a downstream direction. The method takes into account the dynamic characteristics of an earthquake as it is transmitted through the foundation material and propagates through the rockfill in the embankment. The Bray method does not provide an estimate of potential vertical settlement of the embankments, nor does it take pore pressures into account (discussed further under “Post-Liquefaction Analysis”). Estimates of horizontal and vertical displacement for mine site embankments would be further analyzed for current embankment designs during future seismic analysis as part of the detailed design. That work is anticipated to be performed after the EIS is completed.

In a pseudo-static analysis, a horizontal force (seismic coefficient) is applied to the embankments to simulate earthquake loading and determine the critical (yield) acceleration (ky) required to reduce the FoS to 1.0. Embankment deformation could occur if the yield acceleration is lower than the predicted maximum ground acceleration along the critical slip surface. These values are then used in the Bray method to estimate potential deformations. The earthquake magnitude, ky, and spectral acceleration value corresponding to the fundamental period, are all used in the Bray method to predict displacement along the critical slip surface.

Input parameters used in the preliminary pseudo-static analyses are described in PLP 2019-RFI 008g and RFI 008i, and included the following:

- Material parameters used in the analysis for the foundation and embankment fill were as listed in Table K4.15-5. As noted in the table, bedrock was defined as a homogeneous geological unit for the purpose of preliminary stability analyses.
- An estimated rockfill shear modulus ($K2_{max}$) value of 180 was applied to each embankment to determine an average shear wave velocity (Vs) of the sliding mass; this defines the stiffness of the embankment and was used with embankment height to calculate the fundamental period of each structure.
- A dam height of two-thirds the total height was used for the bulk TSF main embankment as it provided a more conservative result, in that the shorter dam reduced the fundamental period of the structure and increased the estimated deformations

under the design earthquakes. Embankment heights for other embankments were as listed in Table K4.15-1.

- The magnitudes of each of the four MCEs evaluated are shown in bold in Table K4.15-9.
- Spectral accelerations for the degraded fundamental period (1.5 times the initial fundamental period, Ts) for embankments founded on bedrock were obtained from the Knight Piésold (2019d) seismic hazard analysis (Table K4.15-10). For the open pit WMP to be founded on overburden, Vs in the top 100 feet of the foundation was estimated using SPT data in site-specific drillholes, which was then used with appropriate ground motion prediction equations to develop site-specific response spectra for the four MCE events.
- The calculated ky of the bulk TSF main embankment was 0.30, and for the other dams the ky ranged from 0.41 to 0.59. Because the Bray method is considered valid for values of ky up to 0.4, for the purposes of the preliminary analysis, a ky of 0.4 was assumed for the other embankments; this results in more conservative (higher) predicted deformations, because the calculated ky is higher than that applied to the structure.

The results of the preliminary pseudo-static analyses are summarized in Table 4.15-2. Estimated displacements ranged from negligible (less than 0.03 feet) to 0.23 feet for the open pit WMP under the deep intraslab earthquake scenario. For the bulk TSF main embankment, results for modified centerline construction (Applicant's Preferred Alternative) were slightly higher (by 0.04 feet) than those of the downstream-constructed embankment under Alternative 2 for the two MCEs with the highest ground shaking predictions (deep intraslab and background earthquakes), though displacement estimates are minimal in either case and would not affect the integrity of the structure.

Previous seismic deformation analyses were conducted on an earlier concept (2011) of the bulk TSF main embankment that do not necessarily apply to the current concept dam but are useful for comparison purposes (PLP 2018-RFI 008; PLP 2019-RFI 008g). The earlier concept dam was about 100 feet higher and had a steeper overall downstream slope (2.3H:1V) than the current concept (2.6H:1V). Potential displacements under earthquake loading from the OBE and different MCE scenarios were estimated for the 2011 concept using multiple methods (Newmark 1965; Makdisi and Seed 1977; and Bray and Travasarou 2007). While minimal deformations were predicted as a result of an OBE event, displacements were estimated to be up to 5 feet along the potential slip surface under MCE loading conditions using the various methods. Based on the Bray method alone, the displacement estimates for the 2011 bulk TSF main embankment ranged from 0.05 to 0.2 feet, up to 0.13 feet higher than those based on the current concept (Table K4.15-11). The changes in dam geometry in the current concept resulted in a higher yield acceleration value for the dam that reduced the predicted seismic deformations. Potential settlement of the bulk TSF main embankment crest was also estimated for the 2011 concept using the empirical relationship of Swaisgood (2003), with settlement estimated to be on the order of 4 feet under MCE loading conditions. These displacements were not large enough to truncate the engineered filter zones or affect the functionality of the embankment (Knight Piésold 2018c; PLP 2018-RFI 008).

Seismic stability and crest deformation analyses would be updated for each embankment structure as design progresses and additional field data are collected to support the understanding of geotechnical and hydrogeological conditions. The estimated crest deformation/settlement values would be added to the minimum freeboard requirements for the embankments, so that the minimum required freeboard would be maintained after the MDE event.

Potential additive effects on dam stability from multiple earthquakes such as aftershocks would also be assessed as design progresses (Knight Piésold 2019d).

It is acknowledged that the current pseudo-static analyses are based on preliminary estimates of homogeneous foundation conditions, and that deep-seated slide risks on potential weak zones can be triggered by earthquakes. As described in Chapter 5, Mitigation, additional geotechnical investigations and detailed assessment of embankment foundation conditions would be completed as the preliminary and detailed designs progress to support refinements of the stability analyses. Future programs would include additional investigation along embankment alignments to further evaluate their location relative to faults, clays, or other weak zones. Potential weak foundation materials or conditions would be mitigated by more detailed stability analyses to determine their effect on embankment stability, removal of the materials, or flattening of downstream slopes if required (PLP 2018-RFI 008a; PLP 2019-RFI 008g; PLP 2019-RFI 014b).

Preliminary Post-Liquefaction Analyses—Liquefaction occurs when porewater pressures in soil exceed the total gravity load of the soil, while the solid particles become buoyant and lose their ability to carry a load. While liquefaction is most commonly associated with earthquakes, it can also occur under static loading conditions if the rate of loading is faster than the rate of porewater pressure dissipation (Knight Piésold 2019p; Marr 2019).

Preliminary stability analyses that evaluated the potential effects of tailings liquefaction on the stability of the centerline portion of the bulk TSF main embankment following liquefaction are provided in Knight Piésold (2019p), PLP 2019-RFI 008g, and PLP 2019-RFI 008h. Post-liquefaction analysis of the downstream-constructed embankment under Alternative 2 is provided in PLP 2019-RFI 130. The different cases evaluated are summarized in Table K4.15-11. These assessments were conducted using a limited equilibrium model executed in SLOPE/W. The Morgenstern-Price method was used to estimate the FoS for any given slip surface considered. The method evaluates the effect of tailings liquefaction on FoS but does not provide an estimate of potential deformation along the slip surface. A minimum acceptance criterion of FoS = 1.2 was selected for post-earthquake or post-liquefaction conditions based on Canadian Dam Association (CDA 2014) guidelines.

Table K4.15-11: Post-Liquefaction Stability Cases Evaluated for Bulk TSF Main Embankment

Failure Direction	Depth of Liquefaction (feet)	Tailings Volume/ Density Change	Phreatic Surface	Slip Surface	Result	Reference
Modified Centerline Construction (Applicant's Preferred Alternative, Alternative 1, and Alternative 3)						
Upstream	100	None	Normal operating condition[2]	Extends to about 30 feet deep in liquefied tailings at FoS = 1.2	Rockfill placed on top of tailings would likely undergo settlement; deformations constrained to upstream direction with no containment failure or loss of freeboard	Knight Piésold 2019p: Case 1
Upstream	Full depth	None	Normal operating condition[2]	Extends to about 40 feet deep in liquefied tailings at FoS = 1.2	Rockfill placed on top of tailings would likely undergo settlement; deformations constrained to upstream direction with no containment failure or loss of freeboard	PLP 2019-RFI 008h: Figure 2
Upstream	100	Reduced tailings volume commensurate with 20% strain[1], and increased pond depth up to 15 feet	Normal operating condition[2]	Extends to about 80 feet deep in liquefied tailings at FoS = 1.2	Rockfill placed on top of tailings would likely undergo settlement; deformations constrained to upstream direction with no containment failure or loss of freeboard	Knight Piésold 2019p: Case 2
Downstream	100	None	Normal operating condition[2]	Extends from dam crest to toe; does not go through tailings	Tailings liquefaction does not affect global stability of downstream shell; FoS > 1.8	Knight Piésold 2019p: Case 3, Figure A.3a
Downstream	100	None	Higher phreatic surface: just below crest for ½ width of crest[3]	Extends from dam crest to toe; does not go through tailings	Tailings liquefaction does not affect global stability of downstream shell; FoS = 1.8 to 2, slightly lower than normal phreatic surface case	PLP 2019-RFI 008h: Figure 5

Table K4.15-11: Post-Liquefaction Stability Cases Evaluated for Bulk TSF Main Embankment

Failure Direction	Depth of Liquefaction (feet)	Tailings Volume/ Density Change	Phreatic Surface	Slip Surface	Result	Reference
Downstream	100	Reduced tailings volume commensurate with 20% strain[1], and increased pond depth up to 15 feet	Normal operating condition[2]	Extends from dam crest to toe; does not go through tailings	Tailings liquefaction does not affect global stability of downstream shell; FoS > 1.8	Knight Piésold 2019p: Case 3, Figure A.3b
Downstream	Full depth	None	Normal operating condition[2]	Extends from dam crest to toe; does not go through tailings	Tailings liquefaction does not affect global stability of downstream shell; FoS > 1.8	PLP 2019-RFI 008h: Figure 4
Downstream	Slip surface at bottom of centerline portion of embankment (top of starter dam), 280 feet deep	Tailings unit weight increased to 120 pcf	Normal operating condition[2]	Slip surface forced through embankment at top of starter dam; extends through about 500 feet of tailings upstream and about ½ of embankment width downstream	Slight reduction in FoS (~ 4.0) due to increased tailings density	Knight Piésold 2019p: Case 3, Figure A.4
Downstream Construction (Alternative 2)						
Downstream	Full depth	None	Normal operating condition[2]	Extends from dam crest to toe; does not go through tailings	Tailings liquefaction does not affect global stability of downstream shell; FoS > 1.8	PLP 2019-RFI 130: Figure 1

Notes:
[1]Tailings volume change results from tailings unit weight increase from 90 to 95 pcf.
[2]Phreatic surface drops steeply through coarse tailings and engineered filter zones, as designed.
[3]Assumes engineered filter zones fully blocked, and drainage capacity provided by downstream rockfill shell.
FoS = factor of safety
pcf = pounds per cubic foot
TSF = tailings storage facility

Three cases in Table K4.15-11 evaluated stability in an upstream direction of the portion of embankment rockfill that is centerline-raised on top of tailings beach material. These cases looked at 1) the effect of reducing the volume of tailings post-liquefaction due to expulsion of porewater and contraction of the solid particles; and 2) varying the depth of liquefaction from 100 feet to the full depth of the tailings. In all upstream cases, tailings liquefaction would result in some deformation of the embankment rockfill, particularly the upstream edge of rockfill that is constructed on top of the tailings beach. However, the deformations are expected to be constrained in the upstream zone of the dam due to the buttressing effect of the tailings and would cause no loss of freeboard or compromise to the integrity of the embankment.

Six cases in Table K4.15-11 evaluated the effect of tailings liquefaction on global embankment stability in a downstream direction. Like the upstream cases, the downstream cases evaluated the effect of reducing the tailings volume (increasing tailings density) and varying the depth of liquefaction. In addition, these cases also evaluated the effect of: 1) increasing the phreatic surface by assuming that the engineered filter zone is fully blocked; 2) a slip surface that extends through both the tailings and about half of the embankment; and 3) downstream construction (versus modified centerline). In all downstream cases evaluated, tailings liquefaction does not affect the global stability of the embankment and the FoS remains well above the target of 1.2.

As described in Chapter 5, Mitigation, PLP has committed to conducting additional tailings testing and deformation analyses as part of the preliminary and detailed design processes. Details on the configuration of the upstream zone and the critical filter zones in the embankment would be developed as the design advances. Detailed stability analyses using FLAC, a finite difference program, would be completed to evaluate potential embankment deformation and displacements under seismic loading and post-liquefaction conditions (PLP 2019-RFI 008g, PLP 2019-RFI 008h; Knight Piésold 2019p).

An independent review of the above analyses by AECOM (2019n) identified several areas of uncertainty regarding the liquefaction analyses and effects on embankment stability:

- It is uncertain whether the thickened tailings at 55 percent solids would segregate enough, with coarse tailings forming the tailings beach near the spigots and finer tailings in the middle of the impoundment, to promote reduction of the phreatic surface near the bulk TSF main embankment, which has implications for embankment stability. The coarse fraction of the tailings is expected to consist primarily of silty fine sand (Figure K4.15-2). Future tailings testing and analysis committed to by PLP in PLP 2019-RFI 008h and described in Chapter 5, Mitigation, would further the understanding of tailings deposition behavior and help address this concern.
- Uncertainties remain regarding the range of embankment stability effects under different phreatic surface, pore pressure, and ground shaking conditions, leading to lingering concerns that some and perhaps all of the entire centerline part of the bulk TSF main embankment (not just the shallow raises) could slide into potentially undrained tailings and have consequent effects in a downstream direction. Future stability analyses planned during the preliminary and detailed designs would reduce these uncertainties. Additional recommendations are provided in Appendix M1.0, Mitigation Assessment, for incorporating the following in the future stability analyses:
    - Continue to evaluate tailings liquefaction under static conditions and for liquefaction depths up to the full depth of the centerline portion of the embankment
    - Include a tailings liquefaction case during an earthquake (not just after), when strong ground motions cause pore pressures to increase leading to liquefaction; the seismic cases should be based on a full time-dependent dynamic analysis that

includes pore pressure effects (FLAC or equivalent) implemented for each applicable earthquake time history

- Include additional cases assuming deeper slide planes in the centerline raises and through the full embankment section
- Assume shallower phreatic surfaces and increased pore pressures in the embankment materials, including cases where flow-through is impeded in the rockfill downstream of the engineered filter zones and seeps out of the face of the embankment

Numerical Modeling—As described under the "Preliminary Pseudo-static Analysis" subsection, the Bray method provides a preliminary estimate of potential displacement that accounts for some of the dynamic characteristics of earthquake ground motions in the foundation material and rockfill embankment. However, it is acknowledged that the design of the mine site embankments is at a conceptual stage, and dynamic response analyses using numerical modeling methods would need to be carried out to further evaluate the potential amplification of seismic waves as they propagate through the foundation material, tailings deposit, and embankments (Knight Piésold 2019d). ADNR (2017a) indicates that for high-hazard dams (Class I and II) located in a highly seismic region with PGA values greater than about 0.3 to 0.4 g (which is the case at the Pebble mine site), seismic design should use advanced modeling techniques to more accurately model the behavior of materials subject to earthquake loading.

The application of numerical modeling to the design at its current conceptual stage would be inappropriate, as it would rely on ongoing geotechnical analyses that have not been completed yet. PLP (PLP 2018-RFI 008a; PLP 2019-RFI 008g) has committed to conducting additional detailed modeling, including FLAC analyses during detailed design of the facilities to better define embankment displacements under seismic loading and post-liquefaction conditions. The scope of additional seismic and stability analyses would be specified in an initial design package to ADSP to be negotiated after the EIS is complete, and the work would be completed as part of a later Preliminary Design package (PLP 2019-RFI 008g).

Concerns have been expressed regarding the potential for transverse (tensional) cracking of the bulk TSF main embankment, which is typically evaluated using finite element techniques that take into account boundary conditions and stress-strain characteristics of the materials. Appendix M1.0, Mitigation Assessment, provides a recommendation to address the potential for transverse cracking as part of numerical modeling studies in a later phase of design.

Post-Closure Phase—As described above under "Seismic Hazard Analysis," the mine site embankments would be designed to withstand an earthquake with a return period up to 10,000 years (Table K4.15-8). Two of the four MCEs selected as the MDE have PGA values greater than the 10,000-year probabilistic event (Table K4.15-9). Preliminary static, pseudo-static, and post-liquefaction stability analyses have been completed based on end-of-operations conditions when the pond, tailings, and phreatic surfaces would be at their maximum or highest condition. Given that tailings would continue to consolidate, runoff off the closure cover would be promoted and infiltration restricted, and the phreatic surface would continue to lower over time, the results of these analyses are expected to be protective of conditions following closure.

The tailings and dam SMEs at the EIS-phase FMEA technical meeting rated the likelihood of bulk TSF main embankment crest deformation in post-closure causing a breach to be very low (AECOM 2018l), given the results of preliminary stability analyses conducted to date, that the embankment would be constructed of compacted rockfill founded on bedrock with limited potential for dynamic settlement, and that design advancement would include further seismic stability analysis.

The calculated ground shaking estimates used in the seismic hazard analyses assume a design life of 50 years, which extends 30 years into the closure period. As indicated in Knight Piésold (2019d: Figure 3.2), the effect of extending the design life would be to increase ground shaking predictions. For example, an OBE with a PGA of 0.16g based on a 50-year design life (Table K4.15-8) would increase to a PGA of about 0.21g if the design life were doubled to 100 years (80 years post-closure). These relationships break down at higher values of design life and ground shaking, however, as they do not account for the material strength of the earth and the inability of rocks to transmit energy above a finite limit.

The extreme earthquake events selected for the MDE would be used for initial TSF design, the design of ongoing raises during operations, and for closure, although subsequent events and other seismic scenarios may be considered during detailed closure design. Longer dam performance for closure of the TSFs would consider the potential additive effect of multiple seismically induced dam settlements over time, such as impacts on freeboard, the closure spillway, and other water management structures (Knight Piésold 2019d). As described in Chapter 5, Mitigation, stability and seepage analyses specific to the closure conditions of the facility would be conducted during detailed closure design and would include an independent panel review. These analyses would be updated as required under state permitting throughout the latter stages of operations.

During closure and post-closure, equipment and personnel would be maintained on site to support ongoing bulk TSF monitoring and water management activities (Chapter 5, Mitigation). In the event that an earthquake causes damage to the bulk TSF reclaim pipelines in post-closure, it is estimated that the time it would take for the bulk TSF main SCP to fill to capacity ranges from 3 weeks to 15 months, depending on precipitation conditions at the time. Redundant equipment would be stored onsite and available in the event repairs are required (PLP 2019-RFI 130).

K4.15.1.6 Analysis of Open Pit Wall Stability

Referring to Figure 2-4 and Figure K4.15-13, the open pit would be constructed in the easternmost portion of the mine site. The pit would be 6,800 by 5,600 feet in width and 1,970 feet deep (PLP 2020d). As described in Section 3.13, Geology, the geology of the open pit area is complex, and consists of a variety of rock types. The surface is blanketed with mostly glacial deposits that are underlain by bedrock consisting of a mixture of Mesozoic andesitic sedimentary flysch with Cretaceous quartz monzodiorite, granodiorite, and diorite sills.

Methods and Input Parameters—Pit wall stability analyses were calculated by SRK (2018c, 2019b) and PLP (PLP 2018-RFI 023a; PLP 2019-RFI 023b) through four sections of the pit, as shown on Figure K4.15-14 and summarized in Table 4.15-2. The method used in modeling was a finite element analysis for static stability using the two-dimensional software RS2 (RocScience 2018), with horizontal peak ground acceleration applied in a dynamic (pseudo-static) case to analyze the effect of earthquake loading on the pit walls (SRK 2019b). Geotechnical parameters used in the model are listed in Table K4.15-12 for three rock domains, as well as for joints and fault features that were within 30 degrees of the vertical plane of each section analyzed.

Input parameters also included disturbance (D) factors that represent zones of bedrock damage caused by relaxation and rebound of the rock mass from pit excavation and blast damage close to the excavation surface (Hoek 2012). Values of D can range from 0 for undamaged rock to 1.0 for highly disturbed rock. Three D zone thresholds were used in the pit wall model: 0.85 at about 100 feet behind the bench face, and 0.7 and 0.5 at successively shorter distances behind the pit walls (PLP 2018-RFI 023a).

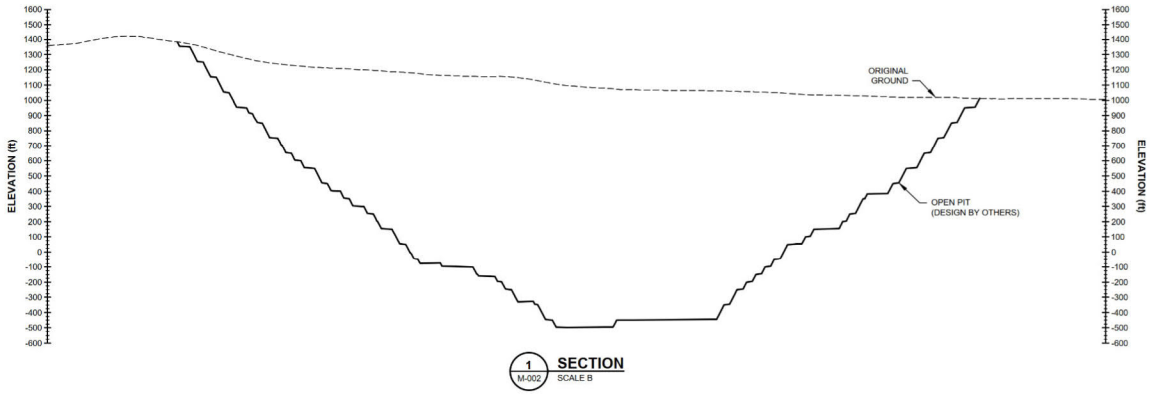

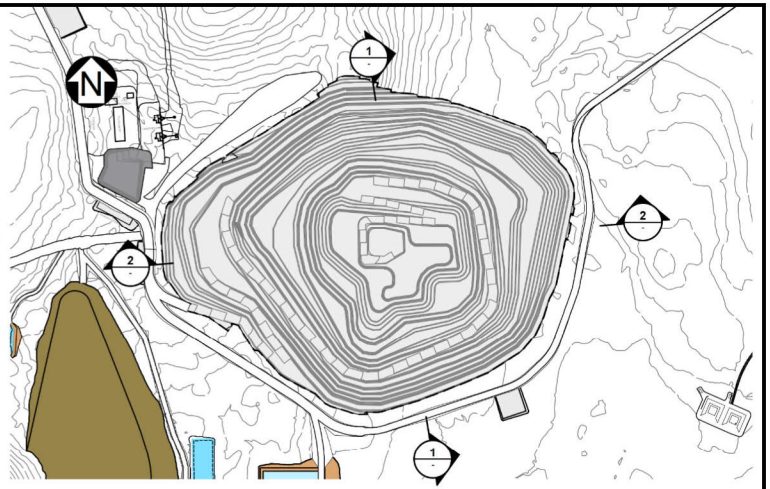

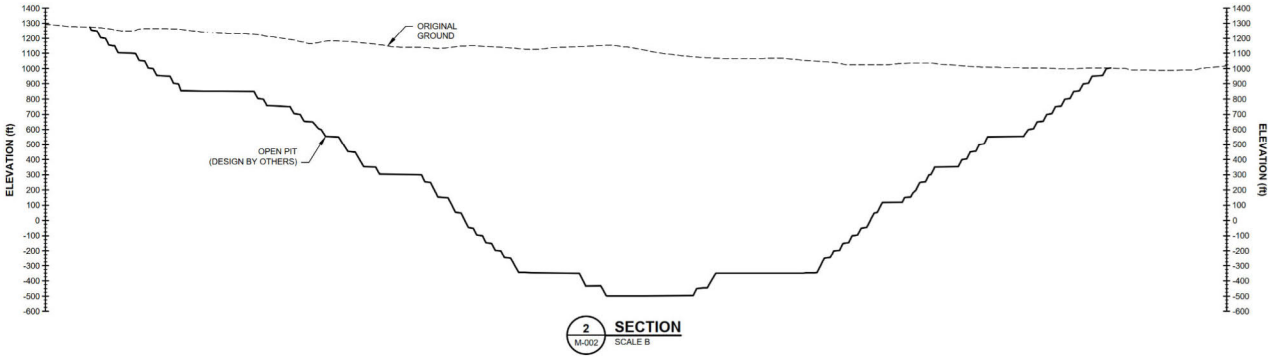

NOTES:

1. COORDINATE GRID IS UTM NAD 83, ALASKA STATE PLANES ZONE 5.
2. CONTOUR INTERVAL IS 25 FEET.
3. DIMENSIONS AND ELEVATIONS ARE IN FEET, UNLESS NOTED OTHERWISE.
4. OPEN PIT SURFACE PROVIDED BY TETRA TECH JUNE 2019.

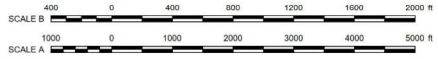

Source: PLP 2019h

US Army Corps of Engineers®

OPEN PIT TOPOGRAPHIC CROSS-SECTION

PEBBLE PROJECT EIS

FIGURE K4.15-13

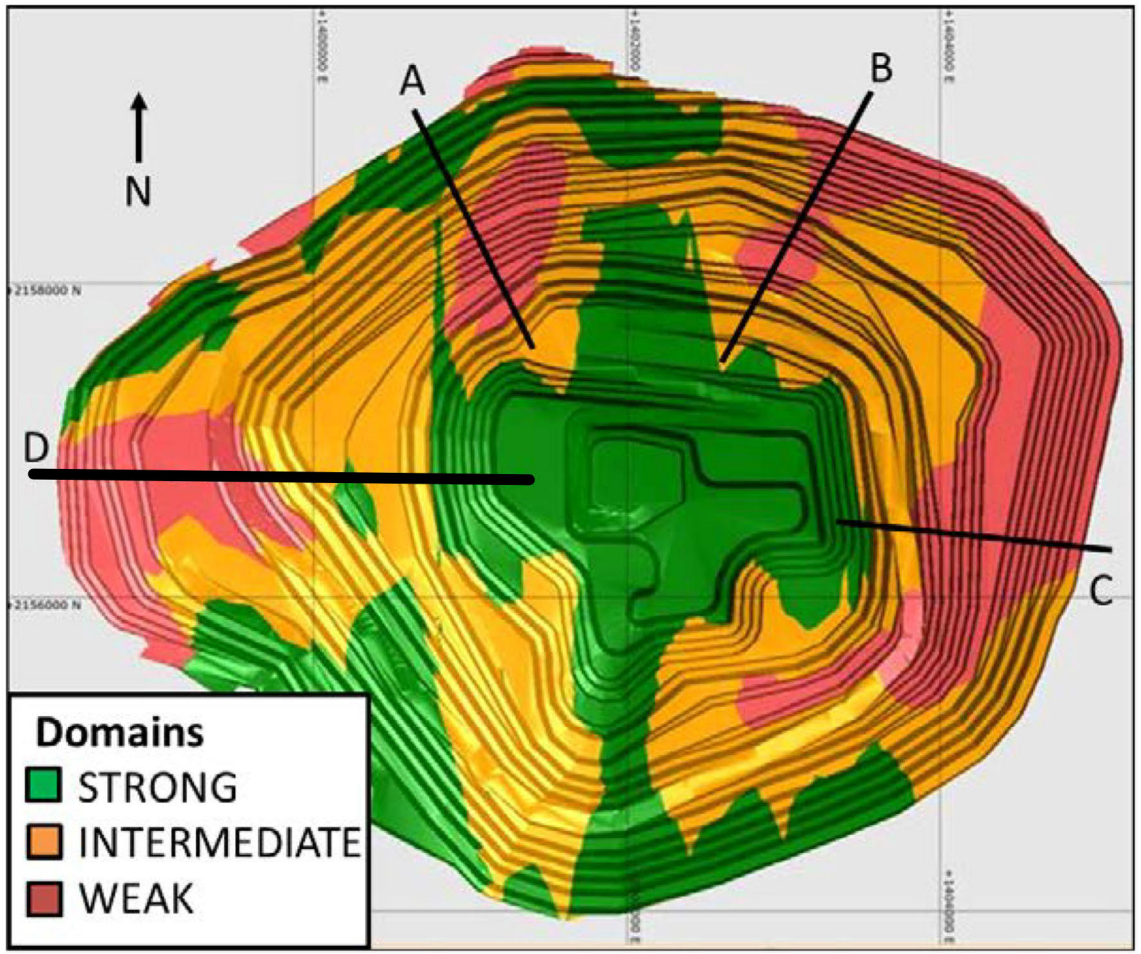

Source: SRK 2019b; PLP 2019-RFI023b

US Army Corps of Engineers

GEOTECHNICAL DOMAINS AND PIT WALL STABILITY SECTIONS

PEBBLE PROJECT EIS

FIGURE K4.15-14

Table K4.15-12: Pit Wall Stability Modeling Input Parameters

Cretaceous Rock Domain	Intact Rock Strength (MPa)		Geological Strength Index	Material Constant (mi)	Youngs Modulus (MPa)	Specific Gravity
	Base Case	Reduced Values Used in Senstivity Analysis				
Weak	27	20	34	17	16,875	2.61
Intermediate	47	35	39	21	27,965	2.66
Strong	66	50	42	25	35,970	2.63
Faults	10	10	25	5	2,000	2.61

Notes:
mi = intact material constant
MPa = mega pascal
Source: SRK 2018c

The modeling evaluated five different water table scenarios as shown in Figure K4.15-15:

1. At the end of operations with groundwater levels below the pit bottom and back from the walls due to dewatering
2. During early closure when active drains would still be used during in-pit backfilling of pyritic TSF materials
3. After discontinuation of groundwater drawdown when the water table begins to rebound
4. With water levels recovered to about a half full pit lake, to evaluate the effect of the lake in buttressing certain unstable slopes
5. After the lake has filled to its final managed lake level

Based on industry guidance (Martin and Stacey 2018), a PGA of half of 0.14g (slightly less than the 1-in-475-year earthquake from the probabilistic seismic hazard analysis, and similar to the OBE selected for embankment design [Table K4.15-8]), was used for the dynamic (seismic) modeling base case. The use of half the PGA is derived from documented experiences at a number of open pit mines in South America and Asia, in which few significant slope instabilities have been produced following major earthquakes, even as slope monitoring devices confirmed high ground-shaking levels. Studies suggest several possible factors for this: 1) natural slope failures commonly occur on ridgetops due to topographic amplification, which may not occur on one-face or valley-face pit slopes; 2) the amplification, if present in pit slopes, is too weak to promote failure or the rock mass is too strong; 3) cut slopes reduce the stiffness contrast amplification between bedrock and overburden compared to natural slopes; and 4) active open pit slopes are typically dewatered, whereas natural slopes are not (Read and Stacey 2009; Azhari 2016).

A sensitivity analysis was conducted to evaluate the effect of increasing earthquake size on wall stability using the most unstable water table scenario, that of early closure after the dewatering pumps have been turned off and the water table begins to rebound. In this analysis, three different levels of ground shaking were evaluated, with PGAs set at half of 0.1g, 0.2g, and 0.3g.

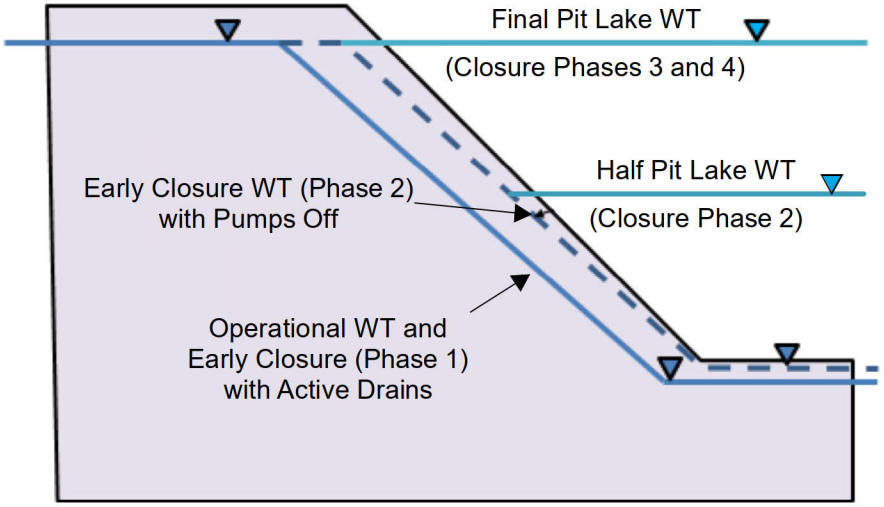

Source: PLP 2019-RFI023b

US Army Corps of Engineers®

WATER TABLE SCENARIOS EXAMINED IN PIT WALL STABILITY ANALYSIS

PEBBLE PROJECT EIS

FIGURE K4.15-15

An additional sensitivity analysis was run on the wall section with the lowest initial FoS results (section A) to test the effect of 25 percent less strength parameters for the three rock strength categories than those used in the base case (Table K4.15-12). This analysis utilized a finite element deformation model, FLAC3D (Itasca 2017), to remodel section A during the worst water table condition (that of early closure with dewatering pumps turned off) using the same input parameters as those used in the R2S model, then reduced the input parameters to the weaker rock assumptions. The strength of the fault domains was not altered in this analysis.

Initial Stability Modeling Results—Table 4.15-2 presents the initial results of the open pit wall modeling. The minimum acceptable FoS for the open pit walls during operations was set at 1.3 for static conditions and 1.05 for dynamic conditions (Read and Stacey 2009). These values were selected as the upper bound, because there is only a single entry into the pit, and any instability involving the ramp would likely result in a loss of production. Acceptance criteria for the pit just after closure would be set at 1.1 because of the lack of access required into the pit during this time, but this would be reviewed during detailed design.

The initial results indicate an FoS below 1.1 for section A on the northwest side of the pit under both static and dynamic conditions during the worst scenario, that of early closure after dewatering pumps are turned off and the water table has rebounded. Two inactive faults that intersect section A appear to affect wall stability in this area, along with heavily jointed rock represented by the white cross-hatching in Figure K4.15-16 and Figure K4.15-17. The results for sections B through D indicated an FoS of 1.1 or greater.

The modeling that simulates the end of operations represents the maximum depressurized wall height prior to lake development. As the pit is deepened, there do not appear to be any large intersections of weaker rock exposed, other than localized areas near the faults. Future designs would investigate improved optimization angles of the interim walls. At closure, the pit walls would be stabilized and monitored to meet ADNR (2006) requirements so that they would not be expected to collapse (PLP 2018-RFI 024). However, the results for section A in early closure suggest that depressurization caused by dewatering and lowering the water table would need to continue until the pit lake rise could buttress/stabilize the area of potential instability, which is below the faults.

The results of the early closure scenario with active drains continuing and the half-full pit lake analysis for section A (Figure K4.15-16 and Figure K4.15-17), indicate FoSs for the two scenarios of 1.3 and 1.4, respectively. This suggests that with continued depressurization in the localized area of section A during early closure activities (e.g., backfilling), the wall stability would meet acceptability criteria, and that when the pit lake rises to above the level of fault instability, the buttressing effect of the lake improves the FoS to above the target criteria.

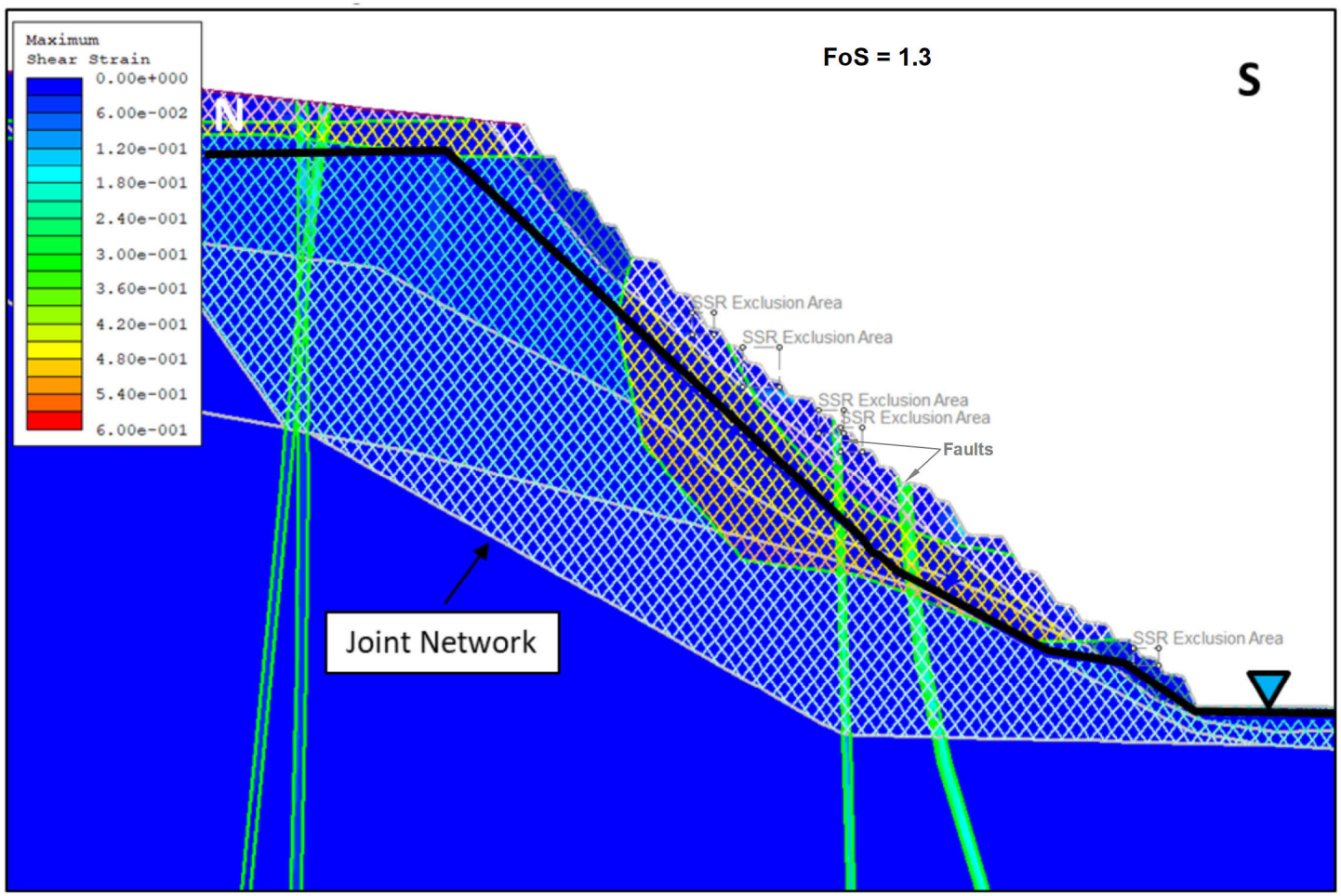

Note: Shows pit water table below the faults in the slope

Source: PLP 2018-RFI 023a; PLP 2019-RFI023b

US Army Corps of Engineers®

PIT WALL STABILITY SECTION A - SCENARIO WITH ACTIVE DRAINS IN EARLY CLOSURE

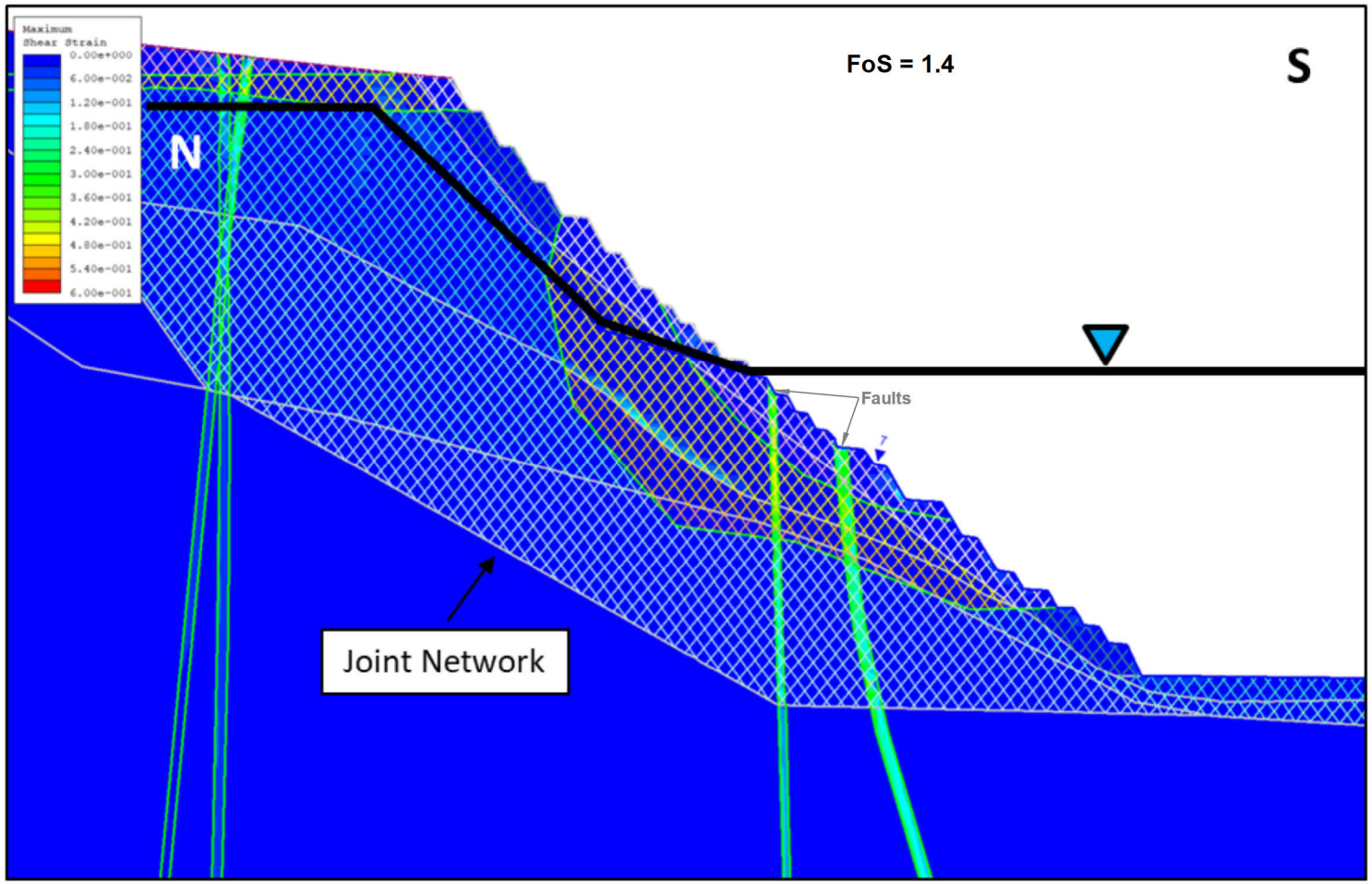

Note: Shows pit lake above the faults in the slope

Source: PLP 2018-RFI023a; PLP 2019-RFI023b

US Army Corps of Engineers

PIT WALL STABILITY SECTION A - SCENARIO WITH HALF-FULL PIT LAKE

PEBBLE PROJECT EIS

FIGURE K4.15-17

Sensitivity Analyses—The results of the sensitivity analysis for earthquake ground-shaking levels are summarized in Table K4.15-13. These were conducted for the worst early closure scenario in which the dewatering pumps have been turned off and the water table has rebounded. The results indicate that in addition to the unstable condition at section A during the early closure described above, section D reaches an unstable FoS (below the target criteria of 1.05) at ground-shaking levels above a PGA of 0.20g, which is roughly equivalent to the 1 in 1,000-year earthquake in the probabilistic seismic hazard analysis (Table K4.15-8).

Table K4.15-13: Pit Wall Stability Sensitivity Analysis for Various Values of PGA

Section[1]	FoS for PGA = 0.10[2]	FoS for PGA = 0.14 (Base Case[3])	FoS for PGA = 0.20	FoS for PGA = 0.30
A	0.8	0.7	0.7	0.7
B	1.4	1.2	1.1	1.1
C	1.1	1.1	1.0	0.9
D	1.3	1.2	1.1	1.1

Notes:
[1]Results are for the worst scenario from the initial modeling results (Table 4.15-3), which is during early closure after dewatering pumps are off.
[2]All PGAs used in the model are half of those shown due to industry experience with lack of significant wall failures following major earthquakes, as described in text (Read and Stacey 2009).
[3]Same as the results presented in Table 4.15-3 for dynamic analysis.
Source: SRK 2019b; PLP 2019-RFI 023b.

The results of the sensitivity analysis that examined the effect of reducing the rock strength parameters in the model for the worst early closure scenario at section A are depicted in Figure K4.15-18. While the initial model results highlighted the area of fault instability in the lower part of the wall, the sensitivity results with the weaker rock assumptions showed the potential for increased risk of movement associated with a fault zone higher in the section, which intersects the ground surface about 650 feet back from the pit rim (Figure K4.15-19). The results are considered conservative in that they do not take into account the buttressing effect of the backfilled tailings and waste rock, which would be placed in the pit as the water table rebounds (Knight Piésold 2018d: Figure 5.1).

The risk of failure along section A would be highest during the phase 2 closure period when the water table is rebounding, but before the lake provides additional buttressing capacity above the backfilled material. According to Knight Piésold (2018d), this period of time could last for about 15 years, extending from about the middle of the closure phase 1 (closure years 5-10 when some of the backfill is complete and lower dewatering pumps may be turned off) to about closure year 20 at the end of phase 2 when the pit lake is at its final level. In post-closure (lake at final level), about 450 vertical feet of the section A weaker rock near the upper fault would remain exposed without any active drains or buttressing by the lake, based on the difference in elevation between the final lake level (890 feet) and the northwest pit rim (about 1,340 feet).

Chemical and physical weathering of the pit slopes could have an added effect on slope instability. Long-term mineralization alteration from core yard observations was taken into account in assigning slopes to the weak rock category in the model. Additional physical (freeze/thaw) weathering could occur on the slopes over time. This is expected to be a surface effect, extending roughly 50 to 100 feet into the slopes, which could result in sloughing at bench crests and inter-ramp slopes, but is unlikely to result in deep-seated failure (SRK 2019b).

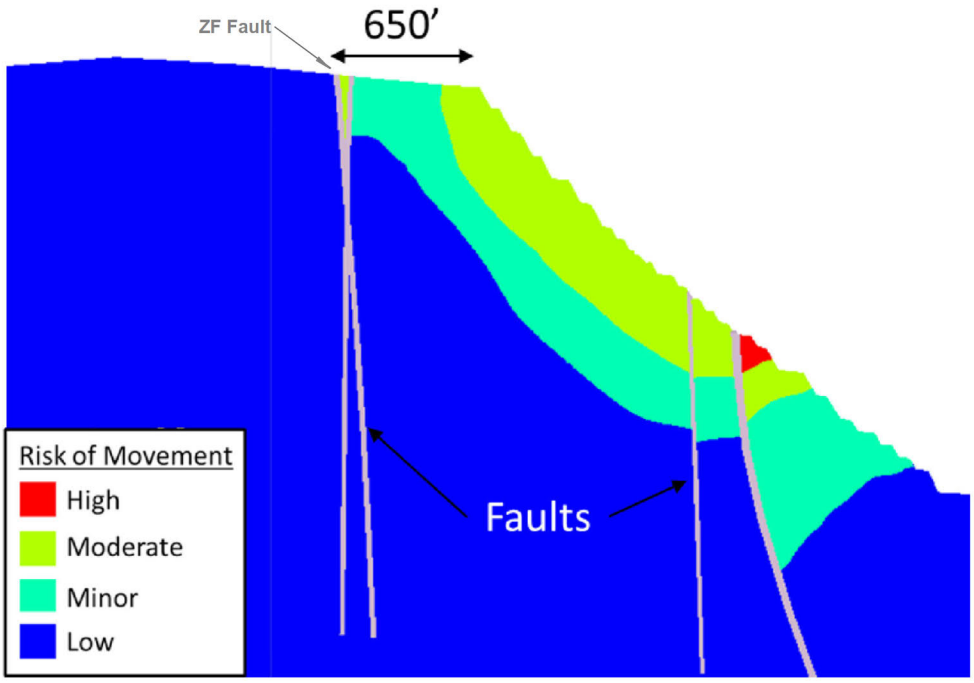

Figure K4.15-18a: FLAC3d model of section A showing the extent of failure risks using base case input parameters for rock strength.

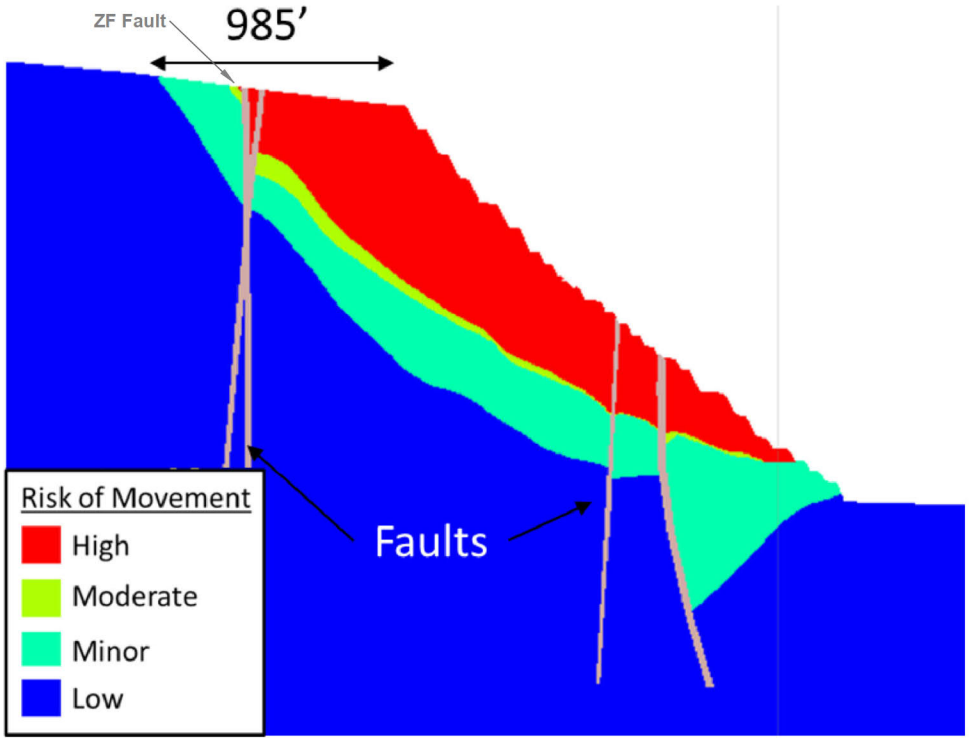

Figure K4.15-18b: FLAC3d model of section A showing the extent of failure risks using 25% weaker rock strength parameters.

Source: SRK 2019b; PLP 2019-RFI023b

US Army Corps of Engineers

PIT WALL STABILITY SENSITIVITY ANALYSIS - REDUCTION IN ROCK STRENGTH PARAMETERS

PEBBLE PROJECT EIS

FIGURE K4.15-18

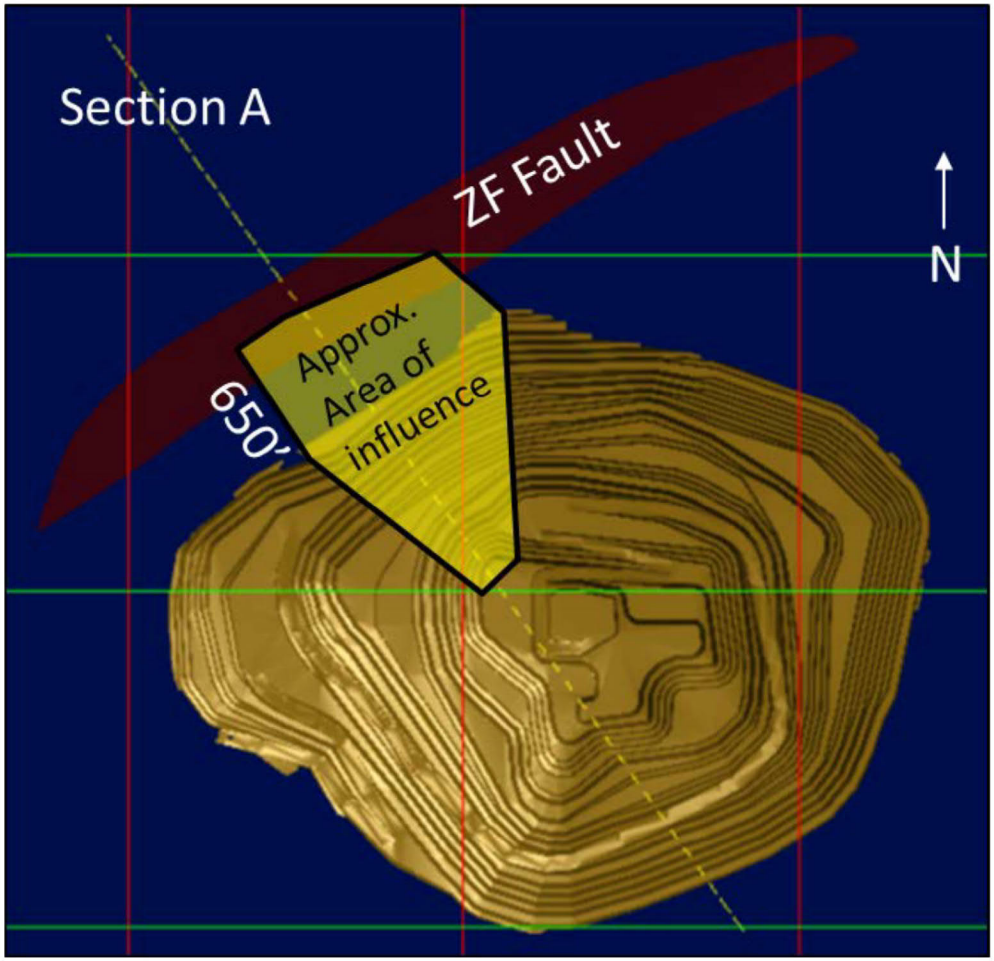

Source: SRK 2019b; PLP 2019-RFI023b

US Army Corps
of Engineers®

AREA OF FAULT INFLUENCE ON SECTION A PIT WALL INSTABILITY

PEBBLE PROJECT EIS

FIGURE K4.15-19

Landslide-Induced Pit Lake Wave—Based on the results of the seismic stability case for the pit walls (see Table 4.15-3), an analysis was conducted to examine the effect of a potential earthquake-induced landslide into the full pit lake in post-closure, and the likelihood that such an event could create a tsunami wave that overtops the pit rim. Tsunamis were computed for two potential landslide scenarios, along sections A and D (Figure K4.15-14). These were selected because they exhibited the lowest FoSs in the dynamic (seismic) stability analysis in Table 4.15-3 for the full pit lake scenario (FoSs of 1.4 and 1.1, respectively). Low FoS cases in the seismic sensitivity analysis shown in Table K4.15-13 were not considered in this analysis, because they assumed no pit lake is present.

The methods and results of the tsunami modeling are presented in AECOM (2019p, 2020). The dimensions of the slides assumed in the model were based on approximations of weak rock zones in figures and cross-sections (see Figure K4.15-14 and Figure K4.14-18; SRK 2019b: Figure 13). Slide dimensions assumed for section A were 1,600 feet wide by 660 feet long by 330 feet thick, or a total of about 13 million cubic yards (cy); dimensions assumed for section D were 980 feet wide by 660 feet long by 160 feet thick, or a total of about 4 million cy. These dimensions were considered conservative in that adjacent areas of intermediate strength rock were included, and the backfilled tailings and waste rock would have a buttressing effect on deep (thick) failure surfaces.

The lake depth was initially assumed to be 250 feet in AECOM (2019p) model runs, based on final water surface and lake bottom elevations of 890 feet and 640 feet, respectively, as provided in an early version of the *Pebble Mine Site Operations Water Management Plan* (Knight Piésold 2018d). Additional model runs were later conducted assuming a deeper lake depth of 420 feet (final water surface elevation and lake bottom elevations of 890 feet and 470 feet, respectively) based on revised mine plans (Knight Piésold 2019s). The initial acceleration value assumed in the model (i.e., the slope-parallel component of gravitational acceleration) was 20 ft/sec^2 and maximum velocity was 80 ft/sec. The initial acceleration is considered conservative because it assumes negligible bottom friction between the slide and lake bottom and between the slide and the water.

The tsunamis were computed using JAGURS (2019), a non-linear long-wave algorithm that is a standard approach used in tsunami computations. Initial maximum wave amplitudes of up to approximately 300 feet (Figure K4.15-20) were propagated around the lake in model runs conducted for both lake depth scenarios. Even with the conservative approximations, the waves do not overtop the rim, although they reach close to the rim in the slide scenario for Section A under both lake depths.

K4.15.2 Port Sites

The port sites would be at Amakdedori for Alternative 1a and Alternative 1, at Diamond Point for Alternative 2, and just north of Diamond Point for Alternative 3 (see Figure 2-1). As shown in Figure K4.15-10, the port sites are situated in a seismically active area. Therefore, seismic hazard analyses were conducted for the port sites in conjunction with the analysis for the mine site using the same methods, including analyses of probabilistic and deterministic seismic hazards.

K4.15.2.1 Probabilistic Seismic Hazard Analysis

Table K4.15-14 shows the results of the probabilistic seismic hazard analyses completed for the two port sites.

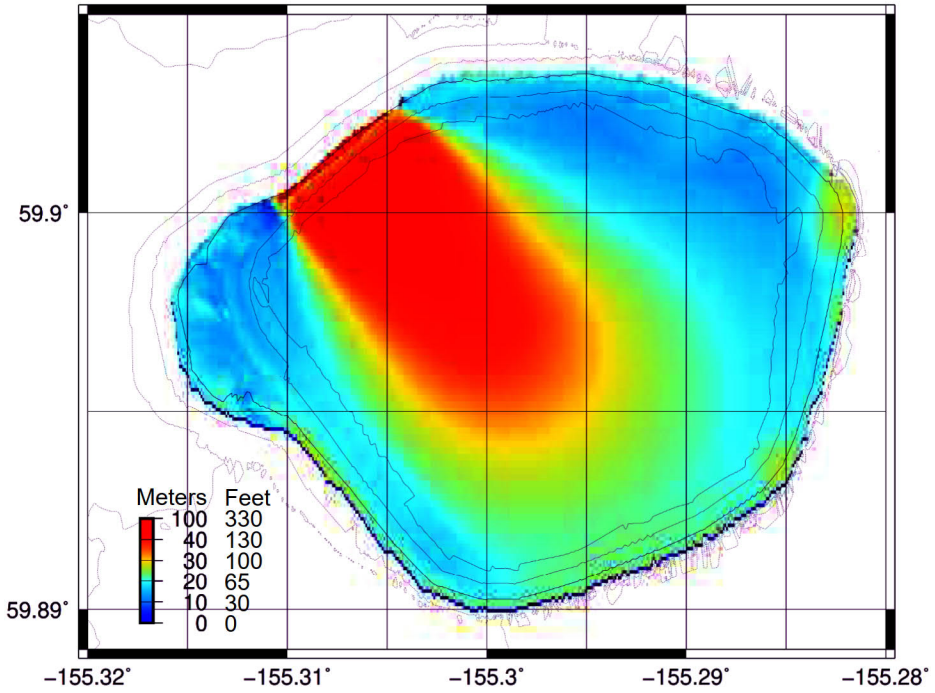

Figure K4.15-20a: Maximum wave amplitudes for Slide A scenario.

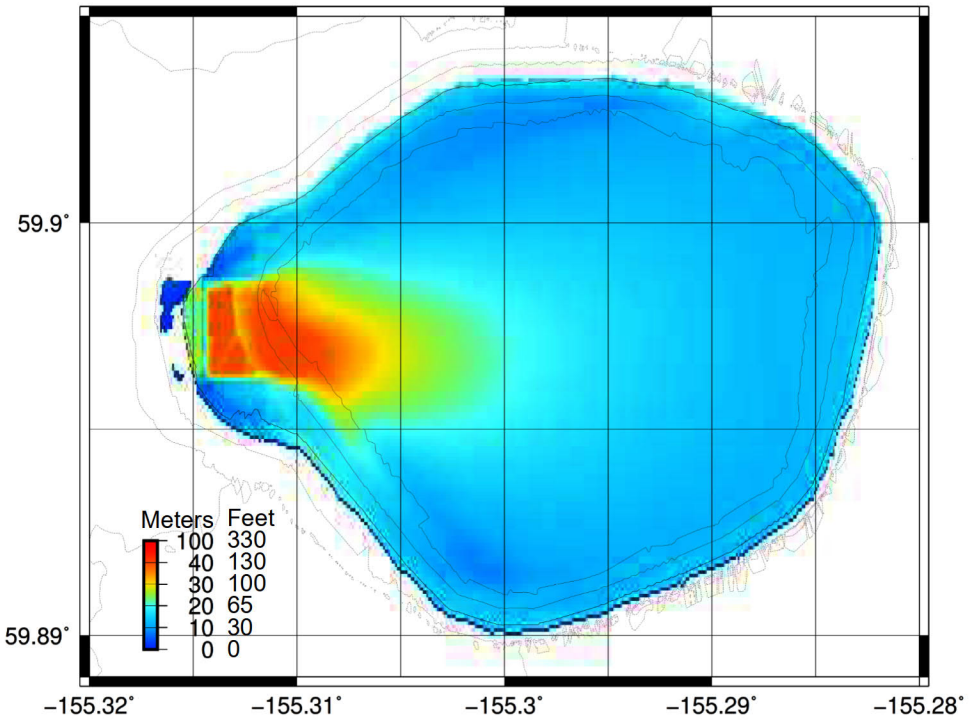

Figure K4.15-20b: Maximum wave amplitudes for Slide D scenario.

Source: AECOM 2020

US Army Corps of Engineers

MAXIMUM WAVE AMPLITUDES FOR EARTHQUAKE-INDUCED LANDSLIDES INTO PIT LAKE

PEBBLE PROJECT EIS

FIGURE K4.15-20

Table K4.15-14: Probabilistic Seismic Hazard Analysis for Port Sites

Return Period (Years)	Probability of Exceedance[1] (%)	Peak Ground Acceleration[2,3] (g)	
		Amakdedori (Alternative 1a and Alternative 1)	Diamond Point (Alternative 2 and Alternative 3)
50	63	0.12	0.13
100	39	0.16	0.18
200	22	0.22	0.24
475	10	0.30	0.34
1,000	5	0.39	0.42
2,500	2	0.51	0.56
5,000	1	0.61	0.66
10,000	0.5	0.74	0.79

Notes:
[1] Probability of exceedance calculated for a design life of 50 years: Q = 1 - exp (-L/T). Where Q = probability of exceedance, L = design life in years, T = return period in years.
[2] Maximum accelerations are for values on firm rock.
[3] Information based on the USGS Seismic Hazard Program 2007 database.
Source: Knight Piésold 2019d: Table 3.2

The dock would be designed to withstand an OBE with a return period of 475 years, and an MDE with a return period of 2,475 years (Knight Piésold 2013; PLP 2020-RFI 160). The estimated maximum accelerations for the 1-in-475-year and 1-in-2,500-year earthquakes are 0.30g and 0.51g, respectively, for Amakdedori, or nearly double that predicted for the mine site (Table K4.15-8). This reflects the closer proximity of the port to the potential intraslab subduction earthquakes shown in Figure K4.15-10 and Figure K4.15-11. Ground shaking effects at the Diamond Point port site are slightly higher than those at Amakdedori, with maximum accelerations for the 1-in-475-year and 1-in-2,500-year earthquakes of 0.34g and 0.56g, respectively.

K4.15.2.2 Deterministic Seismic Hazard Analysis

Table K4.15-15 shows the results of a deterministic analysis for the port sites based on the regional seismic sources.

Table K4.15-15: Deterministic Seismic Hazard Analysis for Port Sites

Earthquake Source Type	Earthquake Source Name	Source/ Fault Mechanism	Maximum Magnitude (Mw)	Epicentral Distance (miles)		Focal Depth (miles)	Peak Ground Acceleration[1]			
							Median (g)		84th Percentile (g)	
				Amakdedori	Diamond Point		Amakdedori	Diamond Point	Amakdedori	Diamond Point
Interface Subduction[2]	Alaskan-Aleutian Megathrust	Thrust	9.2 (8.5)	70	70	25	0.15	0.15	0.29	0.29
Intraslab Subduction	Intraslab Event[3]	In-slab	7.5	35	35	45	0.24	0.24	0.48	0.48
			8.0	35	35	45	0.39	0.39	0.77	0.77
	Deep Intraslab Event[3]	In-slab	7.5	0	0	70	0.29	0.29	0.57	0.57
			8.0	0	0	70	0.49	0.49	0.96	0.96
Shallow Crustal Fault[4]	Lake Clark Fault	Reverse (Thrust)	7.5	59	48	3	0.05	0.06	0.08	0.10
	Bruin Bay Fault	Reverse (Thrust)	8.0	1.2	4.3	3	0.57	0.43	1.04	0.79
	Border Ranges Fault	Strike-slip	8.0	73	65	3	0.05	0.06	0.09	0.10
	Kodiak Island / Narrow Cape Faults	Strike-slip	7.5	130	150	3	0.01	0.01	0.02	0.02

Notes:
Mw: Moment magnitude
[1] PGAs are for values on firm rock.
[2] The PGA values for the interface subduction (megathrust) event have been calculated using a representative magnitude 8.5 event.
[3] See Figure K4.15-10 and Figure K4.15-11 for the locations of intraslab subduction earthquakes relative to the Pebble port sites (roughly 40 to 80 miles beneath and away from the port sites).
[4] The adopted faulting mechanism for each shallow crustal fault was based on a review of the available information for defining the fault type. The predominant faulting mechanism assumed for all shallow crustal faults is strike-slip, with the exception of the Bruin Bay and Lake Clark faults, for which reverse faulting was used.
Source: Knight Piésold 2019d: Tables 3.4 and 3.5

The deterministic values for the port sites are generally higher than those presented in Table K4.15-9 for the mine site, with the differences attributable to the respective proximities to the earthquake sources. The deterministic results predict a maximum credible acceleration of 1.04g for the Amakdedori port site location, resulting from a M8.0 earthquake on the nearby Bruin Bay fault. The location of the Bruin Bay fault relative to the two port sites (Figure K4.15-10) has a significant influence on the predicted peak ground motions. In contrast, the PGA at the Diamond Point site from the Bruin Bay fault would be 0.79g. A maximum ground shaking of 0.96g is predicted at both port sites from a deep intraslab earthquake of M8.0.

As described in Chapter 5, Mitigation, the exact location and geometry of the Bruin Bay fault relative to the Amakdedori port site would be reviewed in future studies to confirm the minimum distance between the potential rupture area and the port site, and the maximum ground shaking predictions that would need to be incorporated into port design.

K4.15.2.3 Foundation Conditions at Port Sites

As described in Section 3.15, Geohazards and Seismic Conditions, available subsurface foundation information for the Amakdedori dock site is limited and includes two vibracores to a depth of 3 feet below mudline, a multibeam bathymetric survey, and extrapolation of onshore geophysical data. Near-surface deposits consist mainly of silty sand and gravel, and shallow bedrock may be present (PLP 2018-RFI 039, PLP 2019b; Zonge 2017).

Information on subsurface foundation conditions at the Diamond Point dock sites is also limited. Water depth is shallower at these locations than at Amakdedori, which would require dredging a navigation channel to an elevation of about -18 to -20 feet MLLW (PLP 2020d). Iliamna and Iniskin bays have a mantle of unconsolidated, fine-grained sediment, with particle size typically decreasing with water depth and distance from the shoreline. Coarse-grained sediments with cobbles and boulders occur along the shorelines of both bays (Knight Piésold 2011d). More detailed subsurface foundation information is available for Williamsport, about 3 miles north of Diamond Point. Based on geotechnical borings and a geophysical survey completed by USACE in 1995, depth to bedrock in the vicinity of the existing dock ranges between approximately 65 and 130 feet, and is mainly overlain by fine-grained sediments. Based on available geophysical data, bedrock is not expected to be present to a depth of more than 100 feet at the Alternative 3 dock site (PLP 2020d).

K4.15.2.4 Stability of Sheet Pile Dock

A rockfill causeway and sheet pile dock design is proposed as the base case for the port at Amakdedori under Alternative 1 and the port at Diamond Point under Alternative 2. As described in Chapter 2, Alternatives, at Amakdedori port this would consist of a causeway constructed of an earthfill embankment, and a barge berth and wharf constructed of a sheet pile wall wharf structure filled with granular material (see Figure 2-28 and Figure 2-29). The Diamond Point port would use the same base case design concept as the Amakdedori port, but would have a different, larger layout (see Figure 2-51).

The stability of port structures is typically determined through stability analyses conducted under both static and seismic conditions. Inputs are based on water depths, tidal fluctuations, winter ice formations, subsurface geotechnical conditions, construction materials, and proposed design features. Material site characterization and stability analyses would be conducted for the respective ports' major structures (such as the terminal patio and sheet pile wharf) during final design (PLP 2018-RFI 005).

Design details available for the sheet pile dock at the Amakdedori site are provided in PLP (2018-RFI 005). Construction of the Amakdedori terminal would require installing approximately 2,200

lineal feet of protected rock slope along an access causeway, and 2,000 lineal feet (in plan) of steel sheet piles that may be 110 feet long (the length may be as short as 50 feet), with tie-backs into the fill behind the sheets to provide sufficient lateral capacity. The lineal sheet pile and tie-back design proposed for the wharf is not considered as vulnerable to an "unzipping" type of failure in a large earthquake as the open-cell structure at the Port of Anchorage (CH2MHill 2013). The sheet piles would be installed in 15 to 20 feet of water. The causeway would be constructed by infilling on top of the seabed with competent fill and rock protection for the slopes. The sheet piles would be installed using a vibratory hammer. If it is discovered that bedrock or similarly hard soil is within 20 to 30 feet of the design seabed elevation, driving the sheets for the last 1 to 2 feet may be required to anchor the sheets in the ground. If bedrock or similarly hard soil is found to be very shallow, pile socketing and a revised concept may be required. If investigations find that the seabed is susceptible to liquefaction under seismic conditions, soil improvement work such as stone column installation may be required (PLP 2018-RFI 005).

The types of impacts that could occur at the ports include structural instability and potential failure of the sheet pile wharf as a result of seismic loading or foundation conditions; erosion at the base of the sheet piles; icing that increases gravity load on the sheets; and corrosion requiring regular monitoring of cathodic protection systems. These impacts would be addressed as design progresses. Experience at other sheet pile docks in Cook Inlet (Port of Alaska, Port Mackenzie) suggest that these issues could also be of concern at the Amakdedori and Diamond Point port sites, as discussed below.

Although geotechnical conditions at the port site could be variable, bedrock may be sufficiently deep that marine structures would not need to be socketed, and that sheet piles could be designed for installation to a design embedment depth (PLP 2018-RFI 005). Subsurface conditions (e.g., buried sensitive clay layers like at the Port of Alaska) that have the potential to lead to translational failure of a structure in a major earthquake (Simpson Gumpertz and Heger 2013) likely do not exist at the Amakdedori port site where, based on the information available, subsurface deposits consist primarily of silty sand and gravel (see Section 3.15, Geohazards and Seismic Conditions). It is also unlikely but possible that these conditions exist at the Diamond Point site.

A stability analysis of the sheet pile wharf at the Amakdedori and Diamond port sites that takes seismic loads into account would be considered to be the state-of-the-practice for this type of structure in this seismic setting. The PGA for a major earthquake at this location could range from an estimated 0.3g to 0.5g for a 500-year to 2,500-year event, respectively (see Figure 3.15-2) (Wesson et al. 2007). These values are supported by the probabilistic seismic hazard analyses described above (Knight Piésold 2019d), which indicate a PGAs of 0.51g and 0.56g for the 2,500-year event at the Amakdedori and Diamond Point port sites, respectively. Additional seismic analyses would be completed before detailed design to support engineering and construction (PLP 2018-RFI 005).

Liquefaction of the seabed during a major earthquake could also cause wharf damage, although the expected sand and gravel conditions at the Amakdedori site may be too coarse and inhomogeneous for liquefaction to occur (see Section 3.15, Geohazards and Seismic Conditions) (Youd and Perkins 1978). However, as noted above, the particle size of the relevant sediment at the Diamond Point site is less certain. Should the seabed conditions be found to be susceptible to liquefaction, soil improvement work such as installation of stone columns or other densification methods would be considered (PLP 2018-RFI 005).

Boulders have been documented on the seafloor near both port sites and may be present in subsurface deposits (see Section 3.15, Geohazards and Seismic Conditions). The boulders could prevent the installation of sheet piles and/or possibly damage the piles. Both the Port of Alaska and Port Mackenzie experienced sheet pile damage caused by subsurface obstructions such as

old earthquake fill, riprap, or unexpected hard layers that were not detected by geotechnical investigations (CH2MHill 2013; Port of Alaska 2018; Lockyer 2016).

If sheet pile defects were to occur during construction, they could allow retained fill to escape, potentially covering the seafloor near the wharf, and may damage the wharf's surface and equipment, and interrupt shipping operations.

Another hazard experienced at the Port Mackenzie dock is erosion from seawater and tidal currents undermining the base of the sheet pile at the mudline, and causing a loss of fill (e.g., Hollander 2017). This hazard is unlikely to occur at the Amakdedori port site, given the design depth of sheet pile anchoring and design contingencies described above, but may be a concern at the Diamond Point site.

If struck by a tsunami, the sheet pile bulkhead design would expose the cross-sectional area to the hydrodynamic impact of the wave. A critical loading condition for the bulkhead could be the very low water level during the "retreat phase" of the tsunami, during which the stabilizing effect of water on the outside of the sheet pile is absent or diminished.

Based on the uncertainties and impacts experienced at other sheet pile structures as described above, it is possible that the sheet pile wharf could experience a release of fill material, ranging from partial loss through a damaged or eroded sheet pile to a major loss in an earthquake. The fill material for the Amakdedori port site would be sourced from a local geologic materials site (blasted granitic material) or imported by ship (PLP 2018-RFI 005) and could range from rockfill to material similar to that present on the seafloor (sand and gravel). At the Diamond Point site, the sheet pile wharf is proposed to be backfilled with the material dredged from the adjacent 20-foot-deep navigation channel.

In the event of the loss of fill from the sheet pile, the released material could cause a temporary turbidity plume in the water column. Wharf damage and loss of fill could also disrupt barging and concentrate lightering activities, potentially causing a buildup of concentrate containers at the port and ferry terminals.

In summary, the proposed rockfill causeway and sheet pile dock design would have the potential to result in adverse impacts on the environment during construction, operation, and closure. Additional field investigations would be performed to support detailed design to confirm that the design is feasible, and if so, to ensure that construction, operation, and closure procedures would be protective of the environment.